IN-VITRO AND *IN-VIVO* EXPRESSION ANALYSIS OF PNEUMOCOCCAL VACCINE CANDIDATES: PILUS-1 COMPONENTS

Gabriella De Angelis

Dottorato in Scienze Biotecnologiche – XXIV ciclo
Indirizzo Biotecnologie Molecolari e Industriali
Università di Napoli Federico II

Dottorato in Scienze Biotecnologiche – XXIV ciclo
Indirizzo Biotecnologie Molecolari e Industriali
Università di Napoli Federico II

In-vitro and *in-vivo* expression analysis of pneumococcal vaccine candidates: pilus-1 components

Dottoranda: **Gabriella De Angelis**

Relatore: **Prof. Ettore Benedetti**

Co-Tutore: **Dott.ssa Monica Moschioni**

Coordinatore: **Prof. Giovanni Sannia**

A mio padre,
che ha sempre creduto in me

INDEX

Chapter 2

Riassunto

Streptoccoccus pneumoniae (o pneumococco) è un batterio Gram-positivo in grado di colonizzare asintomaticamente il tratto nasofaringeo di più del 60% dei bambini e del 30% degli adulti, ma è anche annoverato tra i più importanti patogeni umani se si considerano il tasso di mortalità e morbilità ad esso associati su scala mondiale (circa un milione e mezzo di morti ogni anno tra i bambini di età inferiore a 5 anni). Pneumococco è, infatti, l'agente eziologico maggiormente associato alle polmoniti contratte in comunità, ma è anche causa di infezioni invasive e non invasive quali sinusite, otite media, meningite, batteriemia, endocarditi e pericarditi. Le categorie di età maggiormente colpite da infezioni da pneumococco sono i bambini al di sotto dei 2 anni di età e gli anziani (>65 anni) con un andamento di incidenza annuale che segue più o meno quello dell'influenza stagionale. Quali siano i meccanismi molecolari e i fattori di virulenza che permettono/favoriscono la transizione da uno stato di semplice colonizzatore a quello di patogeno non sono stati ancora completamente chiariti e sono oggetto di studi epidemiologici e biomolecolari.
Le malattie da pneumococco sono in generale efficacemente trattabili con penicillina, trimetoprim o macrolidi, tuttavia la diffusione delle resistenze agli antibiotici ha reso necessaria un'effettiva strategia di prevenzione che possa diminuire la rapidità e la diffusione delle infezioni. Il modo più immediato ed efficace per raggiungere questo scopo è una vaccinazione di massa con un vaccino basato su componenti batteriche (polisaccaridi capsulari o proteine superficiali) in grado di prevenire l'infezione causata da tutti gli isolati di *S. pneumoniae*.
Il disegno di un vaccino polisaccaridico che abbia una copertura globale è reso complicato da fattori quali l'elevata eterogeneità della capsula (94 sierotipi capsulari), l'eterogenea distribuzione geografica dei vari tipi capsulari e la capacità dello pneumococco di acquisire nuovi tratti fenotipici attraverso un meccanismo di trasformazione naturale che lo rende geneticamente flessibile e soggetto a frequenti ricombinazioni generanti mosaicismo genetico. In particolare, quando tali eventi di ricombinazione avvengono a livello del locus dell'operone della capsula (fenomeno noto in letteratura come *capsular switching*) in risposta alla presenza di un elevato quantitativo di anticorpi contro un determinato sierotipo capsulare, il microrganismo diventa capace di sfuggire al sistema immunitario.
Ad oggi sono già presenti sul mercato vaccini a base polisaccaridica (Pneumovax 23) e vaccini polisaccaridici coniugati (Prevenar7, Prevenar13, Synflorix); questi ultimi sono immunogenici anche nei bambini al di sotto dei due anni. Sebbene questi vaccini abbiano dimostrato una buona efficacia nel ridurre i casi di malattia invasiva causata da *S. pneumoniae*, il loro uso è limitato dal fatto che inducono un'immunità sierotipo-specifica e pertanto sono in grado di proteggere efficacemente solo contro le malattie invasive causate dai sierotipi contenuti nel vaccino stesso. Questo implica che, in base alla diversa distribuzione dei sierotipi, i vaccini polisaccaridici in commercio possono avere un grado di copertura diverso a seconda della regione esaminata. Un ulteriore fattore da tenere in considerazione per quanto riguarda la copertura del vaccino è il fatto che nei paesi in cui è stata introdotta la vaccinazione, è stato evidenziato un certo grado di redistribuzione dei sierotipi, associato ad un aumento della diffusione di quelli non coperti dal vaccino stesso, fenomeno noto in letteratura come *serotype replacement*.
L'alternativa concreta per ampliare la copertura di un vaccino e superare i problemi di *serotype replacement* potrebbe essere quella di sviluppare un vaccino sierotipo indipendente, basato su proteine di superficie conservate. Per *S. pneumoniae*, sono

note più di 100 proteine superficiali, molte delle quali sono fattori di virulenza o giocano comunque un ruolo importante nella patogenesi. Tuttavia, la variabilità genetica di tali proteine, i loro profili di espressione, e come queste possano determinare il tropismo tissutale, l'invasività e lo sviluppo della malattia, sono degli aspetti che, seppur investigati estensivamente, sono ancora poco conosciuti.
Tra le proteine selezionate recentemente come potenziali antigeni vi sono le subunità che costituiscono il pilo-1, una struttura fibrillare identificata sulla superficie di alcuni ceppi di *S. pneumoniae*. Questi ceppi contengono nel loro DNA genomico un elemento genetico di 12Kb noto come *pilus islet -1* (PI-1), contenente 7 geni codificanti per: le tre subunità strutturali del pilo (la subunità principale RrgB e due proteine ancillari RrgA ed RrgC); un regolatore trascrizionale positivo (RlrA); e tre transpeptidasi o sortasi (SrtC-1, StrC-2, SrtC-3), enzimi in grado di assemblare covalentemente le tre subunità strutturali e di ancorare il pilo alla parete batterica.
La dimostrazione che il pilo contribuisce alla virulenza batterica e favorisce l'adesione alle cellulle dell'epitelio dell'ospite, unita all'evidenza che l'immunizzazione con le diverse subunità (espresse in forma ricombinante) è protettiva in un modello animale di infezione intraperitoneale, ne fanno un potenziale candidato per un vaccino. In particolare, la subunità strutturale più abbondante del pilo (RrgB), nonché la più protettiva, è considerata il principale candidato per un vaccino a base proteica contro lo pneumococco. Questa proteina, ben caratterizzata dal punto di vista strutturale, è conosciuta in tre diverse varianti (note come clade I, II e III) con un grado di omologia nella sequenza proteica compresa tra il 48 e il 60%. Dato questo basso grado di omologia, le tre varianti di RrgB inducono una risposta immunitaria variante-specifica non in grado di assicurare una cross- protezione tra ceppi che esprimono pili con RrgB di varianti diverse. Al fine di ampliare la copertura di un vaccino contenente il candidato RrgB a tutti i ceppi di pneumococco che possiedono PI-1 (e quindi con ogni probabilità esprimono il pilo-1 sulla loro superficie), è stata generata una proteina di fusione (RrgB321) contenente le tre varianti di RrgB legate covalentemente testa-coda. RrgB321, in animali immunizzati, è in grado di stimolare la produzione di anticorpi contro le tre varianti di RrgB in maniera equivalente e di proteggere efficacemente contro infezioni causate da ceppi piliati di *S. pneumoniae* (contro ceppi rappresentativi delle tre varianti).
Il lavoro di tesi di questi tre anni ha avuto due obiettivi principali, entrambi volti ad una migliore caratterizzazione del candidato per il vaccino RrgB e, più in generale del pilo-1, quale determinante antigenico:

1- Caratterizzare l'espressione di RrgB e degli altri componenti del pilo-1, cercando di identificare i determinanti molecolari che ne favoriscano l'espressione;

2- Verificare come l'espressione del pilo possa influenzare la protezione indotta dalla vaccinazione con RrgB321.

In merito al primo obiettivo sono stati condotti esperimenti volti a chiarire il ruolo ed analizzare l'espressione di tutte le proteine costituenti il pilo e in particolare di RrgB. In dettaglio, l'espressione del pilo è stata valutata mediante FACS (*Fluorescence-activated cell sorting*), microscopia a immunofluorescenza e *Western blot*. Le analisi condotte su differenti ceppi contenenti PI-1 hanno rivelato che, diversamente da quanto visto per altri antigeni, in ogni ceppo è sempre possibile individuare due sottopopolazioni batteriche, una esprimente e l'altra non esprimente il pilo. Le due

sottopopolazioni coesistono nelle condizioni analizzate *in vitro*, in proporzioni variabili a seconda del ceppo analizzato e tali da non essere correlabili nè con il sierotipo o con il genotipo del ceppo stesso, né con la variante di RrgB espressa. Utilizzando le medesime metodiche è stato possibile dimostrare che quando il pilo è presente sulla superficie, anche tutti gli altri componenti codificati da PI-1 sono espressi (viceversa quando il pilo non è presente gli altri geni non sono espressi), indicando che l'espressione del pilo è finemente regolata tramite un meccanismo di tipo *on-off*.
Allo scopo di identificare eventuali condizioni o stimoli ambientali in grado di modulare il grado di espressione del pilo ed in particolare di aumentare la percentuale di batteri che lo esprimono, diversi ceppi di *S. pneumoniae* sono stati cresciuti in differenti condizioni di coltura e l'espressione del pilo è stata poi analizzata mediante FACS. In particolare, sono stati analizzati: a) diverse fasi di crescita batterica; b) diversi terreni di coltura (solidi oppure liquidi, terreni ricchi – THYE, BHI, RPMI- e un terreno minimo); c) diversi valori di pH (5.5; 6.4; 8.4); d) differenti quantità di ossigeno (condizioni atmosferiche e 5% CO_2). È stato inoltre valutato se l'aggiunta di metalli quali ferro e manganese ($MnSO_4$, $FeCl_3$) o di siero (FBS) al terreno di coltura potesse avere un effetto sull'espressione del pilo. Allo stesso modo è stata analizzata l'espressione del pilo dopo crescita in presenza di cellule epiteliali umane o con supernatanti di coltura provenienti da colture cellulari. Infine è stata valutata la percentuale di batteri esprimenti RrgB in presenza di 5 o 10% di sangue (montone o coniglio) in coltura liquida. Nessuna delle molteplici condizioni analizzate in diversi ceppi si è dimostrata in grado di modificare la percentuale di batteri non esprimenti il pilo a vantaggio di quella esprimente, o viceversa. L'unica condizione capace di contribuire positivamente all'espressione del pilo è stata la crescita in presenza di sangue. Tuttavia, data la notevole variabilità sperimentale dei risultati ottenuti nei diversi ceppi analizzati, non è possibile affermare in maniera univoca che la presenza di sangue nel terreno di coltura sia in grado di stimolare l'espressione del pilo.
Per poter meglio caratterizzare e cercare di individuare i determinanti che sono alla base dell' espressione differenziale all'interno di una popolazione dello stesso ceppo sono state individuate e successivamente separate colonie con un diverso grado di espressione del pilo. Mediante *Colony blot* (*Western blot* su singole colonie) e passaggi successivi di selezione e ricrescita è stato possibile isolare, per 6 diversi ceppi, due sottopopolazioni arricchite in batteri esprimenti (*High*) e non esprimenti il pilo (*Low*). Le due sottopopolazioni arricchite sono risultate stabili in coltura *in vitro* (anche in seguito a diversi passaggi consecutivi su piastra) ma non è stato possibile ottenere una popolazione omogenea per l'espressione del pilo (100% dei batteri esprimenti o non esprimenti). I profili di espressione delle due sottopopolazioni arricchite (H ed L) sono stati confrontati tramite *expression profile microarray* per cinque diversi ceppi (utilizzando RNA totale da coltura *in vitro*) al fine di individuare eventuali determinati genetici deputati o che contribuiscono alla regolazione dell'espressione del pilo. Dal confronto dei livelli di RNA tra la popolazione H ed L dello stesso ceppo, risulta che l'espressione di tutte le proteine codificate da PI-1 (incluso il regolatore positivo *rlrA*) sono regolate a livello trascrizionale. I livelli di RNA di tutti i componenti dell'isola risultano infatti significativamente più alti nelle popolazioni esprimenti il pilo. I dati ottenuti, confermati anche da *real-time* PCR, suggeriscono inoltre, come già proposto in precedenti lavori, la presenza di più di un promotore all'interno dell'isola, dal momento che i livelli di RNA delle subunità strutturali risultano significativamente più alti di quelli delle sortasi (enzimi deputati all'assemblaggio). L'analisi poi dell'intero *dataset*, attraverso il confronto dei livelli di

RNA degli altri geni esterni all'isola per le due sottopopolazioni non ha evidenziato altre differenze significative che fossero indice di un coinvolgimento di altri geni nella regolazione dell'espressione del pilo. Tale osservazione risulta in disaccordo con alcune recenti pubblicazioni che descrivono diversi regolatori negativi del pilo, la cui assenza, sembrerebbe in grado di stimolarne l'espressione.
Al fine di meglio caratterizzare la regolazione dell'espressione ed, in particolare, di dimostrare che l'espressione del regolatore positivo RlrA è sufficente ad indurre la trascrizione e la polimerizzazione di tutti i componenti del pilo, sono stati generati plasmidi per l'espressione costitutiva del regolatore positivo (RlrA), della proteina strutturale RrgB e di una delle sortasi necessarie all'assemblaggio (SrtC-2). Tali plasmidi sono stati utilizzati per trasformare la popolazione L di un ceppo e verificare poi tramite *Western blot* e microscopia a immunofluorescenza l'espressione dei singoli componenti del pilo e del loro assemblaggio sulla superficie batterica. I risultati hanno dimostrato che l'espressione costitutiva di SrtC-2 e di RrgB non ha alcun effetto sulla polimerizzazione o sull'espressione degli altri componenti dell'isola. Al contrario, quando nella popolazione L si ha l'espressione costitutiva di RlrA, il 100% della popolazione batterica presenta il pilo sulla propria superficie. Ciò indica che l'espressione di RlrA, differentemente da RrgB e SrtC-2, è sufficiente ad indurre l'espressione di tutti i componenti dell'isola, permettendo così l'assemblaggio del pilo sulla superficie di tutta la popolazione batterica.
I risultati ottenuti sopra descritti indicano che l'espressione del pilo cambia in risposta a stimoli che agiscono attivando l'espressione del regolatore RlrA. Nonostatante siano state analizzate molteplici condizioni di coltura *in vitro* non è stato possibile individuare quali siano questi stimoli e se essi agiscano direttamente o indirettamente modulando l'espressione del regolatore positivo.
Tuttavia, la scoperta che l'espressione del pilo è bifasica ha portato alla necessità di valutare l'espressione del pilo durante l'infezione per capire se le condizioni *in vivo* siano in grado di modulare il rapporto tra batteri esprimenti e non esprimenti il pilo all'interno di una stessa popolazione, o se, per ragioni ancora sconosciute la presenza di una popolazione eterogenea per l'espressione del pilo possa costituire un vantaggio nelle diverse fasi di colonizzazione e sviluppo della malattia nei diversi tessuti dell'ospite.
Per questi motivi, e per investigare ulteriormente l'efficacia protettiva di RrgB321 sono stati condotti esperimenti utilizzando un saggio di opsono-fagocitosi *in vitro* ed un modello di infezione animale murino, monitorando il grado di espressione ad inizio e fine esperimento.
I saggi di opsono-fagocitosi (OPA) permettono di misurare la funzionalità degli anticorpi generati dall'immunizzazione con l'antigene, verificando la loro capacità di mediare, in presenza di proteine del complemento, la fagocitosi/uccisione dei batteri da parte dei macrofagi, mimando così uno dei meccanismi che il nostro sistema immunitario utilizza per difendersi dalle infezioni. Saggi di OPA, condotti utilizzando le due sottopoplazioni arricchite in batteri esprimenti e non esprimenti il pilo (H e L) di un particolare ceppo, hanno dimostrato che l'attività fagocitica osservata in presenza di siero anti-RrgB321 dipende dalla proporzione di batteri esprimenti il pilo all'interno della popolazione. Infatti, la presenza di siero anti-RrgB321 induce la fagocitosi soltanto nella popolazione H in proporzione dipendente dalla concentrazione di siero utilizzato; al contrario non si osserva fagocitosi, anche ad alte concentrazioni di siero, per la popolazione L. Analisi al FACS, condotte sui batteri della popolazione H sopravvissuti al saggio di OPA, hanno inoltre dimostrato che la percentuale di batteri non esprimenti aumenta all'aumentare della concentrazione di siero utilizzato per il

saggio di opsono-fagocitosi, dimostrando ulteriormente la fagocitosi selettiva anticorpo-mediata.
Per verificare che i risultati ottenuti fossero dovuti alla reale fagocitosi dei batteri e non ad un effetto di inibizione dell'espressione del pilo da parte del siero anti-RrgB321 tre differenti ceppi di *S. pneumoniae* sono stati cresciuti in presenza di anticorpi contro l'RrgB ed è stata verificata la loro capacità di replicare per sette generazioni. L'espressione del pilo analizzata tramite FACS ha rivelato che la presenza del siero non è in grado di alterare la proporzione di batteri esprimenti in favore di quelli non esprimenti e vicecersa.
Questi dati hanno confermato che l'aumento, proporzionale alla diluizione del siero utilizzato nell'OPA, dei batteri non esprimenti il pilo è soltanto causato dalla fagocitosi anticorpo-mediata dei batteri esprimenti il pilo.
Dati i risultati ottenuti nei saggi di OPA si è voluto verificare se l'RrgB321 fosse in grado di proteggere da infezioni contro ceppi di *S. pneumoniae* indipendentemente dal loro grado di espressione del pilo. Per verificare tale ipotesi sono stati condotti esperimenti di immunizzazione passiva e attiva utilizzando diversi modelli di infezione murini.
Negli esperimenti di immunizzazione passiva, animali trattati con sieri derivati da immunizzazione con RrgB321 sono stati infettati sia con la popolazione H che con la popolazione L di uno stesso ceppo. Seguendo il corso dell'infezione e l'andamento della mortalità ad esso associata, si è potuto costatare che animali immunizzati con siero anti RrgB321 sono significativamente protetti contro l'infezione effettuata con la popolazione H, ma hanno un buon grado di protezione anche se il ceppo infettante ha un livello di espressione del pilo pressoché irrilevabile (popolazione L) al momento dell'infezione.
Allo stesso modo, gli esperimenti di immunizzazione attiva condotti vaccinando gli animali con RrgB321 hanno confermato che la proteina di fusione è in grado di proteggere contro le infezioni di ceppi di *S. pneumoniae* pressoché indipendentemente dal grado di espressione di quest'ultimo al momento dell'infezione. Infatti, sono stati osservati una significativa riduzione della batteriemia e un aumento della sopravvivenza negli animali immunizzati sia se infettati con la popolazione H sia se infettati con la popolazione L per tre differenti ceppi.
I dati ottenuti indicano che in entrambi i modelli animali utilizzati la vaccinazione con RrgB321 è in grado di produrre una risposta immunitaria efficace anche quando vi è una piccola parte di batteri che esprimono il pilo al momento dell'infezione. Una possibile spiegazione può essere rintracciata nella natura bistabile dell'espressione del pilo. É infatti possibile che durante lo sviluppo della malattia le interazioni dei batteri con i tessuti dell'ospite inducano un cambiamento nello stato dell'espressione delle componenti batteriche, favorendo l'espressione del pilo in batteri prima non esprimenti, e che quindi, in animali immunizzati con RrgB, diventerebbero aggredibili dal sistema immunitario. Un'ipotesi alternativa è che durante l'infezione, l'uccisione di batteri esprimenti il pilo, a seguito dell'immunizzazione con RrgB321, potrebbe indurre l'espressione nei batteri prima non esprimenti per ri-stabilire quell'equilibrio tra batteri piliati e non che si mantiene anche *in vitro* in molteplici condizioni colturali differenti. Per verificare la veridicità di queste ipotesi, l'espressione del pilo è stata valutata tramite FACS nei batteri recuperati dal sito di infezione (sangue) in topi immunizzati e in topi non immunizzati. Per tutti e tre i ceppi su cui è stata condotta l'analisi e per tutti i gruppi analizzati si è potuto osservare che nel caso dell'infezione con la popolazione H, nei batteri recuperati dal sangue si è osservata una lieve diminuzione nella proporzione (10%) dei batteri esprimenti il pilo; al contrario, nel

caso dell'infezione con la popolazione L, i batteri recuperati dal sangue hanno mostrato un lieve aumento nella proporzione (10%) di batteri esprimenti il pilo. Ciò avvalora l'ipotesi che l'espressione del pilo di *S. pneumoniae* può essere modulata nell'ospite, pur tuttavia in maniera indipendente dall'immunizzazione dell'animale. Infatti, non è stata osservata nessuna differenza nell'espressione del pilo tra i batteri recuperati dal sangue nei topi immunizzati rispetto ai topi non immunizzati.
In conclusione, il lavoro di tesi svolto ha permesso di caratterizzare l'espressione dei componenti del pilo-1 di *Streptococcus pneumoniae*, portando evidenze della sua natura bifasica. Allo stesso tempo è stato dimostrato che una proteina di fusione costituita dalle tre varianti della principale proteina strutturale costituente il pilo (RrgB321) è in grado di proteggere in maniera efficace da infezioni contro ceppi di pneumococco positivi per la presenza di PI-1 (codificante i componenti del pilo) indipendentemente dal grado di espressione dello stesso. Nonostante non sia stato possibile chiarire il meccanismo attraverso il quale ciò avvenga, i dati ottenuti supportano l'inclusione di RrgB321 in un vaccino a più componenti contro le infezioni da *Streptococcus pneumoniae*.

Summary

Streptococcus pneumoniae (*S. pneumoniae*) is a Gram-positive commensal of the nasopharyngeal tract of both children and healthy adults. However, *S. pneumoniae* is also a leading cause of morbidity and mortality worldwide, being responsible for non-invasive and invasive diseases such as acute otitis media, pneumonia, sepsis and meningitis. Despite the unquestionable efficacy of the available pneumococcal glycoconjugate vaccines, the limited coverage, along with the observed phenomenon of serotype replacement, could reduce their long-term effectiveness. For these reasons, the development of a serotype-independent vaccine relying on the use of surface-exposed protein antigens represents a valid alternative. In this context, pneumococcal pilus-1 components, and in particular the pilus backbone RrgB, demonstrated significant efficacy in protecting mice from lethal challenge.

The *S. pneumoniae* pilus-1 is encoded by pilus islet 1 (PI-1), which has three clonal variants (clade I, II and III) and is present in about 30% of clinical pneumococcal isolates. Since a combination of the three RrgB variants could broad the efficacy of a pilus-based vaccine, a fusion protein (RrgB321) containing the three RrgB variants in a head to tail organization was constructed. It was recently reported that RrgB321 elicites an antibody response against each of the variants and protectes mice against piliated pneumococcal strains of the three clades both by active and passive immunization, supporting the validity of this candidate as a potential antigen for the generation of a multi-component protein-based vaccine against *S. pneumoniae.*

The data reported in this work contribute to the characterization of pilus-1 expression regulation in *in vitro* and *in vivo* experiments providing evidence that pilus expression is biphasic and demonstrating that the pilus expression level does not impair the protection induced by RrgB321 immunization in mouse models of infection.

Analyzing the strains at the single-cell level, two phenotypically different sub-populations of bacteria (one that expresses the pilus, while the other does not) could be identified. The proportions of these two phenotypes are variable among the strains tested and are not influenced by genotype, serotype, growth conditions, colony morphology or by the presence of antibodies directed toward the pilus components. Two sub-populations, enriched in pilus expressing or not expressing bacteria were obtained by means of colony selection and immuno-detection methods for five strains. PI-1 sequencing in the two sub-populations revealed the absence of mutations, thus indicating that the biphasic expression observed is not due to a genetic modification within PI-1. Microarray expression profile and western blot analyses on whole bacterial lysates performed comparing the two enriched sub-populations, revealed that pilus expression is regulated at the transcriptional level (on/off regulation), and that there are no other genes, in addition to those encoded by PI-1, concurrently regulated across the strains tested. Moreover, evidence that the over-expression of the RrlA positive regulator is sufficient to induce pilus expression in pilus-1 negative bacteria, was reported. Overall the *in vitro* data presented suggest that the observed biphasic pilus expression phenotype is an example of bistability in pneumococcus.

Additionally, in this study, the ability of RrgB321 antibodies to kill both H and L *S. pneumoniae* populations in the opsonophagocytosis assay, as well as the ability of RrgB321 to confer protection *in vivo* against both populations were analyzed.

The results obtained demonstrate that: i) the opsonophagocytic killing mediated *in vitro* by RrgB321 antisera is strictly dependent on the pilus expression ratio of the strain used; ii) during the opsonophagocytosis assay pilus-expressing pneumococci

are selectively killed, and iii) no switch towards the pilus non-expressing phenotype can be observed. Furthermore, in sepsis and pneumonia models, mice immunized with RrgB321 are significantly protected against challenge with either the H or the L pilus-expressing population of strains representative of the three RrgB variants. This suggests that the pilus-1 expression is not down-regulated, and also that the expression of the pilus-1 could be up-regulated *in vivo*. In conclusion, these data provide evidence that RrgB321 is protective against PI-1 positive strains regardless of their pilus expression level, and support the rationale for the inclusion of this fusion protein into a multi-component protein-based pneumococcal vaccine.

Introduction

Overview on *Streptococcus pneumoniae* and vaccine prevention of pneumococcal disease

Streptococcus pneumoniae (pneumococcus) is a Gram-positive, alpha-hemolytic, bacterium isolated and described for the first time by George Miller Stenberg and Louis Pasteur, in 1881 [1,2]. (Figure 1)

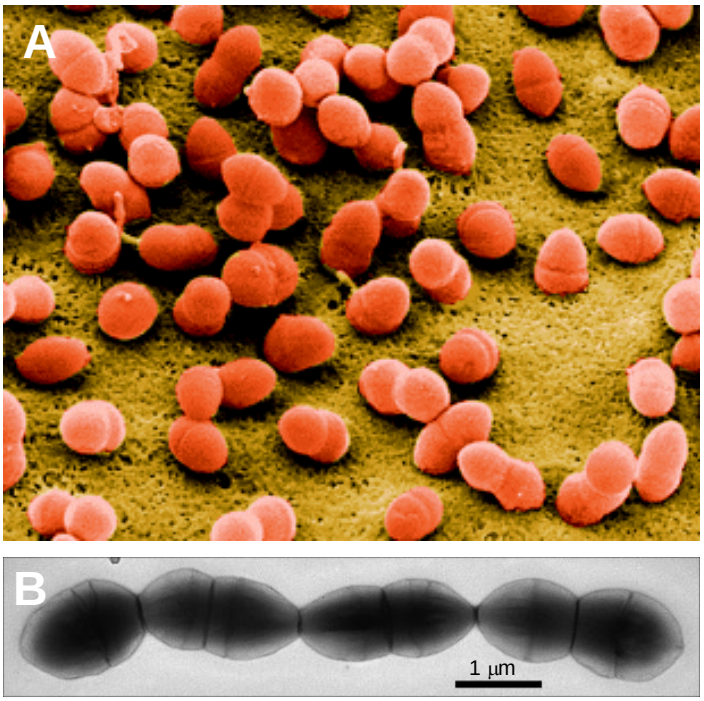

Figure 1. (**A**) Electron microscope photomicrograph of *Streptococcus pneumoniae* from MicrobeWiki and (**B**) negative stain TEM image showing a chain of *S. pneumoniae* TIGR4 bacteria [3].

Primarily a commensal, pneumococcus asymptomatically colonizes the nasopharynx of children and healthy adults. However, it is also a significant pathogen, able to spread from the site of carriage and to cause a range of infections such as otitis media, pneumonia, bacteremia and meningitis, especially in infants, ederly and immunocompromised persons [4,5]. The significance of *S. pneumoniae* as a human pathogen is highlighted by the estimate that in 2000 among children under 5 years of age were reported about 14.5 million episodes of serious pneumococcal disease with 826000 deaths [6]. Other estimates report the pneumococcus to be responsible for a total of 1.6 million deaths annually [7]. However, invasive pneumococcal disease represents only a small fraction of all pneumococcal clinical syndromes, most of which are represented by nonbacteremic pneumonia (Figure 2).
Many antibiotics such as doxycycline, fluoroquinolones and trimethoprim-sulfamethoxazole have been used for the treatment of pneumococcal infections. However, antibiotic resistance has become a worldwide problem, limiting the choice of antimicrobial agents. Thus, the pneumococcus has been, and remains, a major cause of morbidity and mortality worldwide.

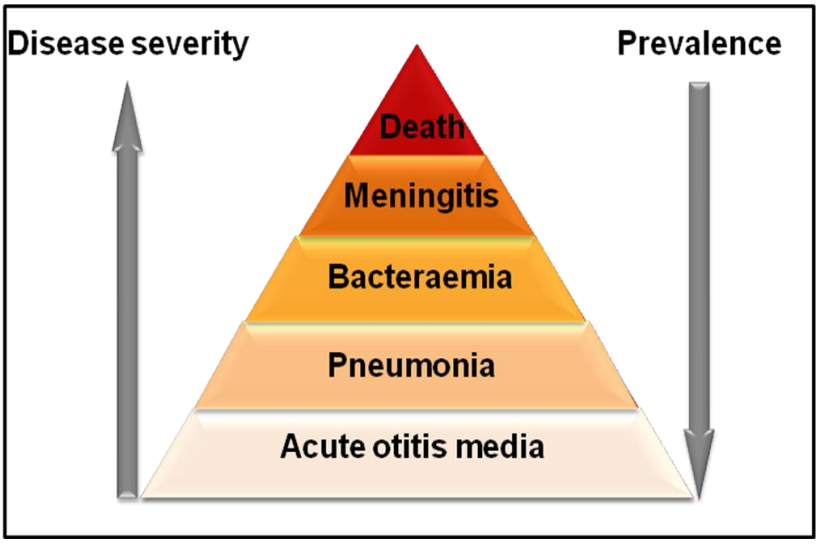

Figure 2. Pneumococcal clinical syndromes. *Modified from* [8]

For the prevention of the pneumococcal diseases, great efforts are being made to develop effective vaccines in both industrialized and developing countries. However, due to the complexity and the multiplicity of the *S. pneumoniae* isolates spread worldwide, none of the current vaccines can address the needs of both the elderly and children in all parts of the world.
S. pneumoniae, in fact, produces a range of different colonization and virulence factors including the polysaccharide capsule, surface proteins and enzymes, and the pneumolysin toxin, that allow the bacterium to escape the host immune system and cause disease (Figure 3).
The polysaccharide capsule is probably the most important pneumococcal virulence factor, as it protects the bacteria from phagocytosis; it is crucial for colonization, prevents mechanical removal by mucus [9] and can also restrict autolysis and reduce exposure to antibiotics [10]. Capsule polysaccharides are highly heterogeneous and, thus far, at least 93 different capsular serotypes have been described, according to their unique serological profiles and chemical structures [11-13].
Capsular serotyping, for historical reasons, is the most used and efficacious strategy for classification of pneumococcal strains; however, to better understand the population structure from the genetic point of view, a nucleotide sequence based method, Multi Locus Sequence Typing (MLST), has been developed in the last decade. The MLST involves the sequencing of internal fragments from seven house-keeping genes (*aroE, gdh, gki, recP, spi, xpt, ddl*), and the unequivocal assignment of the isolates to a Sequence Type (ST) [14]. Moreover, through the algorithm eBURST single STs can be grouped in Clonal Complexes (CCs) based on the number of differences in their allelic profile [15,16], and sequence data can be held on a central database (http://www.mlst.net) and quired through a web server.

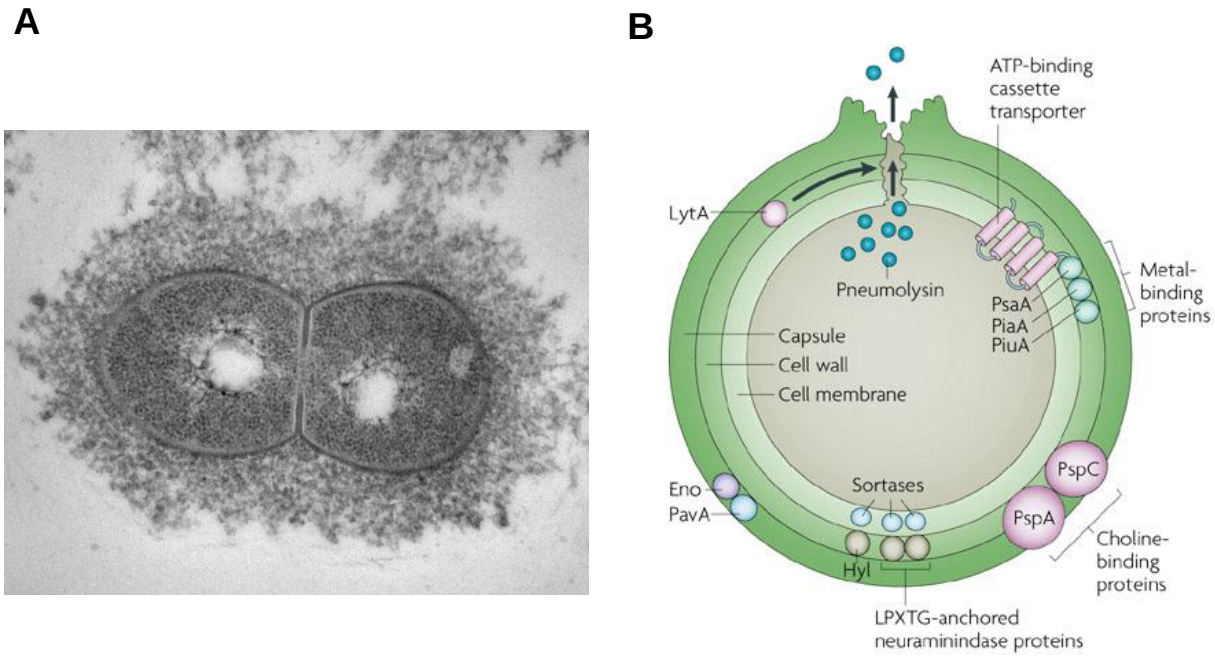

Figure 3. (A) Elettron microscopy analysis of a *S. pneumoniae* 6B strain showing the polysaccharide capsul; **(B)** Schematic rappresentation of *S. pneumoniae* virulence factors [17].

Since capsular polysaccharides (PS) are highly immunogenic and develop an immuno-response able to protect against infection caused by the homologous serotype, pneumococcal vaccines currently on the market are based upon serotype-specific PS alone or conjugated with proteins.
The 23-valent pneumococcal polysaccharide vaccine (Pneumovax 23®, marketed by Merck & Company, Inc.) was licensed in the United States in 1983 and contains 23 different capsular polysaccharides (1, 2, 3, 4, 5, 6B, 7F, 8, 9N, 9V, 10A, 11A, 12F, 14, 15B, 17F, 18C, 19A, 19F, 20, 22F, 23F, and 33F) [18]. This vaccine had a theoretical coverage of more than the 80% of the pneumococci causing infections in adults and children above 2 years of age. Unfortunately, the vaccine was less immunogenic in young children and immunocompromised patients [19] and showed efficacy only against bacteraemia and meningitis in the elderly population, but not against pneumonia, the most prevalent pneumococcal disease of this age group [20,21]. Furthermore, the PS vaccine is not effective against acute otitis media caused by *S. pneumoniae* [22] and does not induce a T cell-dependent immune response, thus limiting the period of protection because of the absence of memory B cells. Moreover, some capsule polysaccharides, including serotypes associated with penicillin resistance, are poorly immunogenic [23]. All these factors have led to the development of new pneumococcal vaccines containing polysaccharide antigens conjugated to carrier proteins, which are effective in developing an immune response also in children under 2 years of age and in reducing nasopharyngeal carriage of vaccine-type pneumococci [24,25]. However, no studies have shown improved efficacy and benefits of conjugate vaccines in the elderly [26]. The first conjugate vaccine (PCV-7 or Prevnar®), targeting seven serotypes (4, 6B, 9V, 14, 18C, 19F and 23F), was approved for use in the United States in 2000 and subsequently adopted in many developed countries [27]. In 2009, a 10-valent vaccine, Synflorix™ (covering serotypes 1, 4, 5, 6B, 7F, 9V, 14, 18C, 19F and 23F), conjugated to *Hemophilus*

influenzae protein-D (PHiD-10), was approved in Europe. In 2010, a 13-valent conjugate vaccine covering serotypes 1, 3, 4, 5, 6A, 6B, 7F, 9V, 14, 18C, 19A, 19F and 23F (PCV-13 or Prevnar-13) was approved in the United States for use among children aged from 6 weeks to 71 months and replaced PCV-7 [28]. (Figure 4)

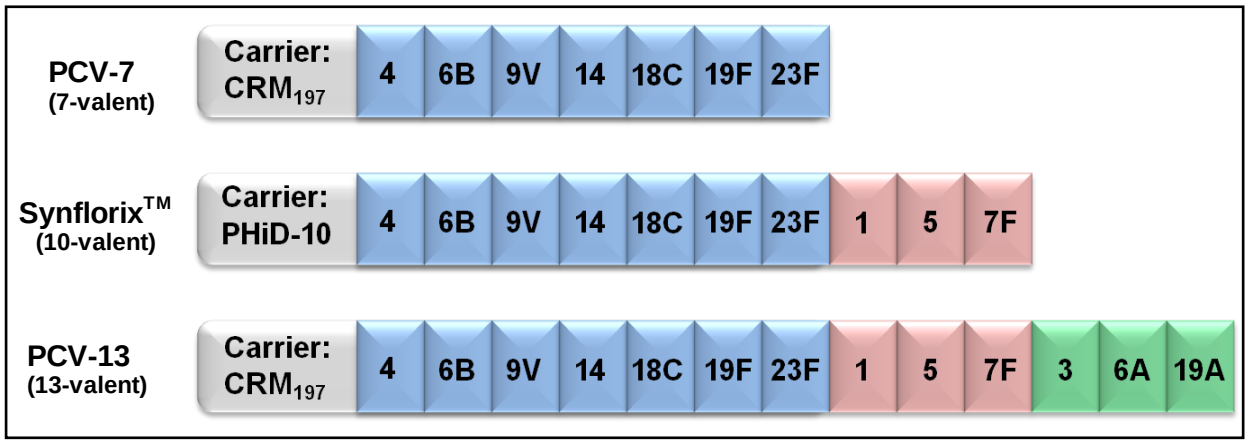

Figure 4. Serotype composition of pneumococcal conjugate vaccines currently on the market.

Unfortunately, these multi-valent vaccines only partially cover the diseases caused by *S. pneumoniae* serotypes circulating in developing countries, and the high manufacturing costs make them too expensive for the populations with the greatest need. Most importantly, events like serotype replacement induced by vaccination, and capsular switching (due to the horizontal transfer of the capsular loci from a strain to one other), have already been clearly demonstrated in several clinical and surveillance studies [29,30]. For this reason, the prospective vaccine failure has become a serious concern.

Consequently, concerted global efforts are currently focused on developing alternative pneumococcal vaccine strategies. One of these approaches involves the development of vaccines based on pneumococcal proteins that contribute to pathogenesis and are common to all serotypes [31]. Such proteins, being T-cell-dependent antigens, should be both highly immunogenic and able to elicit immunological memory in human infants [32]. Furthermore, proteins can be engineered for high-level expression at relatively low cost, and formulation is likely to be simpler, thereby making such vaccines more affordable for the developing countries.

Pneumococci are estimated to express over 100 surface proteins, some of which are known to have a role in pathogenesis and virulence; however the function of the majority of them is still unknown [33]. Some of the surface proteins are currently under investigation as vaccine candidates such as: PspA and PspC (Choline-binding proteins); PsaA (metal-binding lipoprotein); PhtB and PhtE (poly-histidine triad proteins); NanA (neuraminidase) and other proteins that are covalently linked to the bacterial cell wall by a carboxy (C)-terminal sortase (LPXTG; in which X denotes any amino acid) motif [34]. Another well-studied protein that is secreted by all known clinical isolates of *S. pneumoniae* is Ply, the pneumolysin toxin. Although Ply is not a surface protein, it is an important virulence factor, belonging to the family of pore-

forming toxins synthesized by Gram-positive bacteria that can directly damage epithelial surfaces and reduce the migration of phagocytic PMNs [35]. The roles for these proteins in bacterial physiology and pathogenicity based on mutagenesis studies in *in vitro* experiments and in animal models of pneumococcal disease have summarized in Table 1. Although several of these antigens have been shown to be protective immunogens [36], thus far the high sequence variability of these antigens or their toxicity (pneumolysin) limit their use as vaccine candidates. Recently, the availability of the complete genome sequence of virulent and non-virulent isolates of *S. pneumoniae* (http://www.tigr.org) has provided new classes of potential protein antigens. The chromosome of over 2 million base pairs contains slightly more than 2000 predicted protein coding regions; interestingly, about 30% of the open reading frames (ORFs) still remains un-annotated and displays unknown or hypothetical function [37,38].

Table 1. Role in bacterial physiology and pathogenicity of proteins that have been considered as vaccine candidates

Pneumococcal proteins	Main role in colonization and disease	References
Pneumolysin (Ply)	Membrane pore forming cytolytic toxin that also activates complement	[39]
PspC (known as CbpA)	Involved in adherence and colonization	[40]
PspA	Complement inactivation	[41]
NanA, BgaA	Cleavage of terminal sugars; revealing receptor for adherence, promoting Blood-Brain Barrier interaction	[42]
PavA	binds to fibronectin	[43]
LytA	digest the cell wall, which results in the release of ply	[44]
PsaA	Metal ion transport involved in resistance to oxidative stress	[45]
Pilus-1 components	Promote adherence, colonization and inflammation	[46]
PfbB	mediates bacterial adhesion to human epithelil cells	[47]
PsrP	mediates bacterial attachment to Keratin 1 and promotes the formation of large bacterial aggregates in the nasopharynx and lungs	[48]

Therefore, *in vivo* and *in vitro* techniques that complement *in silico* genomic searches are playing a crucial role in the identification of the proteins that provide the greatest promise in terms of novelty and applicability.
The recent discovery that Gram-positive pathogens possess long filamentous pilus-like structures extending from the bacterial surface has opened a new area of research in the understanding of their function in pathogenesis and their role as protective antigens [49,50].

Streptococcus pneumoniae pili

In *S. pneumoniae* strains, two unrelated pilus gene clusters, coding for two antigenically different pili, have been identified: pilus islet 1 (PI-1) and pilus islet 2 (PI-2) [51,52] (Figure 5).

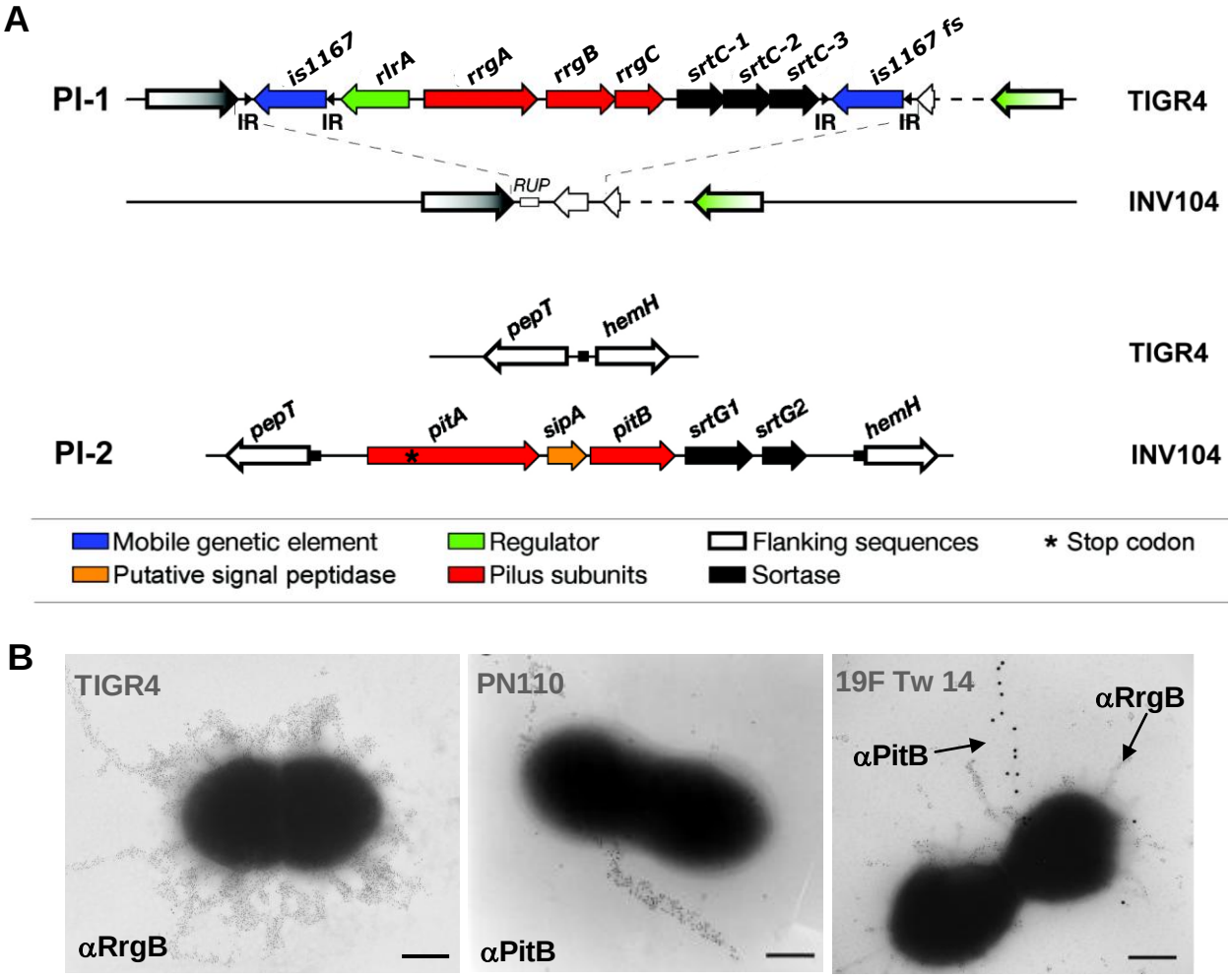

Figure 5. (**A**) Genomic organization of pilus-encoding islets in *S. pneumoniae* [51]. (**B**) Immunoelectron microscopy analysis of whole bacterial cells incubated with polyclonal antibodies (conjugated to 5-nm gold particles) raised against the backbone pilus proteins (RrgB and PitB).

Both pili have the typical features of Gram-positive pili are composed of pilus backbone proteins covalently linked in a head-to-tail organization; have one or two additional (ancillary) proteins linked to the backbone structure and are assembled by specialized transpeptidases also referred to as sortases [49,53].
Each pilin subunit has a C-terminal cell wall sorting signal (CWSS), consisting of an LPXTG-like motif required for the covalent attachment to either the cell wall or to the flanking pilus subunits and a hydrophobic domain, followed by a stretch of basic amino acid residues. The covalent linkage of pilus subunits consists in an amide

bond between the side chain of a lysine residue and the threonine in the CWSS [50,54].
The PI-2, identified by Bagnoli *et al*. [51], is a 7-kb region located between the genes that encode the peptidase T (PepT) and ferrochelatase (HemH) and flanked by putative 7-bp (TCCTTTT) insertion sites. The PI-2 has been reported to be present in about the 16% of the isolates and prevalent in emerging, non-PCV7 serotypes [51,55]. The islet is composed of 5 genes, which are predicted to encode the two surface protein, PitA and PitB (with *pitA* a pseudogene due to a stop-codon), a signal peptidase-like protein (SipA), and 2 sortases (SrtG1 and SrtG2); SrtG2 is nonfunctional in most of the strains. Pilus-2 appears to consist solely of PitB polymers, and has been shown to mediate adhesion of *S. pneumoniae* to eukaryotic cells [51].
The *S. pneumoniae* pilus-1 is encoded by a 12-kb genomic region (PI-1) and is also referred to as *rlrA* pathogenicity islet. This region is flanked by conserved mobile genetic elements characterized by direct inverse repeats, known as Insertion Sequence (IS) elements [46,49]. The PI-1 contains seven genes coding for: a Rof-A-like transcriptional regulator (RlrA), which positively regulates pilus expression [56] and its own expression, three pilus structural subunits with LPXTG-type CWSSs (RrgA, RrgB and RrgC) and three sortase enzymes (SrtC-1, SrtC-2 and SrtC-3 also named SrtB, SrtC and SrtD respectively), which covalently assemble the pilus subunits on the bacterial surface [52,57-59] (Figure 5).

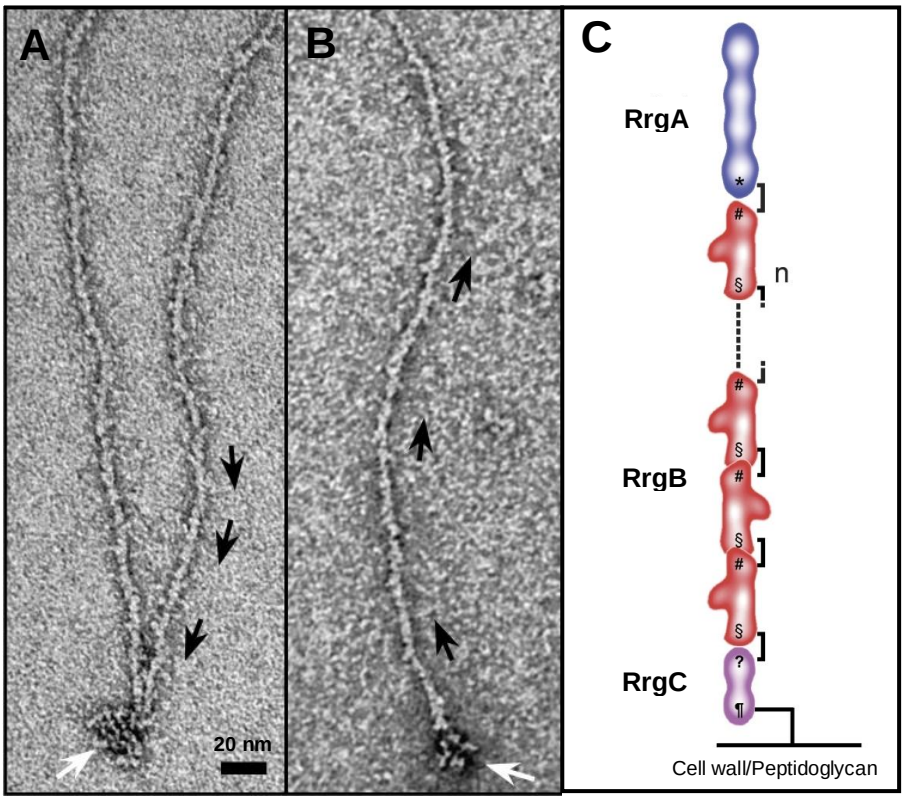

Figure 6. Molecular architecture of *S. pneumoniae* pilus-1. (**A, B**) Negative stain TEM image showing the localization of the ancillary proteins RrgA and RrgC of TIGR4 pili. The white arrows indicate RrgA in panel **A** and RrgC in panel **B**. The black arrows point away from the bacterium. (**C**) Model of *S. pneumoniae* pilus. The symbols indicate the LPXTG motifs for each pilin: * YPRTG (RrgA), § IPQTG (RrgB), ¶ VPDTG (RrgC) and the pilin motif (#) [3].

In pilus-1, RrgB is the major subunit that forms the backbone of the structure, RrgA is the major ancillary protein, localized at the pilus tip and responsible for the host adhesion properties of the pilus, whereas RrgC is the minor ancillary protein, likely located at the pilus base and responsible for the putative cell wall anchoring [3,60,61] (Figure 6).
PI-1 exists in three variants, namely clade I, II and III. Most of the gene variability is concentrated in the genes coding for the pilus components: *rrgA* and *rrgB*. In terms of protein sequence variability RrgB is classified into three variants (I, II and III), RrgA exists in two major groups (clades I and II) whereas RrgC and all the sortases are highly conserved [62] (Figure 7).

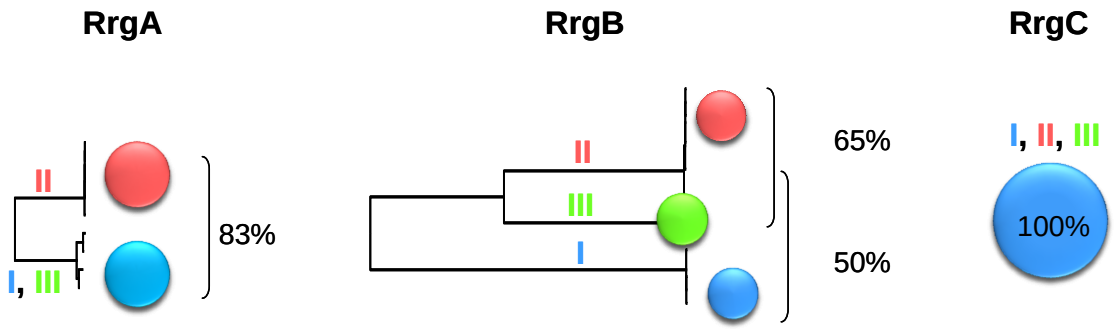

Figure 7. Genetic variability among the pilus-1 subunits. The protein sequence conservation between the clades (I, II, III) is reported in percentage for each pilin.

The contribution to the pilus formation of the three sortases (srtC-1, srtC-2, srtC-3) has recently been reported [57]. The three sortases are redundant, as they are all able to polymerize the structural backbone (RrgB) as well as to link RrgA and RrgC to the pilus shaft.
Considerable effort has been directed also to unravel the structure and the mechanisms of biogenesis of pilus-1. The crystal structures of the adhesin RrgA and of the major pilin RrgB were recently resolved [63,64], while no structure is available for the cell wall anchor protein RrgC.
Despite molecular epidemiological reports highlight that PI-1 is present in about 30% of the pneumococcal isolates, regardless of the geographical origin and the disease outcome analyzed [62,65,66], several studies have already demonstrated the role of the pilus in virulence and host inflammatory responses. In detail, mutants lacking PI-1 are impaired in adhesion to cultured epithelial cells (mostly due to RrgA) and are less virulent in murine models of colonization, pneumonia and invasive diseases [46,67]. Interestingly, immunization of mice with pilus structural antigens was shown to induce protection against lethal challenge by piliated strains. These studies indicate that vaccination with pilus subunits confers the same protection as vaccination with heat killed bacteria, supporting the possibility to use pilus antigens in a multivalent pneumococcal vaccine [68] (Figure 8).
However, whether all PI-1 positive pneumococci express pili (*in vitro* and *in vivo*) and if genetic differences and growth conditions could influence pilus-1 expression levels was still not clear.

Moreover, while protection against invasive disease was demonstrated when pilus antigens were used as vaccines in mouse models, it was not yet reported if the level of the pilus expression could impair the protection against piliated pneumococci.

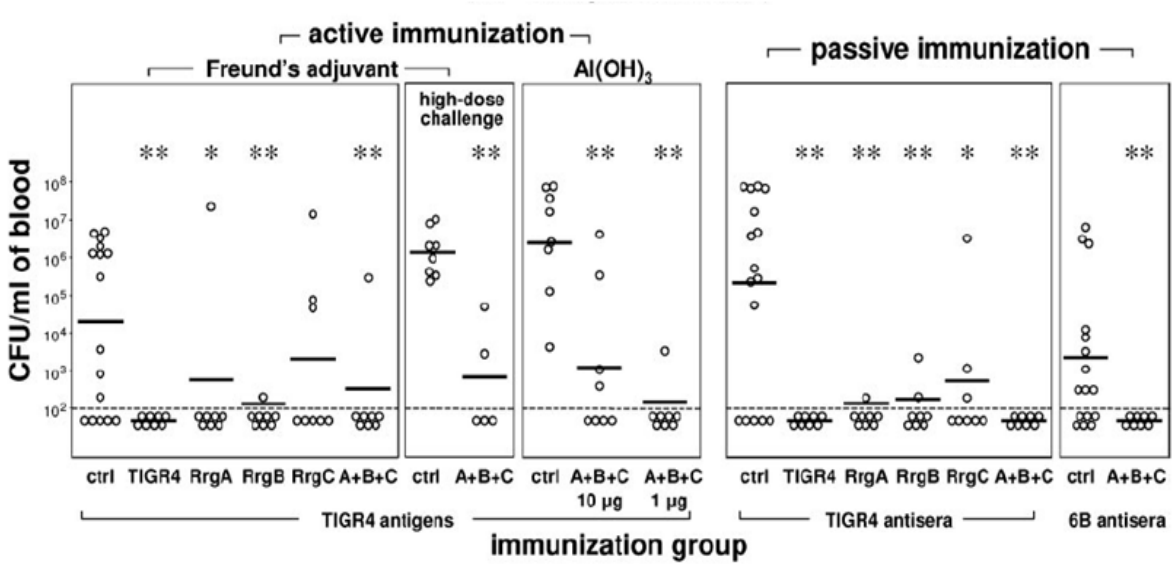

Figure 8. Protective efficacies of pilus subunits in mice. Bacteremia at 24h postchallenge (TIGR4) of vaccinated mice are shown; ctrl indicates mice receiving only the corresponding adjuvant plus saline; * and ** indicate *P* values of <0.05 and <0.01, respectively (one-tailed Mann-Whitney U test), for comparison with the corresponding control groups [68].

For this reason, the focus of this work has been to characterize the expression of the pneumococcal pilus-1 using strains of clade I, II and III, both in *in-vitro* and *in-vivo* conditions.

Chapter 1

Based on:

"The *Streptococcus pneumoniae* Pilus-1 Displays a Biphasic Expression Pattern."

Gabriella De Angelis, Monica Moschioni, Alessandro Muzzi, Alfredo Pezzicoli, Stefano Censini, Isabel Delany, Antonia Sinisi, Claudio Donati, Vega Masignani, Michèle A. Barocchi.

Plos One 2011, 6(6):e21269

Introduction

Streptococcus pneumoniae pilus-1 is a virulence factor involved in adherence to host cells, and its components are able to protect against piliated strains. For this reason, pilus proteins are regarded as promising antigens of new generation protein-based vaccines. Considerable effort has been directed to unravel the structure, the mechanisms of biogenesis and the epidemiology of pilus-1. Moreover, several reports have focused on the evaluation of genetic regulators that are able to modulate pilus expression and therefore bacterial virulence. Seven proteins, in addition to the PI-1 positive regulator RlrA, were demonstrated by different groups to negatively influence *in vitro* pilus expression levels (MgrA, HK343, MerR, CbpS, TCS08, mntE, PsaR) [67,69-71].

Despite a significant increase in pilus prevalence was recently observed, suggesting that the pilus confers important selective advantages in colonization, its prevalence in all population does not exceed the 30% [72]. This potential fitness advantage led us to further investigate the mechanism of regulation of pilus expression in pneumococcus.

Indeed, gene expression in bacteria is traditionally studied as the average behaviour of cells in a population, with the assumption that under a particular set of conditions all cells express genes in an approximately uniform manner. However, the advent of techniques that facilitate the investigation of individual cell behaviour has revealed that, within isogenic populations, bacterial cells can display heterogenous phenotypes. These mechanisms, used by several bacterial species to generate intra-population diversity, increase bacterial fitness and are important in niche adaptation, or to escape host defenses [73].

Various processes can contribute to this variability within a bacterial population and can be based on genetic rearrangement (phase variation) or can be epigenetic in nature and not be accompanied by changes in DNA sequence (phenotypic variation).

Phase variation in many bacterial species is often mediated by frequent and reversible changes in the lengths of short DNA sequence repeats (termed microsatellites) located in protein-coding regions or upstream regulatory regions, leading to deactivation or alteration of the associated genes [73]. Phase variation events can also be due to DNA rearrangements of fragments up to several kilobases, such as: i) homologous recombination occurring between a silent allele of a gene and

the gene located at the expression site; ii) site-specific recombination events caused by inversion, insertion or excision/transposition of a DNA region [74]; iii) duplication events as is the case of the genes involved in the capsular biosynthesis in some serotypes of *S. pneumoniae* [75]. Otherwise, epigenetic regulation of phenotypic variation occurs in the absence of a change in DNA and can involve differentially methylated sequences in the regulatory regions of the phase-varying gene or operon. Some epigenetic traits can also depend on the presence of positive or double-negative feedback loops in the regulatory network that determine the activity of key regulators, generating multistable bacterial populations. Phenotypic variation based on this type of network architecture is known as bistability and is characterized by the existence of two (or more) distinct phenotypes within an isogenic population [76]. Indeed, bistability occurs when in a bacterial cell the expression level of a gene comes through a threshold and the quantitative change becomes qualitative with the coming out of a new pattern of gene expression and the splitting of the bacterial population into coexisting cell types. This regulation system implies that it is possible to switch between two alternative states but not to rest at an intermediate state [77].
Two mechanisms have been proposed to drive this kind of bifurcation. The first mechanism requires that the master gene is positively auto-regulated and establish a positive feedback loop. A second mechanism is a double-negative regulatory circuit involving the mutual repression of two repressors (Figure. 1.1).

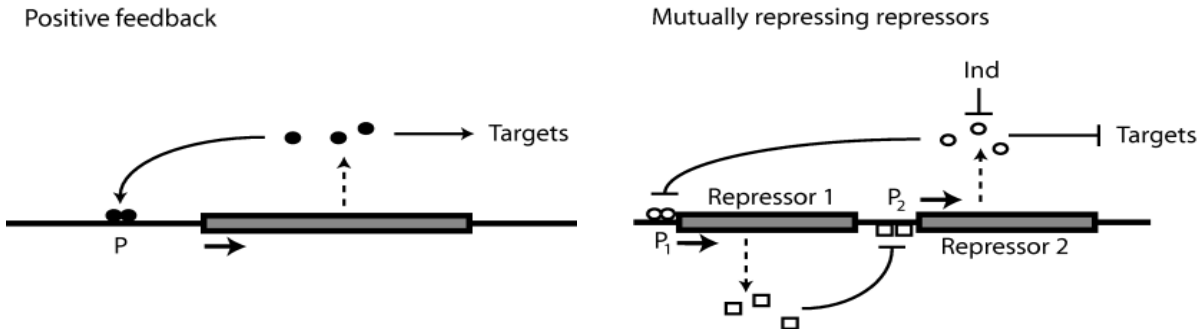

Figure. 1.1 Two network configurations that lead to bistable expression. The first involves a positive transcriptional autoregulatory loop together with cooperativity in promoter activation. The second involves two mutual repressing repressors. An inducer antagonizes the action of repressor 1, throwing the switch in the direction of derepression of target genes under the control of repressor 2. Open symbols denote repressors and closed circles denote activators *Modified from* [77].

Bistability may provide a selective advantage for subsets of bacteria under adverse conditions and has been described in many different organisms (i.e. competence development in *Bacillus. subtilis* and also in S*treptococcus. pneumoniae*) [74,78]. In addition, a bistable expression was already demonstrated for the Ebp-type pili in *Enterococcus faecalis* [79] and for the FCT-3 pili in *Streptococcus pyogenes [80]*.
Furthermore, regulation of gene expression allows the bacterium to be optimally suited to its growth environment. Thus, the expression of phase-variable genes would also be under environmental control. Iron starvation, for example, increases the frequency of antigenic and phase variation of *Neisseria gonorrhoeae* pili [81], and

stimuli such as temperature, pH, carbon source and amino-acid concentration affect the expression of phase-variable pili in *Escherichia coli* and *Salmonella enterica* [82,83].
Herein, given the implication that the *S. pneumonia*e pilus-1 might have in disease development, pilus expression was characterized at the single-cell level and under different growth conditions, providing evidence of its bistable nature.

Results

Pilus-1 has a biphasic expression pattern

In order to elucidate pilus expression in *S. pneumoniae*, bacteria of a serotype 4 strain (TIGR4) were grown in liquid culture, stained with antibodies raised against the pilus components (RrgA, RrgB, and RrgC) and three surface exposed proteins (PspC, PhtA and BgaA), and then analyzed by flow cytometry (FACS) [84-87] (Figure 1.2A).

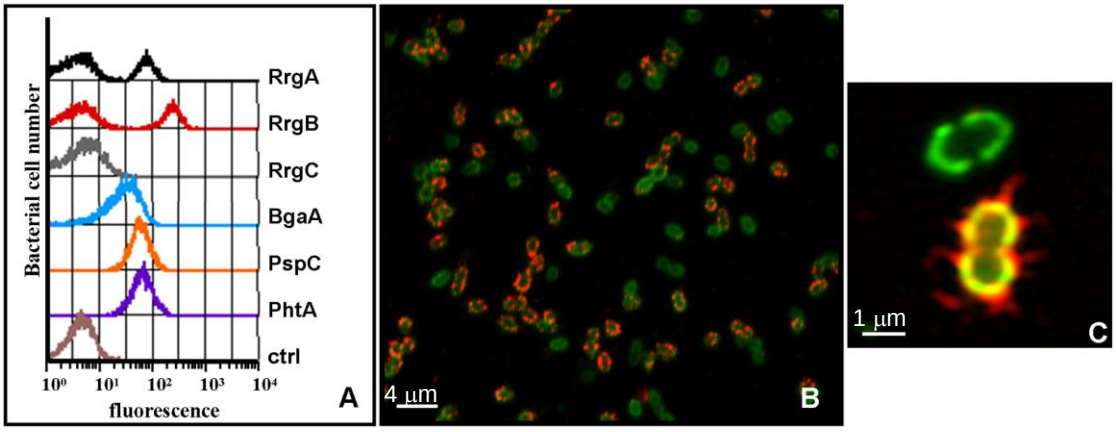

Figure 1.2 Pilus components display a biphasic expression pattern. A) TIGR4 bacteria were labeled with anti-RrgA, RrgB clade I, RrgC, BgaA (beta-galactosidase), PhtA (pneumococcal histidine triad protein A) or PspC (pneumococcal surface protein C) primary antibodies (1:400 dilution), and with FITC anti-mouse IgG secondary antibodies (1:100 dilution). Bacterial staining was analyzed by flow cytometry (FACS-Calibur). Sera of mice immunized with PBS were used as negative control. **B**,**C**) TIGR4 bacteria were processed for immunofluorescence, stained with mouse anti-RrgB antibodies (1:2000 dilution) (red) and with *S. pneumoniae* anti-capsular antibodies (Omniserum 1:2000 dilution) (green). Imaging was performed with a confocal microscope.

While the bacteria were found to uniformly express PspC, PhtA and BgaA, the specific antibodies for RrgA and RrgB revealed the presence of two sub-populations, one expressing high levels of the pilus subunits (Pil+), while the other displayed a mean fluorescence intensity (MFI) comparable to the negative control (sera raised against an unrelated protein) (Pil-). Interestingly, the analysis of bacteria labeled with anti-RrgC antibodies revealed a single homogeneous population with an MFI similar to the negative control, confirming that, in intact bacteria, RrgC is not exposed on the bacterial surface [3]. To support the data obtained by flow cytometry, the bacteria

were incubated with the antisera and then analyzed by immunofluorescence. As shown in Figure 1.2B (and in the enlargement of Figure 1.2C), bacteria were uniformly stained by anti-capsular antibodies, whereas the RrgB pilus specific signal was present only in a subset of bacteria (Pil+) and undetectable in the others (Pil-).

S. pneumoniae pilus expression is not correlated with genotype, clade type and serotype

A worldwide collection of 1366 strains of *S. pneumoniae* (Figure 1.3) including both carriage, AOM (acute otitis media) and invasive clinical isolates from different geographical origins, were characterized for serotype (with conventional methods) and sequence type (ST), for the presence of the PI-1 and for PI-1 clade. Multi Locus Sequence Typing (MLST), Clonal Complex (CC) assignment by E-BURST analysis, and PI-1 detection were performed as previously described [62].

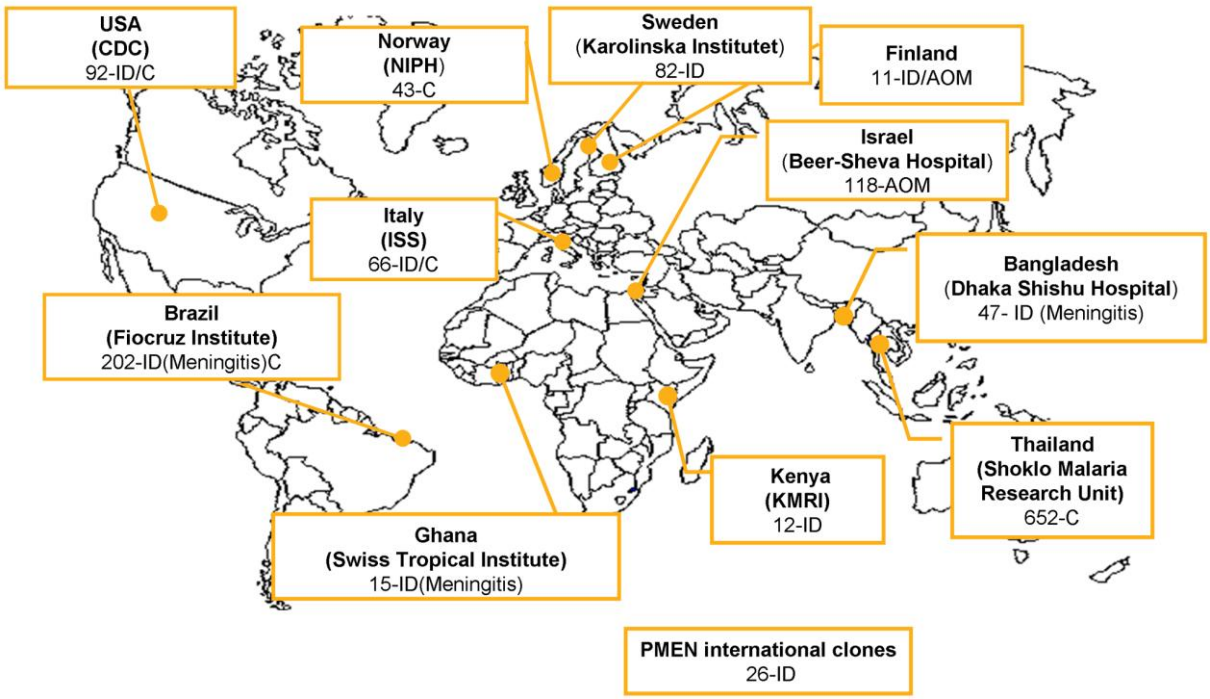

Figure 1.3. Composition of the Novartis _S. pneumoniae_ global collection. Geographical origin, number of strains and disease outcome are indicated (ID: invasive disease, C: carriage, AOM: acute otitis media).

Given the biphasic expression pattern observed in the TIGR4 strain, a panel of 139 *S. pneumoniae* strains, randomly selected among those that resulted PI-1 positive within the entire collection (436), were analyzed for pilus-1 expression by FACS analysis. All of the selected strains revealed a biphasic pilus expression, with the proportion of Pil+ bacteria ranging from 5 to 95%. As presented in Figure 1.4 for a selection of strains, there was no correlation between the ratio of Pil+ versus Pil- bacteria (pilus expression ratio) and the genotype, clade type and serotype. In addition, there was no association with the disease outcome of the isolates, as the

pilus expression ratio was heterogeneous in invasive, carriage and otitis media strains from the same or different geographical origins (data not shown).

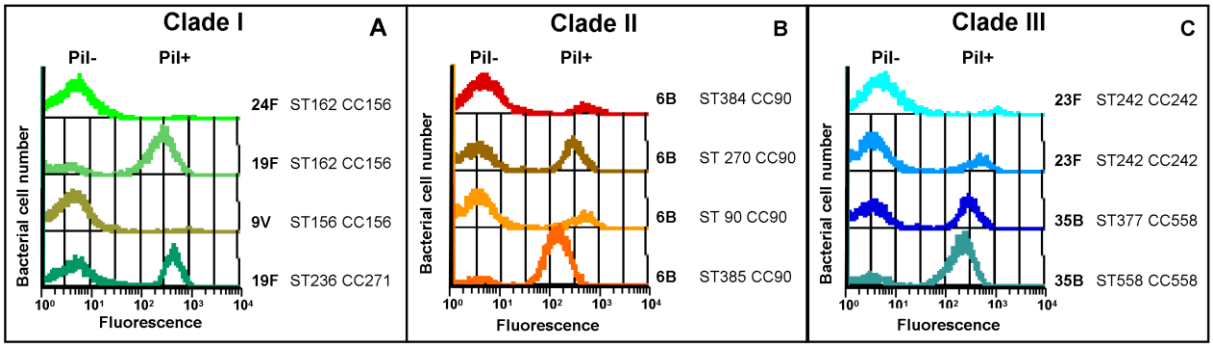

Figure 1.4 Pilus expression ratio is not correlated with serotype, genotype or clade type. Bacteria containing either PI-1 clade I (**A**), clade II (**B**) or clade III (**C**), were labeled with clade specific anti-RrgB antibodies (1:400 dilution) and FITC anti-mouse IgG secondary antibodies (1:100 dilution). Pilus-1 expression was then analyzed by flow cytometry (FACS-Calibur).

A detailed analysis of the PI-1 sequence revealed the presence of variable short nucleotide repeats in the intergenic regions upstream RrgA (2-6 CTATA repeats) and RrgB (poly-A tract containing 5 or 6 adenosine nucleotides). Since in other organisms the presence of different repeat numbers in the promoter region accounts for variable expression of the downstream gene [88-90], we hypothesized that these sequence repeats could act as regulation signals for RrgA and RrgB-RrgC expression. However, we found no correlation between the number of repeats and the pilus expression ratio in the 44 strains analyzed [91] (data not shown).

Pilus expression ratio remains unchanged growing the bacteria under different conditions

The identification of factors able to modulate pilus-1 expression *in vitro*, and, in particular, to enhance the pilus expression ratio could facilitate the understanding of the pilus role *in vivo*. Therefore, three *S. pneumoniae* strains (TIGR4, 6B Finland 12 and 35B SME 15) were grown under several growth conditions and pilus-1 expression was evaluated by flow cytometry.

In detail, pilus expression analysis was performed on bacteria grown in rich media (THYE, Tryptic Soy Broth, Brain Hearth Infusion broth) and in a chemically defined minimal medium (CDM) [92] alone or supplemented with $MnSO_4$ (1 mM), $FeCl_3$ (≥ 50 mM) or Fetal Bovine Serum (20%). Bacteria were also grown until different growth phases (A_{600} ranging from 0.1 to 1.2) (Figure 1.5), at different pH values (5.5, 6.4, 8.4) or in the presence of different O_2 concentrations (air condition or 5% CO_2).

In all the conditions tested the analyses performed by using flow cytometry revealed that pilus-1 expression remained unchanged.

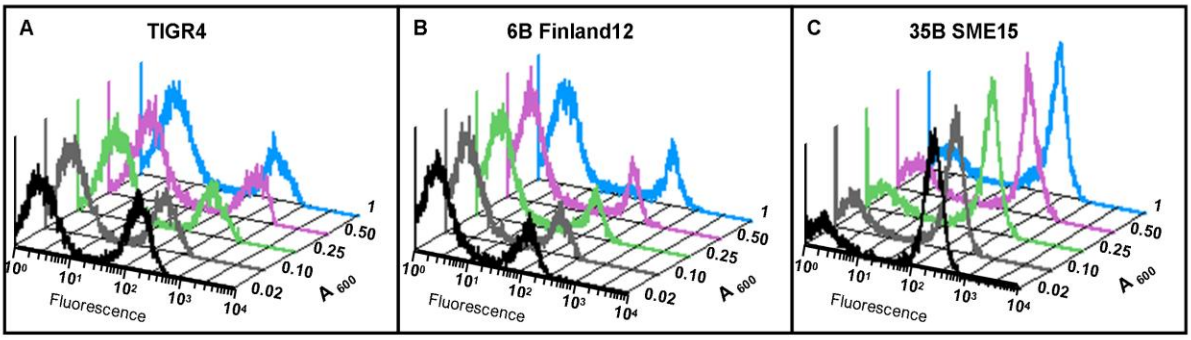

Figure 1.5. Pilus expression ratio is constant at different growth phases. Bacteria expressing pilus-1 of clade I (**A**, TIGR4), clade II (**B**, 6B Finland 12) or clade III (**C**, 35B SME15) were grown in THYE at different A_{600} (0.02, 0.1, 0.25, 0.5 and 1) and labeled with clade specific anti-RrgB antibodies (1:400 dilution), and FITC anti-mouse IgG secondary antibodies (1:100 dilution). Pilus-1 expression was then analyzed by flow cytometry (FACS-Calibur).

Only the addition of 5-10% fresh sheep blood to CDM medium increased the pilus-1 expression ratio to variable extents in TIGR4. As shown in Figure 1.6, when TIGR 4 bacteria were grown in presence of blood and than analyzed by flow cytometry, the proportion of Pil+ bacteria increase of about 30% with respect to the control (bacteria grown in the absence of blood), with the consequent detriment of the Pil- bacteria. The increase observed in wild-type TIGR4 was not reproducible in the other two strains.

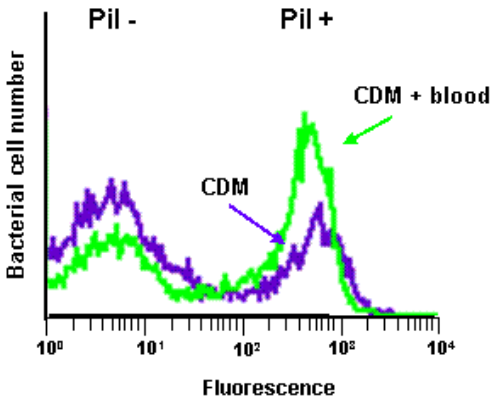

Figure 1.6. TIGR4 pilus-1 expression increases in presence of blood. TIGR4 bacteria were grown in CDM alone (blue line) or supplemented with 10% sheep blood (green line) until A_{600} 0.25 (mid log phase) and labeled with clade specific anti-RrgB antibodies (1:400 dilution) and FITC anti-mouse IgG secondary antibodies (1:100 dilution). Pilus-1 expression was then analyzed by flow cytometry.

Two *S. pneumoniae* sub-populations enriched in Pil+ or Pil- bacteria can be separated by colony selection

In order to verify if Pil+ and Pil- bacteria after duplication maintain their original pilus expression phenotype, bacteria, following a sonication step, were grown on a plate as single colonies and then analyzed for pilus expression. As shown in Figure 1.7A,

when colony blot was performed with anti-RrgB antibodies, the colonies displayed different RrgB intensities, but none were RrgB negative.
Colonies showing differential RrgB staining were selected and re-grown. Analysis performed by flow cytometry revealed that the majority of the colonies gave rise to populations with a ratio of pilus expression similar to the original strain. However, some colonies gave rise to either mostly Pil+ or Pil- sub-populations, defined as H (high pilus expression) or L (low pilus expression) sub-populations (Figure 1.7B).

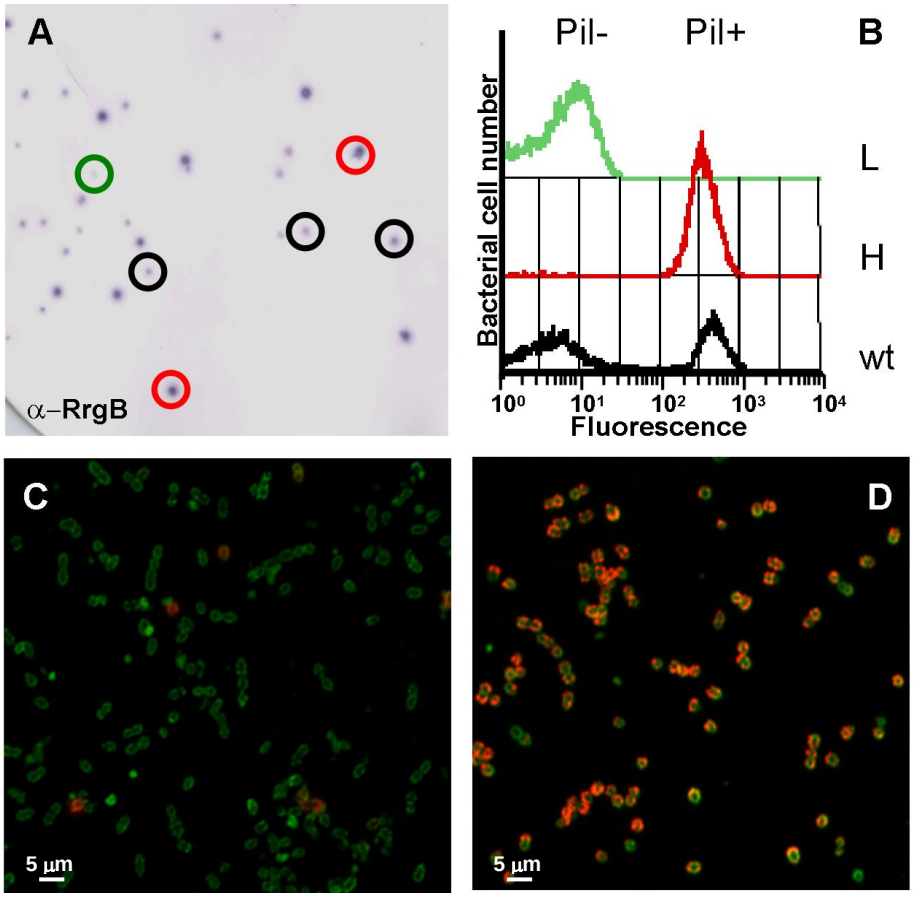

Figure 1.7. Stable separation of enriched high (H) and low (L) pilus-1 expressing sub-populations. A) TIGR4 pilus-1 expression was revealed on single colonies by colony immunoblot using anti-RrgB clade I antibodies (green, red and black circles correspond to colonies displaying low, medium or high RrgB specific signal intensities, respectively). Bacteria recovered from the growth of different colonies were stained with anti-RrgB clade I antibodies and analyzed by flow cytometry (**B**). The bacteria expressing (Pil+) and non-expressing (Pil-) the pilus-1 are indicated in the L (green) and H (red) enriched sub-populations, and in the wt (black). H and L sub-populations were stained for immunofluorescence (**C** and **D**). Bacteria were incubated with mouse anti-RrgB antibodies (1:2000 dilution) (red) and with *S.pneumoniae* anti-capsular antibodies (Omniserum 1:2000 dilution) (green). Imaging was performed with a confocal microscope.

Despite numerous attempts, completely positive or negative sub-populations were never obtained, as there were always Pil+ and Pil- in the L and H sub-populations, respectively (Figure 1.7C and 1.7D). Notably, the two enriched sub-populations (H

and L) were stably maintained after consecutive re-growths and long-term storage at -80°C.

PI-1 components expression is undetectable in pilus-1 negative bacteria

The *S. pneumoniae* pilus-1 polymerization is a complex and tightly coordinated process, not yet fully elucidated, requiring the simultaneous involvement of pilus components and bacterial sortases [57,93,94]. Following this observation, and in order to gain more insight into the pilus polymerization mechanism, the expression levels of the single PI-1 components were evaluated in Pil- bacteria.

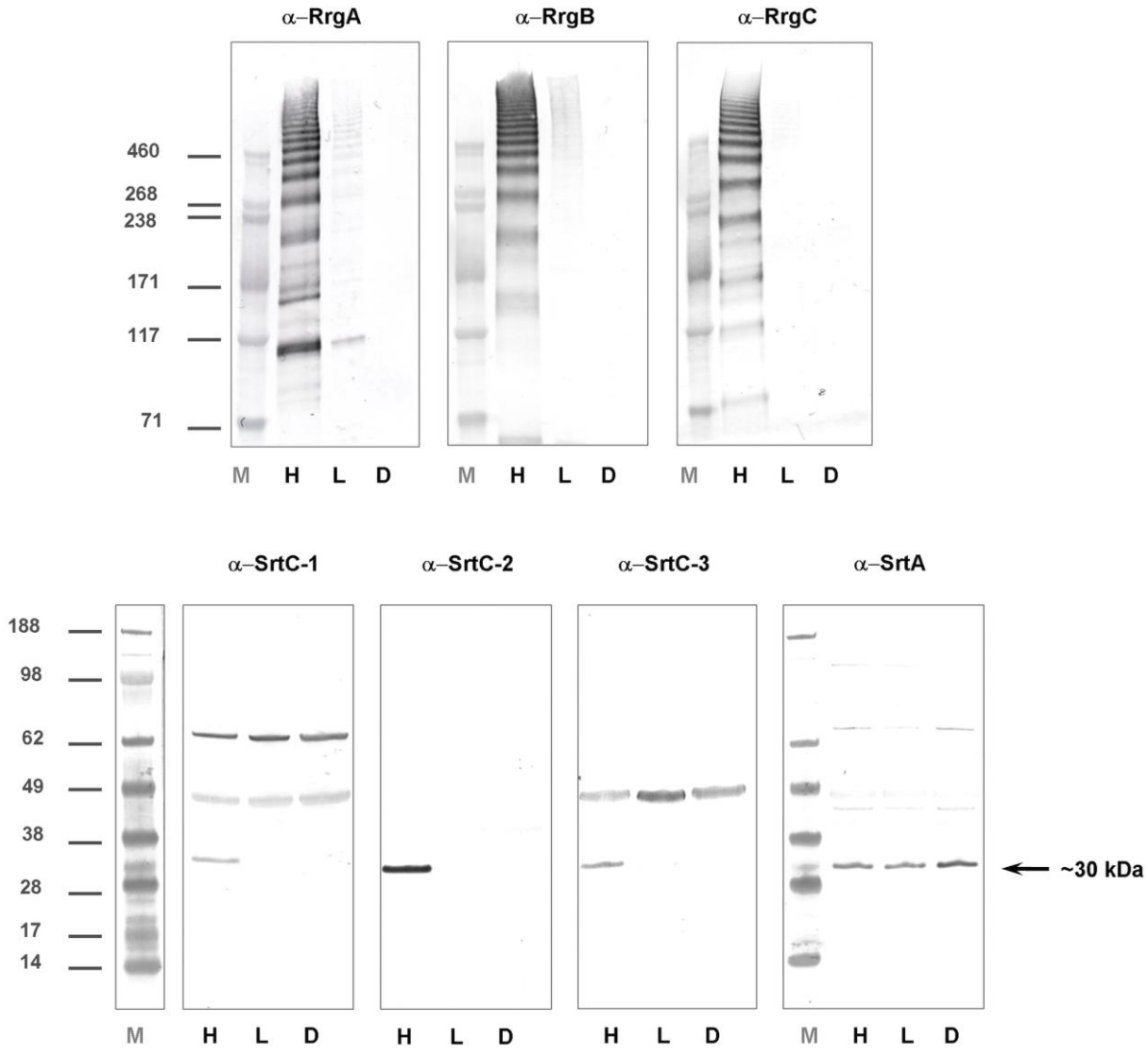

Figure 1.8. PI-1 encoded proteins are not expressed in RrgB negative bacteria. Western Blot analysis performed on whole bacterial lysates of TIGR4 H (H), L (L) or TIGR4 L depleted of RrgB positive bacteria (D), using polyclonal mouse antisera against RrgA, RrgB, RrgC (see High molecular weight ladders), SrtC-1, SrtC-2 ,SrtC-3 (see bands indicated by arrows) and SrtA (used as loading control).

In this regard, whole bacterial lysates of the TIGR4H and TIGR4L sub-populations, along with a TIGR4L sub-population further depleted of pilus positive bacteria (TIGR4 D) (see materials and methods) were probed with antibodies raised against RrgA, B and C and SrtC1, 2 and 3; antibodies raised against the SrtA, a transpeptidase not involved in pilus assembly, are used as experimental control. As reported in Figure 1.8, the impossibility to detect RrgA and RrgB on the surface of bacteria correlates with the lack of expression of all PI-1 components, both pilus-1 subunits and PI-1 sortases as demonstrated by the absence of both the typical pilus High Molecular Weight (HMW) ladder and protein monomers in TIGR4 D.

Biphasic pilus expression is not due to phase variation within the PI-1

To exclude that the biphasic pilus expression pattern was due to phase variation events at the level of the positive regulator (*rlrA*), or, more in general, to point mutations within PI-1, the islet was sequenced for three strains (TIGR4, 19FTaiwan14, OREP4) in the two enriched sub-populations (L and H) and in the wild-type. Neither alterations in the genomic sequence nor uncertainties in the chromatograms were observed, indicating that phase variation events within PI-1 are not responsible for the pilus-1 expression pattern.

Only PI-1 components are differentially regulated between the H and L pilus expressing sub-populations

To evaluate if pilus-1 expression was regulated at the transcriptional or translational level, total RNAs were extracted from the H and L sub-populations of five strains, TIGR4, 19F Taiwan 14, OREP4 (Clade I), 6BFin12 (Clade II) and 35B SME 15 (Clade III) (Figure 1.9). The expression profiles of the L versus the H pilus expressing sub-populations were directly compared by microarray analysis (see materials and methods). As shown in Figure 1.10A, the analysis of the $\log_2$ H/L signal intensity ratio curves for PI-1 components in the five strains revealed that all the PI-1 genes (including *rlrA*) were differentially regulated in all the strains tested. The different $\log_2$ signal intensity ratios observed among the isolates clearly depends on the ability to enrich in Pil+ and Pil- the H and L sub-populations, respectively. The strains 6B Finland 12 and 35B SME 15 showed the lowest $\log_2$ H/L signal intensity ratio, and were the isolates with the least enriched sub-populations (Figure 1.9).

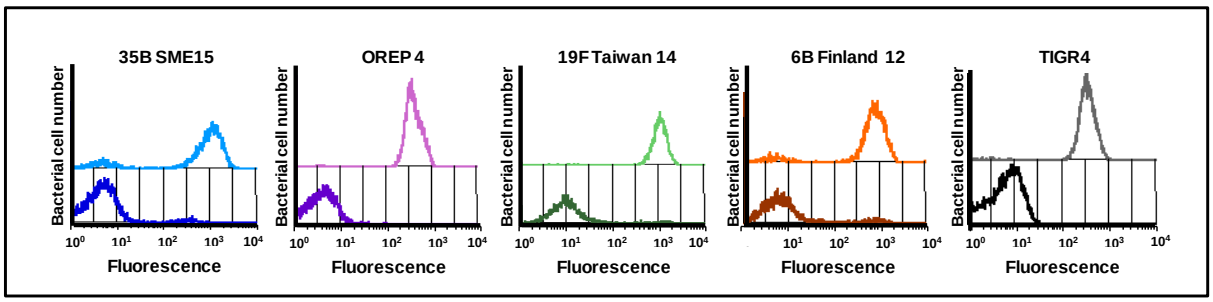

Figure 1.9. Pilus-1 expression profile of the H and L sub-populations. High and low pilus expressing sub-populations of strains TIGR4 (Clade I), 19F Taiwan 14 (Clade I), OREP4 (Clade I), 6B Finland 14 (Clade II) and 35B SME 15 (Clade III) were labeled with clade specific anti-RrgB antibodies (1:400 dilution) and FITC anti-mouse IgG secondary antibodies (1:100 dilution). Pilus-1 expression was then analyzed by flow cytometry (FACS-Calibur).

In addition, the log_2 ratio expression levels measured for the three sortases were consistently lower with respect to the pilus components and the *rlrA* regulator (Figure 1.10A).

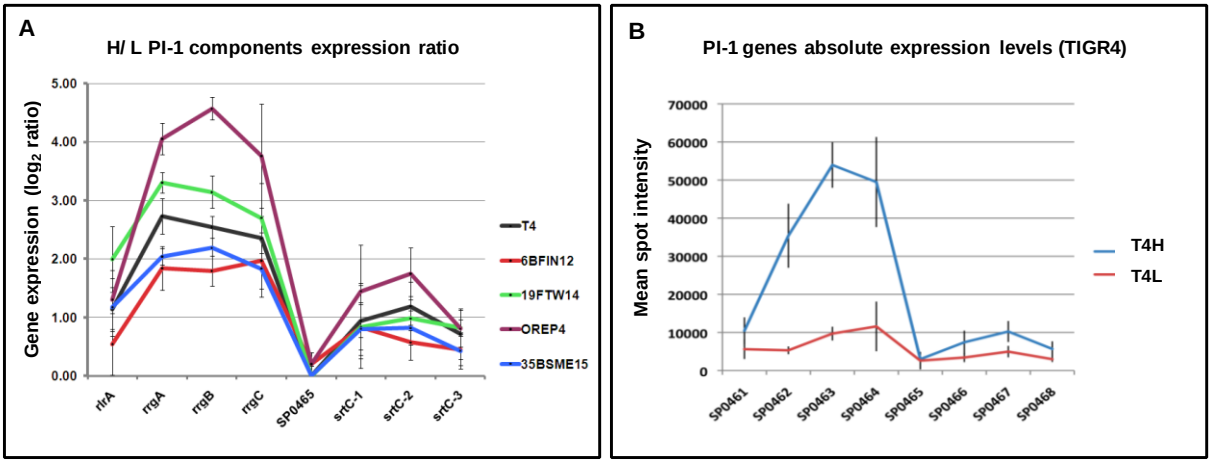

Figure 1.10. Pilus-1 expression is regulated at the transcriptional level.
A) Log_2 ratio values indicating the PI-1 genes differential expression in High vs. Low pilus expressing sub-populations in the five above mentioned strains, as measured by spotted DNA microarray analysis. The data are measures of relative gene expression during *in vitro* growth in liquid cultures. The values reported for each gene are the mean of all the spots and their replicates within the array and of two independent experiments (bars represent standard deviations). **B)** Absolute gene expression levels of PI-1 genes measured for TIGR4 high and low pilus expressing sub-populations by microarray hybridization. Absolute expression levels reported for each gene are the mean of all the spots and their replicates within the array and of two independent experiments (bars represent the obtained standard deviations).

This result is dependent on the different absolute expression levels measured for the PI-1 genes both within the H and the L pilus expressing sub-populations (sortase absolute expression levels were about four-five times lower than pilus components) as reported in Figure 1.10B for the TIGR4 strain. This observation suggests the presence of multiple promoters within PI-1, upstream *rlrA*, *rrgA*, *rrgB* and *srtC-1* as previously published [56]. In addition, the data obtained further confirm the absence of a mRNA coding for the protein annotated as hypothetical protein SP0465 [38].
The ratios of H/L obtained for the PI-1 genes with the microarray transcriptome analysis were further confirmed by qRT-PCR. The relative quantitation method (threshold cycle $\Delta\Delta CT$) was used to evaluate the quantitative variation in gene expression between the high and low pilus expressing subpopulations for the 5 different strains tested, relative to each gene examined. The *S16* and *GAPDH* (glyceraldehyde 3-phosphate dehydrogenase) amplicons were used as the endogenous control for the normalization of the data. (Figure 1.11)

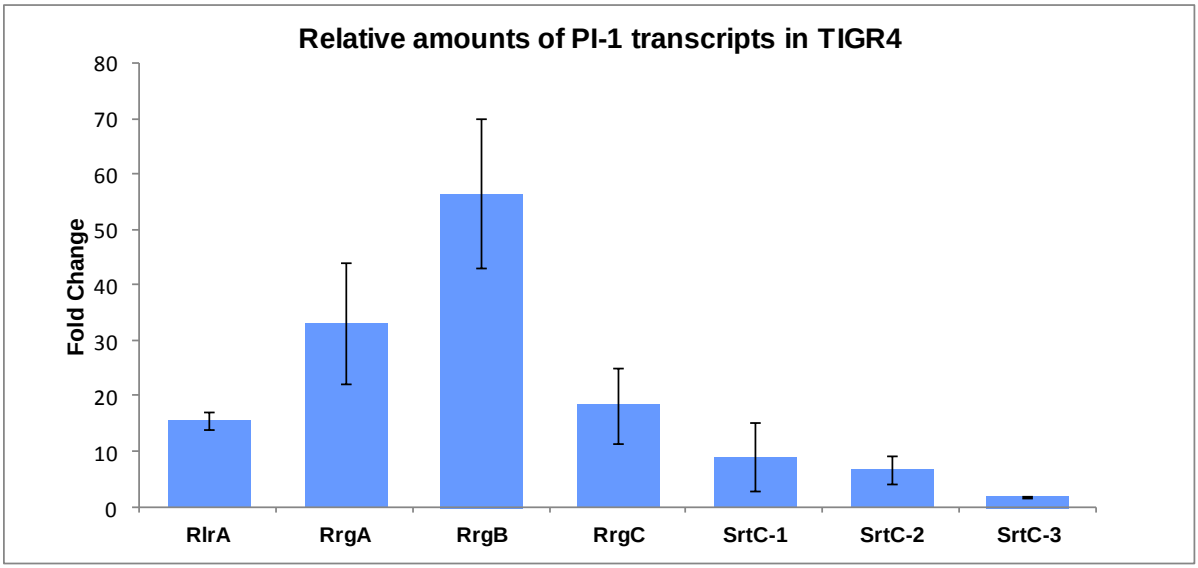

Figure 1.11. Relative increase of mRNA levels of all the pilus islet 1 components in the H sup-population with respect to those in the L sub-population for the TIGR4 strain. The values obtained were normalized for the expression levels of GAPDH and S16 for both the populations. Error bars indicate the standard deviation obtained combining three indipendent experiments. Similar results were obtained for the other 4 *S. pneumoniae* strains tested (OREP4, 19F Tw 14, 6B Fin 12, 35B SME15) (Data not shown).

The microarray data analysis comparing the expression profiles of H vs. the L pilus expressing sub-populations was then extended to all the genes conserved among the isolates, with the aim to identify genes possibly involved in the regulation of pilus expression. Interestingly, no other conserved genes, apart from PI-1 components, were differentially regulated in all the five strains tested (Figure 1.12A, 1.12B). Furthermore, the expression rate of the previously published negative regulators (MgrA, HK343, MerR, CbpS, TCS08, mntE, PsaR) [67,69-71] remained unchanged in the two sub-populations for all the strains tested (Figure 1.12C).
A possible reason that could explain why these genes were not up-regulated in the L sub-population has to be found in the experimental procedures used to determine the involvement in pilus expression regulation. In fact, the putative negative regulators have been identified generating and testing the Knock-out (KO) mutants of each gene with the assumption that under a particular set of conditions all cells were expressing genes in an approximately uniform manner. However, given the biphasic expression of the pilus, the colony selection of the KO mutants could also result in the fortuitous selection of colonies expressing the pilus at high or at a low level.

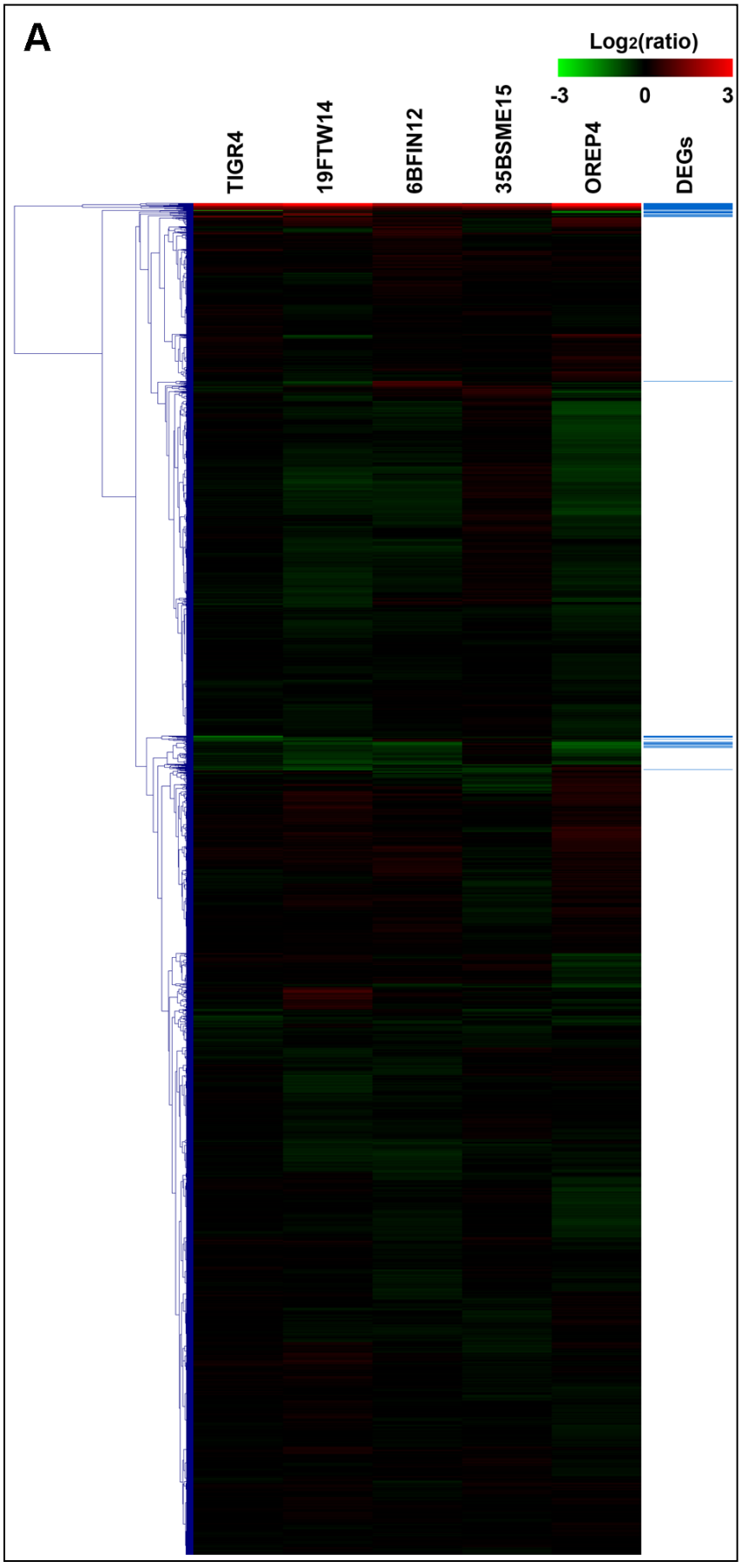
A
Log2(ratio)
-3
0
3
TIGR4
19FTW14
6BFIN12
35BSME15
OREP4
DEGs

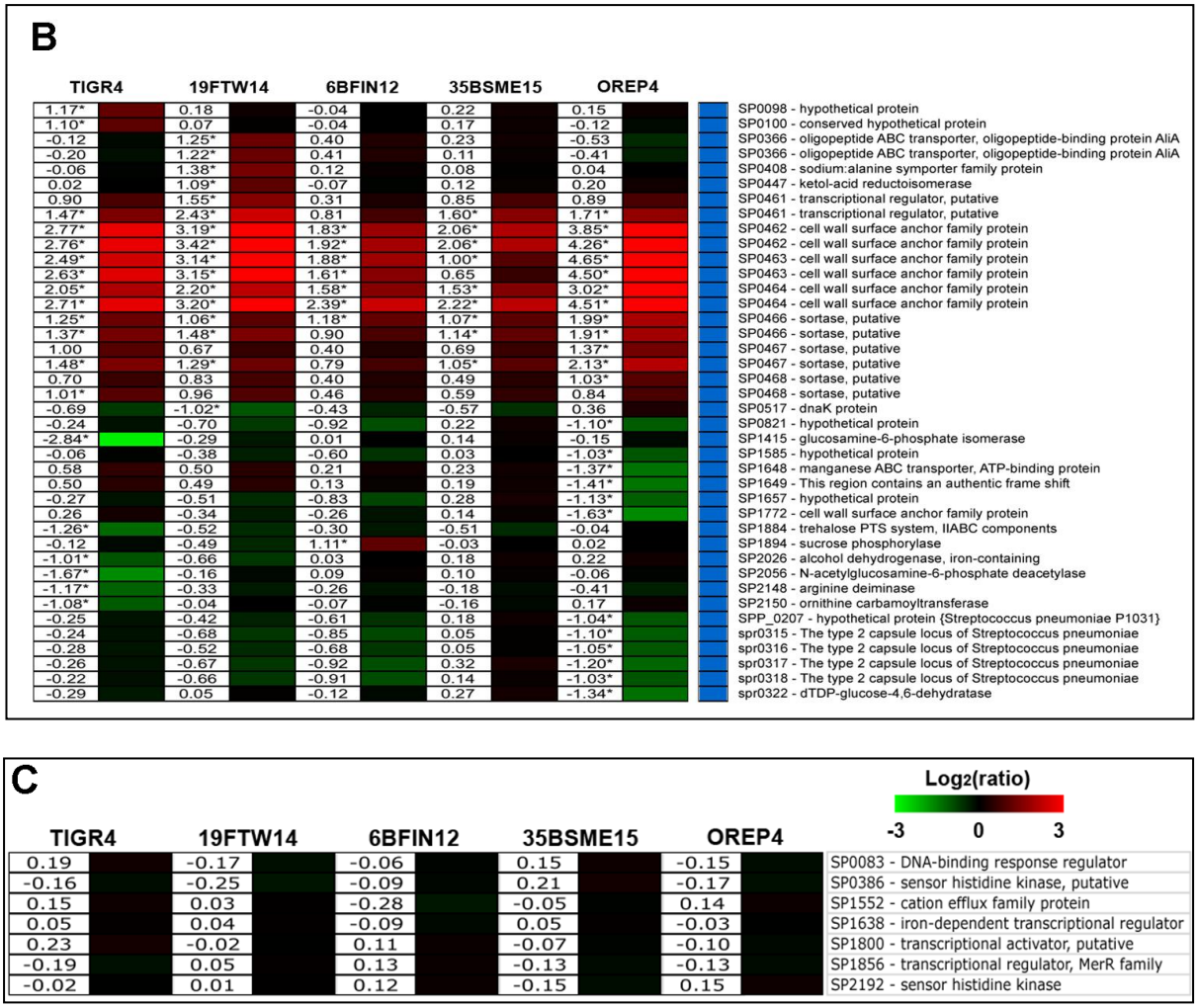

Figure 1.12. Microarray expression profile analysis of the high versus the low pilus expressing sub-populations. A) Hierarchical clustering representation of complete microarray data. Blue bars indicate genes significantly differentially regulated in at least one strain. **B)** Gene expression profiling of the genes differentially regulated in A. Numbers represent the $\log_2$ ratios. * P<0.05. **C)** Pilus-1 expression repressors reported in the literature are not differentially expressed**.** Gene expression profiling of high versus low pilus expressing sub-populations for strains TIGR4 (Clade I), 19F Taiwan 14 (Clade I), OREP4 (Clade I), 6B Finland 14 (Clade II) and 35B SME 15 (Clade III), by spotted DNA microarray analysis. The data are measures of relative gene expression in *in vitro* growth liquid cultures. Red and Green represent high and low experimental high/low pilus expression ratios for the 5 strains tested, respectively (see scale bar). The columns represent arrays of different strains (two hybridizations were performed with independently prepared samples), and the rows represent the genes. Red and Green correspond to high and low experimental high/low pilus expression ratios for the 5 strains tested, respectively (see $\log_2$ ratio scale bar).

Expression of the RlrA regulator in Pil- bacteria is sufficient to induce pilus polymerization

In order to better evaluate the regulation of the pilus locus and to check if the positive regulator RlrA is sufficient to induce the pilus polymerization, the effects induced by the expression of the pilus-1 components under the control of a constitutive promoter within Pil- bacteria, were evaluated. In detail, the pMU1328 plasmid, for which was already demonstrated the ability to epigenetically replicate in *S. pneumoniae* [95], was used to express in the L population of the TIGR4 strain the positive regulator RrlA, the backbone of the pilus RrgB and one of the sortases SrtC-2, required for the pilus assembly. The three genes, amplified from the genome were fused by overlap extention PCR to the erythromycin constitutive promoter (Pc), and than cloned into the pMU1328 plasmid (Figure 1.13). The TIGR4 L sub-population was transformed with a pMU1328 plasmid containing the *rrgB,* the *rlrA* or the *srt-C2* gene (pMU1328 empty vector was used as negative control).

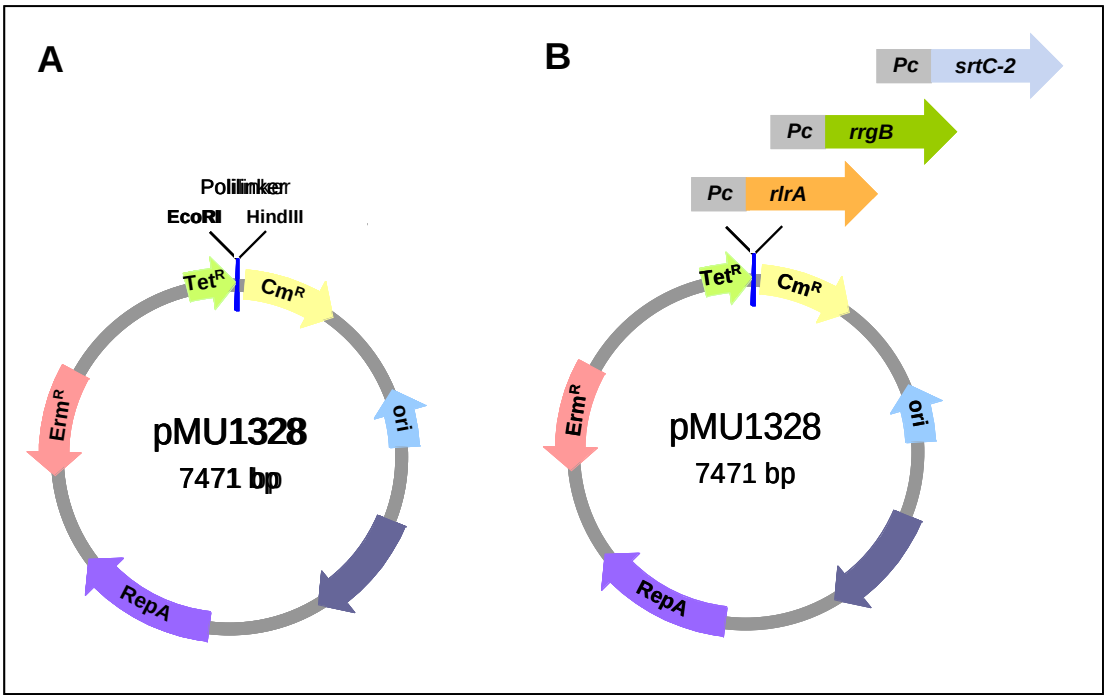

Figure 1.13. (A) Schematic representation of the "empty" plasmid pMU1328 and **(B)** the three constructs cloned in the pMU1328 and used to constitutively express RrgB, RlrA and Srt-C2 in the TIGR4 L population.

Following transformation, bacteria were studied by FACS analysis (data not shown), western blot (Figure 1.14) and immunofluorescence (Figure 1.15). WB analysis performed using polyclonal mouse antisera against RrgB and SrtC-2 on whole bacterial lysates showed that SrtC-2 is expressed in the TIGR4L sub-population when TIGR4L is transformed with *pMU1328 Pc_srtC-2* and its expression does not influence RrgB expression. Moreover the over-expression of SrtC-2 in TIGR4 PI-1

mutant lacking the three sortases and so expressing RrgB in a monomeric form (TIGR4Δ*srtC-1-3*) restores RrgB polymerization. (Figure 1.14)

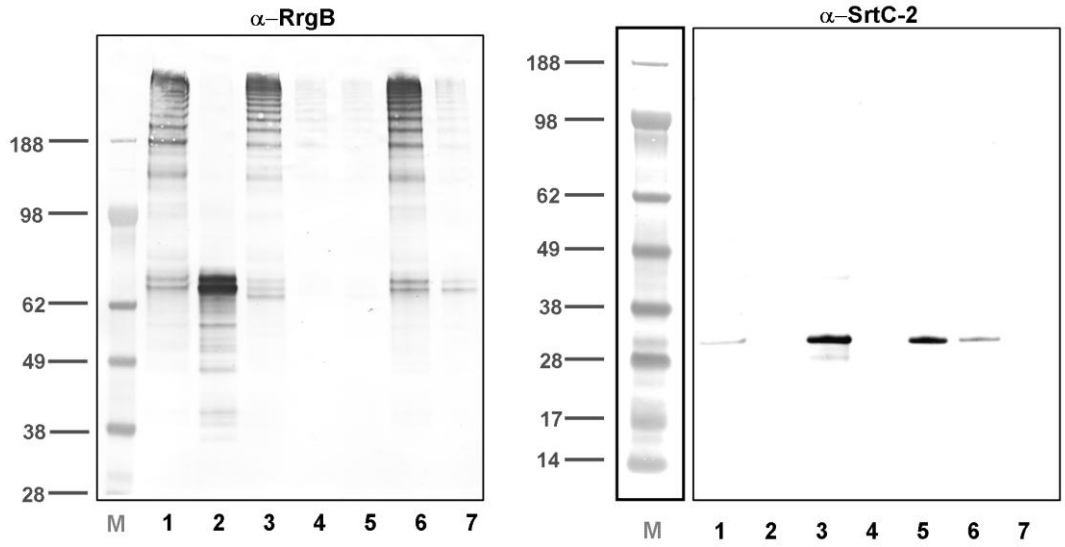

Figure 1.14. SrtC-2 is expressed and functional in bacteria transformed with *pMU1328-Pc-srtC-2*. WB analysis performed using polyclonal mouse antisera against RrgB and SrtC-2 on whole bacterial lysates shows that: SrtC-2 is expressed in the TIGR4L sub-population when TIGR4L is transformed with *pMU1328 Pc_srtC-2;* SrtC-2 expression does not influence RrgB expression; and the over-expression of SrtC-2 in TIGR4Δ*srtC-1-3* expressing RrgB in a monomeric form, restores RrgB polymerization. Samples were loaded as follows: TIGR4 wt (lane 1), TIGR4Δ*srtC-1-3* (lane 2) and TIGR4Δ*srtC-1-3* transformed with *pMU1328-Pc-srtC-2* (lane 3), TIGR4L transformed with *pMU1328* empty vector (lane 4), *pMU1328-Pc-srtC-2* (lane 5), *pMU1328-Pc-rlrA* (lane 6), or *pMU1328-Pc-rrgB* (lane 7).

In the same way, the performed immune-fluorescence analysis showed that the ratio of bacteria expressing the pilus was not altered upon transformation with the pMU1328 empty plasmid (Figure 1.15 panels A-C), while the expression of RlrA induced polymerization of the pilus in 100% of the *S. pneumoniae* population (Figure 1.15 panels D-F). Interestingly, following the expression of RrgB or SrtC-2 (Figure 1.15 panels G-I and J-L, respectively) the proportion of bacteria able to polymerize the pilus on their surface did not change when compared to the control. In detail, when RrgB was over-expressed, RrgB was localized in clusters on the Pil- bacterial surface (Fig. 1.15 panels G-I), but remained un-polymerized (Fig. 1.14) due to the lack of expression of the pilus specific sortases. On the other hand, the expression of a functional SrtC-2, which in the presence of the RrgB monomer is sufficient to induce RrgB polymerization (Fig. 1.15 panels J-L and Fig. 1.14), did not induce in the T4L sub-population any change in pilus components expression or pilus polymerization.
Taken together, these data indicate that the expression of RlrA, unlike that of RrgB and SrtC-2, was sufficient to induce the expression of all the other PI-1 components.

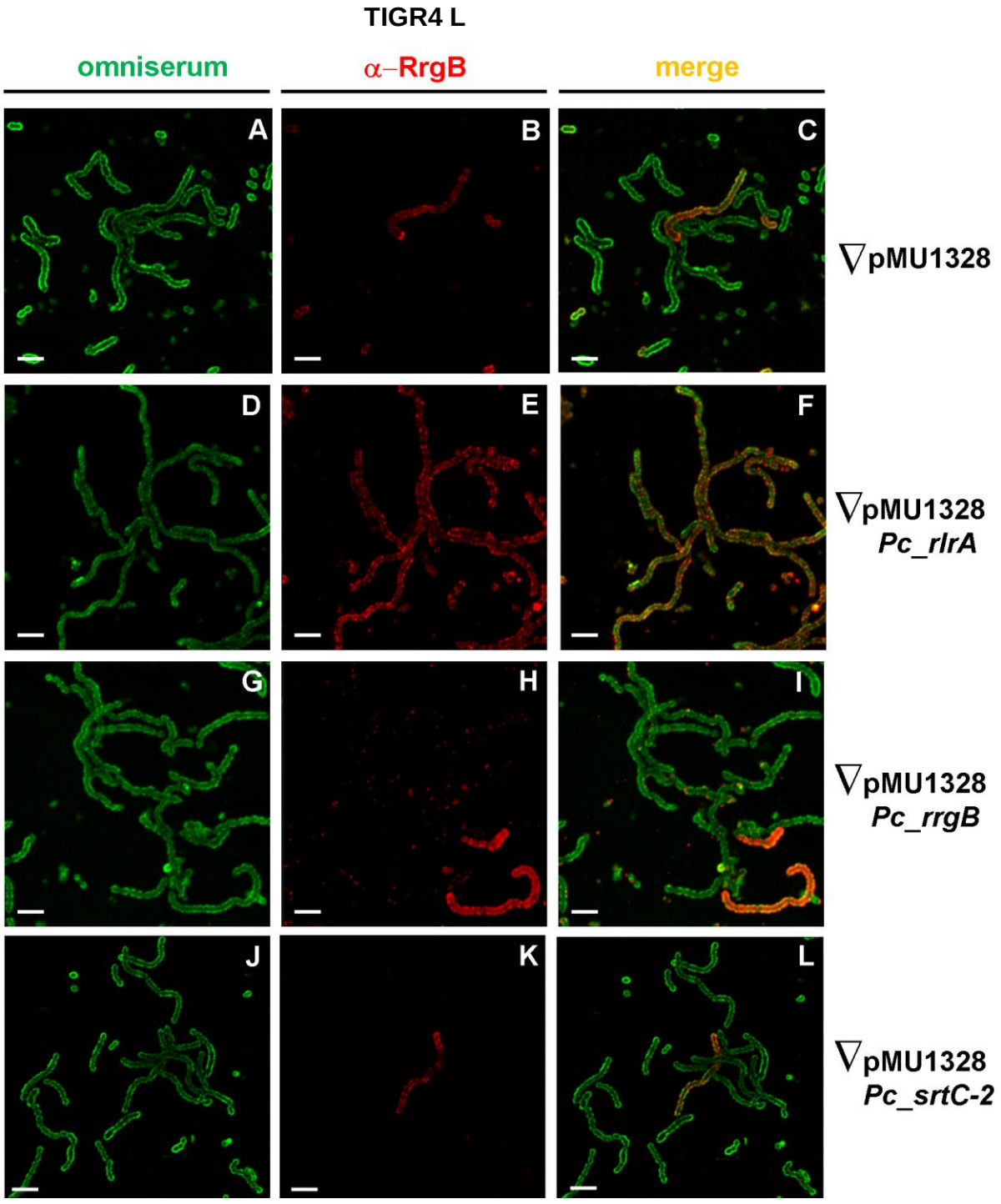

Figure 1.14. RlrA expression in pilus negative (Pil-) bacteria induces pilus polymerization. TIGR4 low pilus expressing bacteria (T4L) transformed with *pMU1328* (panels A-C), *pMU1328-Pc-rlrA* (panels D-F), with *pMU1328-Pc-rrgB* (panels G-I) or with *pMU1328-Pc-srtC-2* (panels J-L) were processed for confocal microscopy immuno-fluorescence analysis by incubating *S. pneumoniae* with anti-capsular antibodies (Omniserum 1:2000 dilution) (green, left panels) and mouse anti-RrgB antibodies (1:2000 dilution) (red, central panels). Right panels represent the merged signal of the left and central panels. Scale bar is 4 µm.

Materials and Methods

Bacterial strains and growth conditions

S. pneumoniae strains were routinely grown over night (ON) at 37°C in 5% CO_2 on Tryptic Soy Agar plates (TSA) (Becton Dickinson) supplemented with 10 mg/L colistine, 5 mg/L oxolinic acid, and 5% defibrinated sheep blood. Liquid cultures were carried out statically at 37°C under 5% CO_2 humidified atmosphere until A_{600} = 0.25 in Todd Hewitt Broth supplemented 0.5% (w/w) yeast extract (THYE) unless otherwise specified (Becton Dickinson).

Genomic DNA extraction and PI-1 sequencing

Genomic DNA extractions were performed from 50 mL of bacterial liquid culture by using the Wizard Genomic DNA purification kit following the manufacturer's instructions (Promega). To obtain PI-1 sequences, oligonucleotides matching on homologous regions inside the islands were designed and used to amplify and sequence the PCR products (Table 1.1). Sequences were obtained by use of an ABI 3730xl DNA Analyzer and assembled with Vector NTI 10.

Table 1.1. Oligonucletides used to amplify and sequence pilus-1 islets of clade I, II and III

Amplifications PI-1 clade I	Primer forward	Primer reverse
1_clade I	AACTGAATTGACACAACGTCTT	AGCGACAAGCCACTGTATCATATT
2_clade I	ACTTTCTAATGAGTTGTTTAGGCG	AGCGACAAGCCACTGTATCATATT
3_clade I	CTGGTCGATAACTCCTTCAATCTT	GTACGACAAAAGTGTGGCTTGTT
4_clade I	GAATGCGATATTCAGGACCAACTA	ATCTCACTGAGTTAATCCGTTCAC
5_clade I	TGTATACAAGTGTGTCATTGCCAG	TTGATAAATTCTCTTTGAAAGTG
6_clade I	GATGTTCAAACACCTTATCAGAT	TAAACATCTGGTAACTTTGCCCATCTC
7_clade I	ACTTTTACTCAGAAAGCTTTGATG	CATCGGATCTGTAATCGTACCATT
8_clade I	ATCCTGGTACGGATGAAGCAACGG	CATCTTCACCTGTTCTCACATTTT
9_clade I	GCGGTCTTTAGTCTTCAAAAACA	ACCTGTTAAGGTTGCTCCATCTTC
10_clade I	TTAACAGAAGCTGAAGGAGCTAA	TACATCATTAGATTCTGGTACTTC
11_clade I	TTAACAGATGCTGGTTTAGCTAA	ACGATTATCTTTATCATTAACTTT
12_clade I	GCTGGAGAAATTGCTGTCAAGAA	CTGTTTTGTTTCTTCTAAGTAATA
13_clade I	TTTGAATGGGTGGCAGATAAGGAC	CAAGAGAAAAACACAGAGCCATAA
14_clade I	TTGCTTAAGTAAGAGAGAAAGGAGC	CAGGAGTATAGTGTCCGCTTTCTT
15_clade I	GGCAATGTTGACTTTATGAAGGTG	TATCAGCATCCCTTTATCTTCAAAC
16_clade I	TGAGATTTTCTCGTTTCTCTTAGC	AATAGACGATGGGTATTGATCATGT
17_clade I	CCGACGAACTTTGATGATTTATTG	ACCAACAGACGATGACTGTTAATC
18_clade I	AATGACTTTGAGCCTGTCTTGAT	TTCTACAATTTCCTGGCCATTATC
19_clade I	GCCATTTGGATCAGCTAAAAGTT	TTTTTCAACCCACTACAGTTGACA
20_clade I	GCCATTTGGATCAGCTAAAAGTT	GCCACACAAGATGTTGATGCTTTT

Amplifications PI-1 clade II	Primer forward	Primer reverse
1_clade II	AACTGAATTGACACAACGTCTT	AGCGACAAGCCACTGTATCATATT
2_clade II	ACTTTCTAATGAGTTGTTTAGGCG	AGCGACAAGCCACTGTATCATATT
3_clade II	CTGGTCGATAACTCCTTCAATCTT	GTACGACAAAAGTGTGGCTTGTT
4_clade II	GAATGCGATATTCAGGACCAACTA	ATCTCACTGAGTTAATCCGTTCAC
5_clade II	TGTATACAAGTGTGTCATTGCCAG	CACTAACCGTCAACTCGATTCC
6_clade II	CATATGAACGTGTGATTCCAGAAG	GTTCAATTCCTCTGCATCTGAT
7_clade II	ACAGCTAAAACTTATAATTATAG	AATCGGTACTAGAGTTAAATGG
8_clade II	GGAGCAGAGAGCTAAATTAGTT	CGACCATTCGTGTCATAGAAT
9_clade II	GAGAAAAGGATTCGTGTAACAGGT	CATCTTCACCTGTTCTCACATTTT
10_clade II	GCGGTCTTTAGTCTTCAAAAACA	GTTAATACTTGCCCATTAGGACCA
11_clade II	TTTGACAACTAAAGATGGACTTA	ATCCATAGCTACATTATTCAAAGT
12_clade II	TATGTTGTTAATACAACAATTC	CCGACTTTCTCACCAGTCTTGGC
13_clade II	GAATACTCCAAAACCAACTAA	GCATCCAATTTTTGTTTTGCAGTT
14_clade II	CCACGTGTAAAAACATACGGT	CAAGAGAAAAACACAGAGCCATAA
15_clade II	TTGCTTAAGTAAGAGAGAAAGGAGC	CAGGAGTATAGTGTCCGCTTTCTT
16_clade II	GGCAATGTTGACTTTATGAAGGTG	TATCAGCATCCCTTTATCTTCAAAC
17_clade II	TGAGATTTTCTCGTTTCTCTTAGC	AATAGACGATGGGTATTGATCATGT
18_clade II	CCGACGAACTTTGATGATTTATTG	ACCAACAGACGATGACTGTTAATC
19_clade II	AATGACTTTGAGCCTGTCTTGAT	TTCTACAATTTCCTGGCCATTATC
20_clade II	GCCATTTGGATCAGCTAAAAGTT	TTTTTCAACCCACTACAGTTGACA
21_clade II	GCCATTTGGATCAGCTAAAAGTT	GCCACACAAGATGTTGATGCTTTT

Amplifications PI-1 clade III	Primer forward	Primer reverse
1_clade III	AACTGAATTGACACAACGTCTT	AGCGACAAGCCACTGTATCATATT
2_clade III	ACTTTCTAATGAGTTGTTTAGGCG	AGCGACAAGCCACTGTATCATATT
3_clade III	CTGGTCGATAACTCCTTCAATCTT	GTACGACAAAAGTGTGGCTTGTT
4_clade III	GAATGCGATATTCAGGACCAACTA	ATCTCACTGAGTTAATCCGTTCAC
5_clade III	TGTATACAAGTGTGTCATTGCCAG	TTGATAAATTCTCTTTGAAAGTG
6_clade III	GATGTTCAAACACCTTATCAGAT	TAAACATCTGGTAACTTTGCCCATCTC
7_clade III	ACTTTTACTCAGAAAGCTTTGATG	CATCGGATCTGTAATCGTACCATT
8_clade III	ATCCTGGTACGGATGAAGCAACGG	CATCTTCACCTGTTCTCACATTTT
9_clade III	GCGGTCTTTAGTCTTCAAAAACA	CCTGGATCTACGAAACCTGCTGCA
10_clade III	TTAATTATTCTGCCGCTTGTAA	TTAGTAATTGTAAGTTCACCG
11_clade III	GTATACTGCAACTTTAAATGCTC	GCTCATTCTTCACAACGAATTGTG
12_clade III	TGGAAAGATGAAAATCCAGAACCAA	TGGAATTGACCATCAGTGTTAGAA
13_clade III	ATGCAGCACAAGCTGTAGTAGAT	CAAGAGAAAAACACAGAGCCATAA
14_clade III	TTGCTTAAGTAAGAGAGAAAGGAGC	CAGGAGTATAGTGTCCGCTTTCTT
15_clade III	GGCAATGTTGACTTTATGAAGGTG	TATCAGCATCCCTTTATCTTCAAAC
16_clade III	TGAGATTTTCTCGTTTCTCTTAGC	AATAGACGATGGGTATTGATCATGT
17_clade III	CCGACGAACTTTGATGATTTATTG	ACCAACAGACGATGACTGTTAATC
18_clade III	AATGACTTTGAGCCTGTCTTGAT	TTCTACAATTTCCTGGCCATTATC
19_clade III	GCCATTTGGATCAGCTAAAAGTT	TTTTTCAACCCACTACAGTTGACA
20_clade III	GCCATTTGGATCAGCTAAAAGTT	GCCACACAAGATGTTGATGCTTTT

Animal immunizations
Animal treatments were done in compliance with the current law, approved by the internal Animal Ethics Committee (AEC numbers 200601, 200602, 200607 and 200911) and authorized by the Italian Ministry of Health. To generate sera against the specific proteins, purified recombinant proteins were used to immunize CD1 mice (20μg, three doses administered intra-peritoneally two weeks apart) or New Zealand rabbits of 2.5 kg body weight (100μg, three doses subcutaneous immunization two weeks apart) (Charles River Laboratory). Two weeks after the third immunization the animals were bled to obtain the sera. A rabbit polysaccharide multivalent antiserum (OMNIserum) was purchased from Staten Serum institute (Copenhagen).

Flow Cytometry on whole bacteria
Bacteria recovered from liquid cultures were stained with mouse antisera raised against pilus-1 components or surface exposed proteins (final dilution 1:300). After labelling with a secondary FITC conjugated antibody (Jackson Laboratories, dilution 1:100), bacteria were fixed with 2% paraformaldehyde. Bacterial staining was analyzed by using a FACS-Calibur cytometer (Becton Dickinson). Sera from mice immunized with PBS (Phosphate Buffered saline) plus adjuvant were used as a negative control. To test the pilus-1 expression in the presence of antibodies directed against RrgB, the bacteria were grown from an A_{600} of 0.01 to 1.2 in THYE supplemented with anti-RrgB rabbit sera at different dilutions (1:20, 1:50, 1:100). The growth was also carried out with rabbit anti-BgaA and with sera derived from animals immunized with adjuvant only (1:20, 1:50, 1:100), used as negative controls. When the desired A_{600} was reached, bacteria were processed for FACS analysis as reported above by using mouse anti-RrgA as primary antibody.

Immuno-fluorescence staining
Bacteria were harvested form a plate after an ON growth, washed with PBS pH 7.4, fixed with 2% (w/v) paraformaldehyde in PBS and then attached to polylysine-coated cover slips. After washing five times with PBS the slides were blocked for 15 min with PBS 3% BSA (w/v) (Bovine serum albumin) supplemented with 10% normal goat serum (Sigma). Primary and secondary antibodies conjugated with fluorochromes (Invitrogen) were diluted in PBS containing 1% BSA and incubated with the bacterial cells for 30 min at room temperature. Between incubation steps the bacteria were washed thoroughly with PBS. To reduce bleaching of the fluorochromes, the slides were mounted in Pro Long Gold antifade reagent with DAPI (Invitrogen). Images were obtained using a Carl Zeiss LSM 7MP Laser Scanning Microscope.

Depletion of RrgB positive bacteria
TIGR4 low pilus expressing bacteria were incubated with rabbit anti-RrgB antibodies (1:400 dilution) and then with goat anti-rabbit IgG biotin conjugated (Abcam, 1:1000 dilution) antibodies. Labelled bacteria were then incubated with Sepharose magnetic beads coated with streptavidin (Invitrogen) for 1 h at 4°C. Finally, RrgB positive bacteria attached to the Sepharose beads were removed by placing the tubes in a magnetic separation rack and recovering the bacterial suspension (containing RrgB negative bacteria).

SDS-PAGE and Western Blot analysis
SDS-PAGE analysis was performed on whole bacterial lysates using Nu-PAGE™ 4-12% Bis-Tris or 3-8% Tris-acetate gradient gels (Invitrogen) according to the

manufacturer's instructions. Hi-Mark™ pre-stained HMW protein standard (Invitrogen) served as a protein standard. Gels were processed for Western Blot analysis by using standard protocols. Mouse and rabbit antibodies raised against recombinant His-Tag-proteins were used at 1:3000 and 1:5000 dilutions, respectively. Secondary goat anti-mouse and anti-rabbit IgG alkaline phosphatase conjugated antibodies (Promega) were used at 1:5000 and the signal developed by using Western Blue Stabilized Substrate for Alkaline Phosphatase (Promega).

Colony immuno-blot

Bacteria were diluted on blood-agar plates to obtain isolated colonies. Before plating the bacteria underwent three sonication cycles (three cycles alternating 15 s of sonication and 15 s of pause at 4°C and 20 kHz, with a Vibracell sonicator, Sonic, at 50% of the maximum power), to ensure that the colonies were derived from single bacteria. The effectiveness of sonication was checked by inspection of the bacteria under the microscope before and after the treatment. Following ON growth, nitrocellulose membrane discs (Millipore) were gently placed on the plates, removed after 5 min, heat-treated with microwave irradiation (300 W for 2 min) and then processed for Western Blot analysis as described above.

RNA extraction

RNAprotect bacterial reagent (Qiagen) was added to 2 mL liquid bacterial culture (2:1) and the mixture vortexed for a few seconds. After 5 min at room temperature the bacterial pellet was recovered by centrifugation (5000 *g*, 10 min), resuspended in 1 mL prewarmed (100°C) SDS solution (SDS 2%, 16mM EDTA pH 8.00) and incubated at 100°C for 2 min, under vigorous shaking. Prewarmed (65°C) acid phenol (1 mL) was then added to the samples, that were incubated for 5 min at 65°C under shaking, and then extracted twice with 1 mL Phenol/Chloroform/Isoamyl alcohol (25:24:1) and once with 1 mL Chloroform/Isoamyl alcohol (24:1). The aqueous phase containing the RNA was recovered by sample centrifugation and the RNA precipitation was carried out by adding 2.5 volumes of ethanol and 1/10 vol of Na Acetate 3M (pH 4.5). After 2 h of incubation at -20°C and centrifugation (16000 *g*, 20 min), the RNA pellet was recovered and purified by using RNeasy Mini Kit (Qiagen) according to manufacturer's instructions. Before the final elution, all RNA samples were subjected two times to a DNase I treatment (Qiagen). Total RNA integrity check was performed on agarose gel.

Microarray design

Gene expression analysis was performed by using a custom made microarray based on dsDNA fragments (200-500 bp), PCR-amplified on TIGR4 genomic DNA. In the design were also included amplicons matching on specific genes selected from additional five *S. pneumoniae* strains (R6, G54, 70585, P1031 and Taiwan-19F 14). Genes were considered non-specific if they had a corresponding homologous gene in TIGR4 with an identity greater than 80% on at least 80% of the gene length. An additional stringency criterion was applied for the gene selection from 70585, P1031 and Taiwan-19F 14 genomes: genes matching with the amplicons already designed on TIGR4, R6 and G54, having an identity of 87% on at least 70 bp of length, and having lengths shorter than 180 bp, were removed. Furthermore, amplicons corresponding to the genes present in two D39 strain plasmids (pDP1 and pSMB1) and in the serotype 2 capsule biosynthesis locus (D39), as well as those

corresponding to the PI-1 genes specific for Clade II (Finland 6B-12) and Clade III (Taiwan 23F-15) were added.
Amplification primers were designed by *Primer3* software (v. 1.0b) [96]. Usually, one pair of primers was designed for each gene; in the case of 337 genes in TIGR4 and 19 genes in R6, multiple primer pairs (ranging from 2 to 7) were designed on the same gene. The resulting coverage in TIGR4 is of 2121/2236 (94.6%) predicted open reading frames (25 fragments cover 2 or more genes that are contiguous, extremely similar or paralogous). For the other *S. pneumoniae* strains, the primer pairs designed on specific genes cover the following number of open reading frames: 144 (R6), 22 (G54), 126 (70585), 120 (P1031), 114 (19F Taiwan 14), 5 (D39 pDP1 and pSMB1) 15 (D39 capsule), 6 (PI-1 Clade II and Clade III). The possible resulting coverage was rechecked by sequence homology between the amplicons and the predicted genes in the additional *S. pneumoniae* strains, requiring at least 70 bp of alignment with an identity of at least 87%. The resulting coverage, based on NCBI annotations is: R6 1879/2043 (92%), G54 1911/2047 (93.4%), 70585 1890/2323 (81.4%), P1031 1955/2254 (87.8%), 19F Taiwan 14 1917/2205 (86.9%).
PCR amplifications were performed on the genomic DNAs (prepared as described above), purified using QIAquick-96 PCR purification plates (Qiagen), eluted in ddH2O before to be checked by gel electrophoresis on a 96-well format and finally diluted with DMSO (dimethyl sulfoxide) 50% (vol/vol). All the PCR-amplified fragments were spotted in quadruplicate by using a Microgrid II spotter (Arrayit Corporation) on Type-VII* aluminium-coated mirrored slides (ArrayJet). Two hundred and one spots were spotted with a higher number of replicas (varying from 8 to 32). Negative controls, such as PCR-processed empty buffer (spots indicated as 'H2O') and spotter-processed empty buffer (spots indicated as 'empty'), were also included.
The chip layout was submitted to the EBI ArrayExpress and is available with the identifier A-MEXP-2001

Probe labeling and microarray hybridization

For RNA labeling, 1 μg total RNA, prepared as described above, was reverse transcribed for two hours at 42°C using Super Script II Reverse Trascriptase (Invitrogen), random nonamer oligonucleotides (GE Healthcare) and the fluorochromes Cyanine3-dCTP or Cyanine5-dCTP (GE Healthcare). Following the reverse transcription reaction, labeled cDNA was treated with RNAse (RNAse One, Promega and RNAse H, Invitrogen) at 37°C for 30 min and than purified by using the Qiaquick PCR purification kit (Qiagen), according to the manufacturer's instructions. The incorporation efficiency of the Cy3 or Cy5 dCTP was measured by NanoDrop analysis. Following heat denaturation (2 min at 95°C), equal amounts of Cy5- and Cy3-labeled cDNAs were used to hybridize microarray slides (over night incubation at 42°C) in microarray hybridization buffer (GE Healthcare) and 50% formamide. Slides were then washed once for 5 min in SSC solution (150mM NaCl and 15mM Sodium Citrate) 0.2% SDS, and twice for 10 min in 0.1x SSC 0.2% SDS. Finally, the slides were dipped 5 times in 0.1X SSC, 2 times in water and then dried with nitrogen. Images were acquired with PowerScanner (Tecan) at 5 and 10 μm resolution and analyzed with Genepix 6.1 (Axon laboratories).

Microarray data analysis and RT-PCR

Data normalization was performed with the application *BASE2* [97] by using a lowess transformation, as implemented in the *R* software environment, by the *loess* function after an intra-slide median centering and a low intensity spot correction (if the

average spot intensity was less than one standard deviation of the background signal the intensity spot was corrected to the same value of one standard deviation of the background signal).
Differential gene expression was assessed by grouping all $\log_2$ ratio values corresponding to each gene within experimental replicas and spot replicas, and comparing them against the zero value by Student's t-test statistics (one tail). Genes having a t-test *p-value* < 0.05 were usually accepted as differentially expressed. Type-I error rate was estimated by *q-value* method [98]. A $\log_2$ ratio threshold filtering was also applied, and genes with a $\log_2$ ratio > 1 or < -1 were accepted and classified as being significantly changed. The threshold was inferred from $\log_2$ ratio distribution widths (standard deviation between 0.25 and 0.44 and an average of 0.31) observed in each sample.
Hierarchical clustering was applied as implemented by *MeV* software (v. 4.2) [99] using the Euclidean metrics and the average agglomeration method.
Microarray data were submitted to the EBI ArrayExpress and are available with the identifier E-TABM-1154.
Gene expression changes were validated by quantitative real-time PCR (qRT_PCR) analysis. The primers used for qRT-PCR analysis are reported in Table 1.2. The qRT-PCR reaction was performed in a Light Cycler 480 II (Roche) by using the Light Cycler RNA amplification kit SYBR green I (Roche) according to the manufacturer's instructions. For each gene, duplicate reactions were performed on the RNA samples isolated from separate assays. Analyses were performed with Light Cycler® 480 SW 1.5 (Roche).

Table 1.2. Oligonucleotides used in qRT-PCR to validate microarray data

Gene name	Forward primer	Reverse primer
rlrA	TTCAATCTTCTGCTCAGTCATC	TACTTAGAGCCACATGCCAACA
rrgA	AACATAAAACCTGGGACATACAC	CGATTCCATATTGGTTATCATCC
rrgB clade I	CACTTGCTAATTATGCAACAGCA	ATGTCTTGGTCAATGTCAAATCG
rrgB clade II	TCAGATGAAATGACAGAAGGTC	CTGTCCCATGTCTTAGTTACTG
rrgB clade III	TCAGATGAAATGACAGAAGGTC	GCATCAGCCCATGTTTTAGTAA
rrgC	GAGATGACCTTCCTTGAGAATCA	GTATTCTCCAATCAAGGGAACCT
srtC-1	AGGCTGACATTGATGAACGAATG	GTCAAATCCGTAAACATCTTAGC
srtC-2 clade I and III	TGATCACTGCTCACAGAGGATT	AATAACCACAACCAGAATTGCC
srtC-2 clade II	GTTGTCACTGCTCATAGAGGATT	AATAACCACAACCAGAATTGCC
srtC-3	GGATCAGCTAAAAGTTGGAGAT	AACCATTGAGAGGTTGCAACAC
S16	AGCAGTAGGGAATCTTCGGCAAT	AAGGGTCTAACACCTAGCACTC
GAPDH	CGACTGGGCTACTGACGGTGTAG	GCGAGCACGGCGAAGGTCACCA

Generation of a TIGR4 *srtC1-3* deletion mutant

A TIGR4 Δ*srtC1-3* isogenic mutant was generated by allelic exchange. Fragments of approximately 500 bp upstream and downstream the target gene were amplified by PCR and spliced into a kanamycin resistance cassette by using overlap extension PCR; the PCR fragments were then cloned into pGEMt (Promega) and transformed in *S. pneumoniae*. To select the bacteria in which the target genes were replaced with the resistance cassette, bacteria were plated on blood-agar plates with kanamycin (500 μg/ml). The presence of the isogenic mutation was confirmed by

PCR and Western blot analysis. To obtain a TIGR4 Δ*srtC1-3* complemented mutant, *pMU1328-Pc-srtC-2* was transformed into TIGR4 Δ*srtC1-3* with conventional methods. Transformants selection was performed by supplementing media with kanamycin (500 μg/mL) and erythromycin (1μg/mL) and complementation confirmed by Western blot analysis.

Expression of RrgB, RlrA and SrtC-2 in TIGR4 low pilus expressing bacteria
The *rlrA,* the *rrgB* and the *srtC-2* genes were amplified from chromosomal DNA of TIGR4 strain by PCR by using the primers listed in Table 1.3. The PCR products were cloned into the complementation plasmid pMU1328 between BamHI and SalI restriction sites [95]. Expression of RlrA, RrgB and SrtC-2 was under the control of the erythromycin constitutive promoter (Pc), which was amplified with the primers listed in Table1.3 and cloned immediately upstream *rlrA, rrgB* or *srtC-2* (EcoRI, BamHI). All plasmids were confirmed by sequencing, and then transformed into TIGR4 low pilus expressing bacteria by conventional methods. Transformant selection was performed by supplementing media with erythromycin (1μg/mL). Bacteria containing the pMU1328 *Pc_rlrA, Pc_rrgB* or *Pc_srtC-2* plasmids were analyzed by PCR. Expression of pili on the bacterial surface was detected by Western blot, FACS and immune-fluorescence analysis of whole cell lysates.

Table 1.3. Oligonucleotides used to constructs pMU1328 plasmids expressing RrgB, RlrA and SrtC-2. Underlined sequences correspond to the restriction sites used for cloning.

Primer name	Primer sequence
Pc _for Eco RI	GTGCGTGAATTCGAAACAGCAAAGAATGGCGGAAAC
rrgB _for_BamHI	GTGCGTGGATCCATGAAATCAATCAACAAATTTTTA
rlrA _for_BamHI	GTGCGTGGATCCATGCTAAACAAATACATTGAAAAA
srtC-2 _for_BamHI	GTGCGTGGATCCATGGACAACAGTAGACGTTCACGA
Pc _rev_BamHI	CAGCGTGGATCCGTAATCACTCCTTCTTAATTACAA
rrgB _rev_SalI	CAGCGTGTCGACTGGCTCCTTTCTCTCTTACTTAAG
rlrA _rev_SalI	CAGCGTGTCGACCTTTTTGTGTGTAGACAGTACGAT
srtC-2 _rev_SalI	CAGCGTGTCGACCGTAGTTTAGTCCTTGACATGACG

The obtained PCR products were then digested with the appropriated restriction enzymes and cloned into the plasmid pMU1328, containing an erythromycin resistance marker [95]. The ligations mixtures were then transformed into competent cells of *Escherichia coli* DH10B. Selection of erythromycin resistant transformants was performed on plates supplemented with erythromycin (100 μg/mL) and insertion was confirmed by sequencing. The obtained plasmids along with the empty pMU1328 plasmid were then transformed in D39 or TIGR4 wt or deletion mutants strains by using conventional methods [100]. *S. pneumoniae* transformants were selected on agarose plates supplemented with antibiotics (erythromycin 1μg/mL with or without kanamycin 500μg/mL), analyzed by PCR to confirm the presence of the plasmid and further investigated for the expression of the proteins of interest.

Discussion

Following their first identification in other Gram-positive bacteria, pili have been detected on the surface of the major human pathogen *S. pneumonia*e and shown to be immunogenic and involved in pathogenicity in *in vivo* and *in vitro* studies [46,61,68]. Epidemiological reports have defined that PI-1, coding for the proteins implicated in pilus-1 biogenesis, is present in approximately 30% of the pneumococcal isolates and exists in three genetically related variants [62,65,101].
The molecular structure of pilus-1 and the mechanism of pilus assembly have been investigated, and a number of putative PI-1 genetic regulators have been described [3,59,63,67,69-71,102]. However, still very little is known about the regulation of pilus expression, the environmental conditions able to modulate it and the complex macromolecular machinery that regulates pili biogenesis. In addition, in all the above mentioned studies, *S. pneumoniae* pilus expression has always been evaluated not on a single cell basis, but as an average behavior of a large population.
In this work, by using detection methods able to discriminate single cells, we have compared the expression of the pilus to other known surface exposed virulence factors in the laboratory reference strain TIGR4. Unlike the other proteins tested, pilus-1 components were found to display a biphasic expression pattern. The two phenotypically distinct sub-populations, Pil+ and Pil-, are present in variable ratios in all the strains tested. The pilus expression ratio is inherited by daughter cells and is not influenced neither by bacterial genetic and epidemiological characteristics nor by the *in vitro* growth conditions tested. Furthermore, the majority of the colonies isolated on solid medium from the same strain show a similar pilus expression pattern, thus indicating that this may be influenced by some genetic traits of the strain, still unidentified. However, some colonies generate bacterial populations displaying different ratios of Pil+/Pil- bacteria. Since the isolation of the clinical isolates from the human host always implies a process of *in vitro* growth and stochastic colony selection, the pilus expression ratios observed may not be representative of the expression of pili *in vivo.* This aspect needs further investigation.
Interestingly, despite numerous attempts using single colony selection, sub-populations containing 100% of either Pil+ or Pil- bacteria were never obtained. Consequently, the analysis of pilus expression (both by microarray and western blot) was performed by comparing two sub-populations, H and L, enriched in Pil+ and Pil- bacteria, respectively. Microarray expression profiling showed that no other genes, with the exception of the PI-1 components, were differentially regulated in the two sub-populations across the five strains tested, including the genes previously reported to be RlrA repressors. Moreover, as clearly demonstrated in this work, RlrA (unlike RrgB) expression was sufficient to induce the polymerization of a functional pilus on Pil- pneumococci, switching the pilus biosynthesis from an “off” to an “on” condition. The latter observation is in agreement with previous reports which demonstrated that RlrA is a positive regulator of PI-1 genes transcription, able to activate its own transcription and to establish a positive feedback loop [56]. Taken together these data indicate either that other transcriptional changes remained undetected by our assay, or that pilus expression is not dependent on regulators located outside PI-1, but directly changes in response to still unidentified external stimuli or noise able to activate *rlrA* transcription. Additional data obtained in our lab by analyzing pilus expression at the single cell level in knock-out mutants of the

known PI-1 repressors, exclude the possibility of their direct involvement in pilus regulation (data not shown), and therefore favor the second hypothesis.
Although the molecular mechanisms triggering such regulation events are still not clear, the data presented in this work suggest that *S. pneumoniae* pilus expression could be an example of bistability, as it was recently suggested for *Streptococcus pyogenes* FCT3 encoded pili and the Ebp-type pili in *Enterococcus faecalis* [79,80]. In fact, this term is usually referred to phenotypic variation examples where: 1) two stable expression states coexist within a population; 2) noise or different factors operate across the entire population driving cells to switch into the alternative expression state and determine the overall switching probability; 3) the regulation occurs through the presence of feedback loops, either positive or double negative [76,77,103]. Moreover, bistability is epigenetic in nature (not caused by a change in the DNA sequence). In this regard, our data exclude the possibility of phase variation events within PI-1, but genetic modifications present elsewhere in the genome (still unexplored) could indirectly influence pilus expression.
The molecular basis and the biological benefit of this bistability phenomenon are currently unknown. Presumably, such switching mechanisms have evolved as a way for bacteria to be phenotypically pre-adapted to survive present or pending adverse conditions. Most likely, this heterogeneity helps the bacterium to utilize different niches within an ecosystem, and even has the potential to increase the overall fitness of the species, and prepare a sub-population of *S. pneumoniae* cells to promptly adapt in response to stress or different environmental conditions.
In conclusion, this study has shown that pilus expression follows a biphasic pattern, and is an on-off regulated mechanism occurring at the transcriptional level and involving all the PI-1 components, included the PI-1 positive regulator RlrA (there could be multiple promoter regions within PI-1 responding to RlrA positive regulation). Further studies are necessary to better clarify the molecular mechanisms responsible for the biphasic pilus phenotype. This finding suggests that new experimental approaches should be devised to assess the contribution of pilus-1 to virulence. In addition, the discovery of this byphasic phenotype points toward the need to evaluate the expression of the pneumococcal pilus during infection and to understand if *in vivo* conditions will modulate the pilus expression ratio, or if, for still unknown reasons, the coexistence of the two heterogeneous sub-populations is necessary to exploit the pilus virulence potential.

Chapter 2

Based on:

"Immunization with the RrgB321 fusion protein protects mice against both High and Low pilus-expressing *Streptococcus pneumoniae* populations."

Monica Moschioni[1], Gabriella De Angelis[1], Carole Harfouche[1], Esmeralda Bizzarri[1], Sara Filippini[1], Elena Mori[1], Giuseppe Mancuso[2], Francesco Doro[1], Michèle A. Barocchi[1], Paolo Ruggiero[1] and Vega Masignani[1].

[1]*Novartis Vaccines and Diagnostics, 53100 Siena, Italy*
[2]*The Elie Metchnikoff Department, University of Messina, 98125 Messina, Italy*

Introduction

Pneumococcal pilus-1 components, and in particular the RrgB backbone pilus subunits, demonstrated significant efficacy in protecting mice from lethal challenge [68], and therefore are evaluated as candidates for the inclusion in a new multi-component protein-based vaccine against *S. pneumoniae* [31,104].
RrgB exists in three variants (I, II and III), which have a degree of protein homology of 48-60% [62]. The three allelic variants are protective *in vivo* against homologous challenge with *Streptococcus pneumoniae* strains, but neither cross-protection nor cross-reaction was observed between clades [105]. Since a combination of the three RrgB variants could broad the efficacy of a pilus-based vaccine, a fusion protein (RrgB321) containing the three RrgB variants in a head to tail organization (Figure 2.1A), was constructed. Harfouche *et al*. have demonstrated that RrgB321 elicites an antibody response against each of the variants and protectes mice against piliated pneumococcal strains of the three clades both by active and passive immunization (Figure 2.1B), supporting the validity of this candidate as a potential antigen for the generation of a multi-component protein-based vaccine against *S. pneumoniae* [105].
The clearance of *S. pneumoniae* from the host following the immunization with capsular polysaccharide is thought to be primarily mediated by antibody-dependent phagocytosis and intracellular killing by alveolar macrophages and polymorphonuclear neutrophils (PMNs) recruited to the infection site [106,107]. Due to this observation an *in vitro* assay based on the bacterial killing mediated by opsonophagocytosis has been developed [108].
The assay measures the functional activity of vaccine-induced antibodies and resembles the mechanism by which antibodies provided *in vivo* protection against infection by encapsulated pathogens.

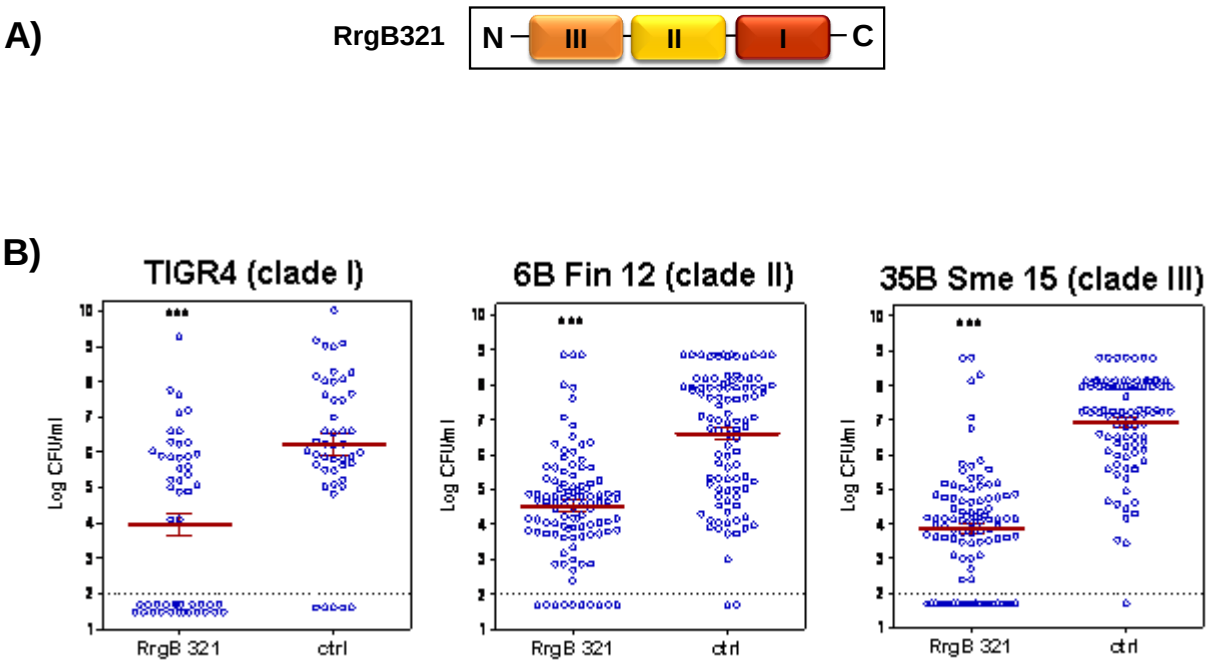

Figure 2.1 (A) Schematic representation of the RrgB321 construct, the three full length variants of RrgB are linked in a head to tail organization. **(B)** Protective efficacy provided by active immunization with RrgB321. BALB/c mice were either immunized with RrgB321 or received alum plus saline (ctrl) and than challenge intravenously with pneumococcal strains of the three RrgB clades. Values of bacteraemia for each mouse were reported: circles represent values of Log CFU/ml for the blood of single animals, horizontal bars represent the mean ± SEM for each group, and the dashed line indicates the detection limit (*i.e.* no CFU were detected in samples positioned below dashed line). Values of $P \leq 0.05$, ≤ 0.01, and ≤ 0.001 are indicated by *, **, and ***, respectively [105].

In detail, the assay is classically performed by incubating HL-60 used as effector cells (a primary pluripotent cell line differentiated to macrophages) with complement and a specific antiserum, and determining the number of surviving pneumococci when the mixture is plated on agar plates [109] (Figure 2.2).
Although the ability to correlate *in vitro* opsonophagocytic activity with a linear increase in *in vivo* protection has not been demostrated yet, in the recommendations of the World Health Organization for pneumococcal conjugate vaccine it has been suggested that the opsonophagocytic activity (OPA) could be considered a surrogate of the effectiveness of new streptococcal vaccines and should be a necessary component of any vaccine development program [110]. Interestingly, RrgB321 is the only protein thus far reported able to induce antibodies which mediate a complement-dependent opsonophagocytic killing (OPK) of strains representing the three RrgB variants at levels comparable to those elicited by antisera against the PCV-7 glycoconjugate vaccine [105].

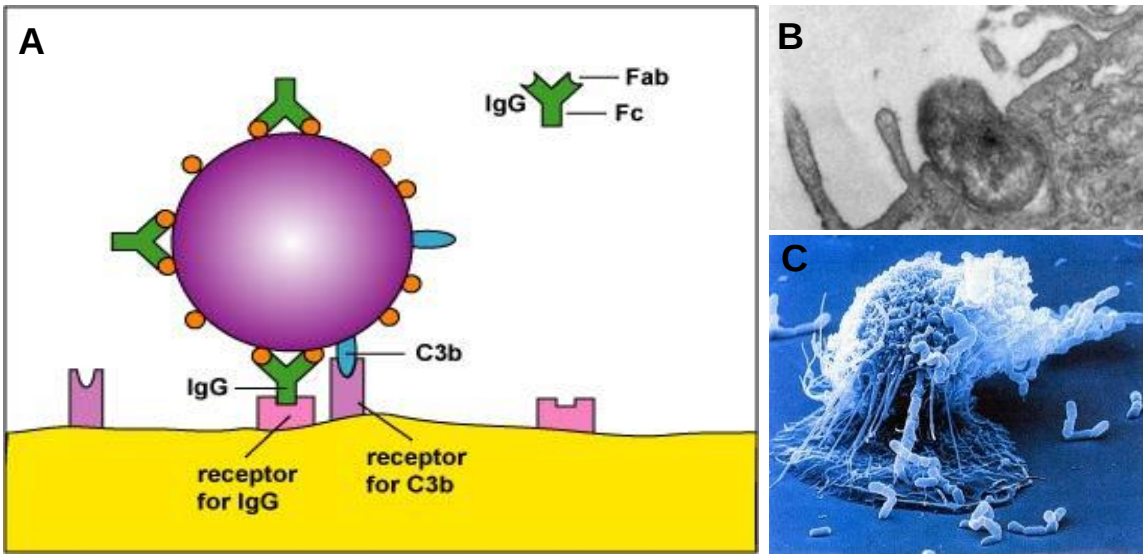

Figure 2.2 (A) Schematic representation of antibodies-mediated opsonophagocytosis by neutrophils; the bacterial uptake into phagosomes is followed by bacterial killing through multiple mechanisms (*From www.cat.cc.md.us/.../ opsonization/u1fig26n.html*); (**B and C)** Electron microscope photomicrographs of a macrophage phagocyting pathogens. *From http://www.squidoo.com/macrophage*

Since, as shown in chapter 1, the expression of the pilus is biphasic, we further investigate if the pilus expression ratio could impair the protection provided by Rrg321. With this purpose, the two stably separated subpopulations expressing the pilus at high (H) and low (L) level, were tested in the OPK assay to investigate whether RrgB321 antibodies are able to kill both H and L *S. pneumoniae* populations. Moreover the ability of RrgB321 to confer protection *in vivo* against both populations was tested in different mouse models of infection.

Results and Discussion

Pilus expression is required to obtain RrgB321 antisera-mediated killing in the OPK assay.

In order to assess if the expression ratio of the pilus in a given strain affects the levels of bacterial killing obtained in the OPK assay with RrgB321 antisera, the H and L (*i.e.* the High- and the Low-pilus-expressing) populations of the 6B SPEC strain (Figure 2.3) (obtained as detailed in Materials and Methods and in [111]) were tested under the same experimental conditions.

While antibodies against RrgB321 were able to kill up to 80% of 6B SPEC H population in a concentration-dependent manner (sera were serially diluted from 1:200 to 1:437400), no detectable killing of 6B SPEC L was observed.

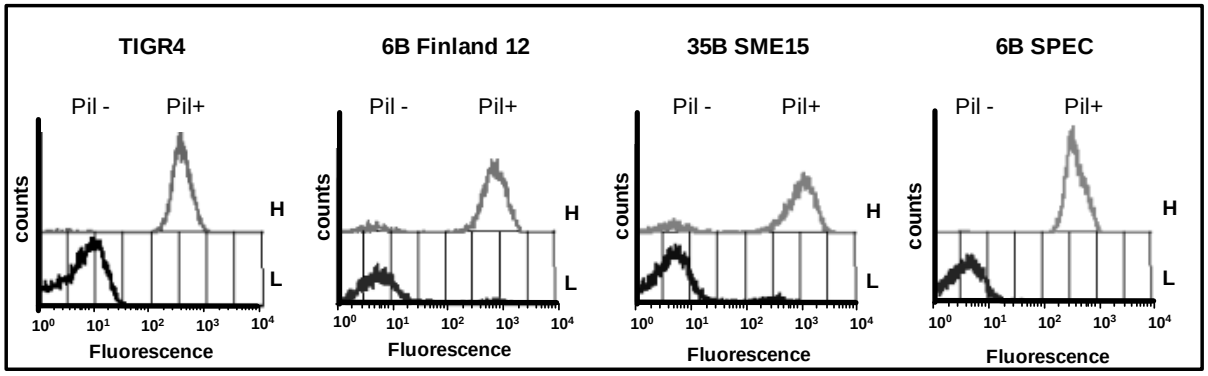

Figure 2.3 Pilus expression profiles of the H and L populations used to perform the *in vivo* and *in vitro* experiments in this study. Pilus expression was analyzed by flow cytometry (FACS-Calibur). RrgB321 antisera (1:400 dilution), and FITC anti-rabbit IgG (1:100 dilution) served as primary and secondary antibodies, respectively.

In contrast, Omniserum, which was used as positive control, showed similar killing of both 6B SPEC H and L, with about 100% killing at the lowest dilutions tested (sera were serially diluted from 1:400 to 1:874800). No bacterial killing was detectable when the assays were performed with negative control sera (Figure 2.4). These data indicate that the OPK activity observed *in vitro* with RrgB321 antiserum is strictly dependent on the proportion of the pilus-expressing bacteria of the strain tested.

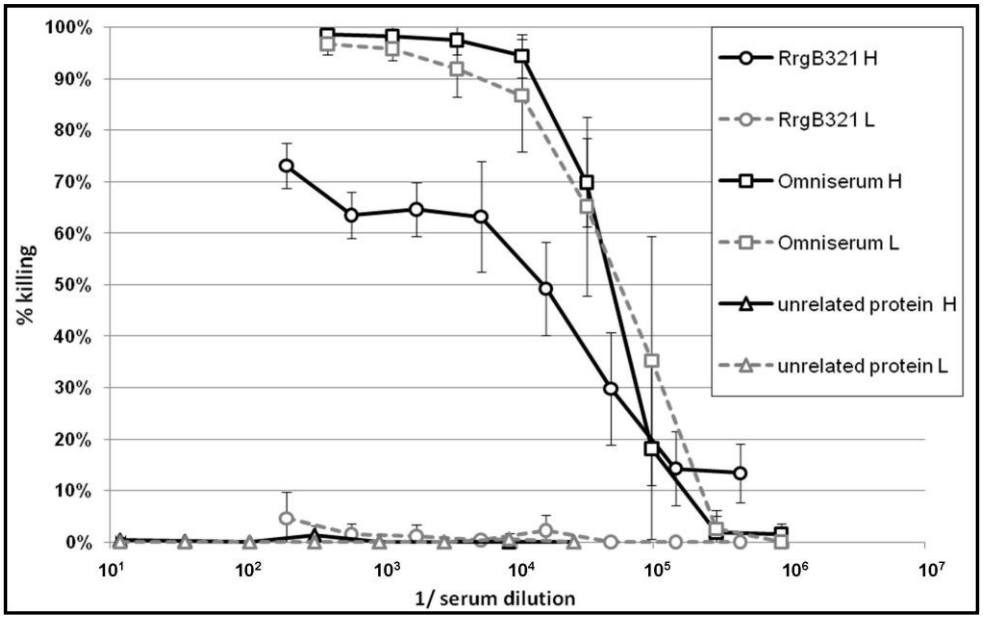

Figure 2.4. RrgB321 antibodies are functional in the OPK assay only against 6B SPEC H *S. pneumoniae*. The OPK assay was performed with both the 6B SPEC H and L populations by using: RrgB321 antisera (serial dilutions from 1:200 to 1:437400), Omniserum (serial dilutions from 1:400 to 1:874800) and a negative control serum (serial dilutions from 1:12 to 1:26244). The X and Y axes represent the sera dilutions and the percentages of killing, determined as detailed in the materials and methods section.

During the OPK assay pilus positive bacteria are selectively killed.
Due to the bistable expression of *S. pneumoniae* pilus-1, the separation process adopted to obtain the H and L populations leads to the isolation of an enriched, but not pure populations of pilus expressing bacteria [111]. In addition, in the OPK assay carried out with anti RrgB321 antiserum, the 100% killing was never obtained even with the H population (see above). Therefore, we sought to determine if during the OPK assay bacteria were switching from an "on" to "off" pilus expression state. With this purpose, 6B SPEC H bacteria surviving the OPK assay performed in the presence of different dilutions of negative control or RrgB321 antisera were analyzed by FACS.

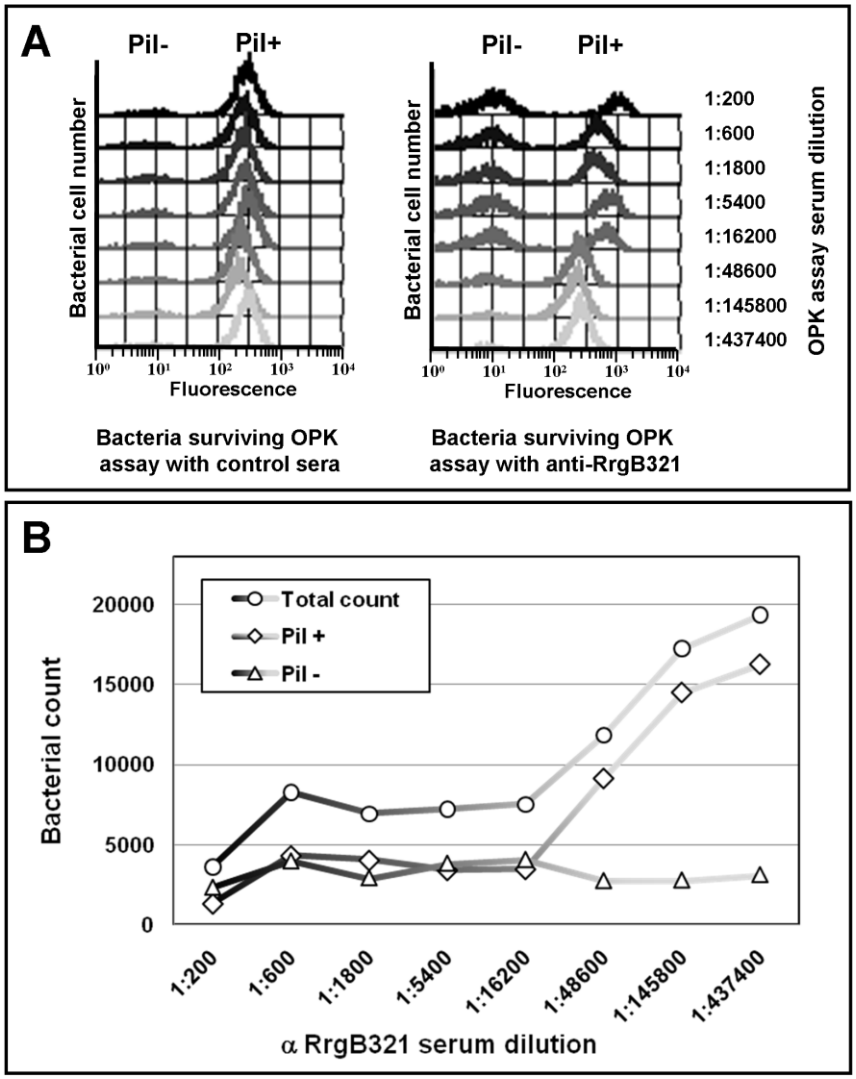

Figure 2.5. Pilus positive bacteria are selectively killed by RrgB321 antibodies in the OPK assay. **(A)** Pilus expression was analyzed by FACS using RrgB321 antibodies on bacteria surviving the OPK assay performed with different dilutions of negative control or RrgB321 sera (serial dilutions from 1:200 to 1:437400). **(B)** Total bacterial counts at different RrgB321 serum dilutions were acquired from the OPK assay experiments. The pilus positive (Pil+) and negative counts (Pil-) for each RrgB serum dilution were estimated normalizing the percentages of pilus positive-negative bacteria obtained by FACS to the total counts. The assay was repeated in triplicate. One representative experiment is shown.

Pilus expression of bacteria incubated with negative control sera (unrelated protein) (Figure 2.5A left panel) was similar, at each serum dilution, to that of bacteria non-incubated and of bacteria incubated with phagocytes and active complement in the absence of specific antibodies (not shown). On the other hand, when the OPK assay was performed by using RrgB321 antisera, the proportion of *S. pneumoniae* not expressing the pilus (Pil-) increased at rising sera concentrations (Figure 2.5A right panel). To estimate the relative number of pilus-positive (Pil+) and pilus-negative (Pil-) bacteria surviving the OPK assay, the percentages of pilus-expressing bacteria at different RrgB321 serum concentrations (evaluated by FACS analysis) were normalized to the actual counts of surviving bacteria. At increasing RrgB321 serum concentrations a proportional decrease in the total and in the pilus-positive counts was observed, while the pilus-negative counts remained constant at all dilutions (Figure 2.5B).
Moreover, in order to demonstrated that the presence of RrgB antisera did not affect *S. pneumoniae* pilus-expression in liquid cultures three *S. pneumoniae* strains (TIGR4, 6B Fin 12, 35B SME 15) were grown in the presence of antibodies directed against RrgB (sera raised against an unreleted protein were used as negative control), and were allowed to replicate seven cycles. The expression of pilus-1 was then verified by FACS analysis revealing that the pilus expression ratio was unaffected by the presence of the RrgB antisera (data not shown). These data further confirm that the observed increased proportion of pilus non-expressing bacteria in those surviving the OPK assay is only due to the specific RrgB321 antisera-mediated killing and not to a switch towards the off-state of pilus expression induced by the presence of the serum.

RrgB321 protects mice against challenge with either H or L *S. pneumoniae* populations by both active and passive immunization.

Given the results obtained in the OPK assay *in vitro*, we set out to determine whether immunization with RrgB321 could protect mice against PI-1 positive strains independently from their pilus expression ratio by using animal models of sepsis and pneumonia.
In the sepsis model, mice immunized intraperitoneally (i.p.) with RrgB321 were challenged intravenously (i.v.) with either the H or L populations of three strains representative of the RrgB variants (TIGR4, 6B Finland 12, 35B SME 15) (Figure 2.3 and Table 2.1). The protective efficacy of RrgB321 against the wild-type strains was already established [105]. Bacteraemia at 48 hours and survival were analyzed as described in the Materials and Methods section.
As expected, when the i.v. challenge was performed with the H populations of the three strains the levels of protection were always significant, in terms of reduction of bacteraemia (ranging from about 1.5 to 3 Logs, according to the challenge strain), increase of median survival (from 4 to 10 days), and survival rates (from 32 to 70%) (Table 2.1 and Figure 2.6, left panels).

Table 2.1 RrgB321 protective efficacy by active and passive immunization against the H and L populations of three pneumococcal strains

	CHALLENGE		N	BACTERAEMIA				SURVIVAL					
strain [RrgB clade]	dose (CFU/mouse)	route [a]		mean Log CFU control	mean Log CFU RrgB321	Log reduction	*P* [b]	median survival control (days)	median survival RrgB321 (days)	median survival increase (days)	*P* [b]	survival rate (%) [c]	*P* [d]
ACTIVE IMMUNIZATION													
TIGR4 H [clade I]	4,4E+05	i.v.	18	6,30	3,15	3,15	**0,0002**	5,50	15,50	10,00	**0,0002**	72	**< 0.0001**
TIGR4 L [clade I]	3,3E+05	i.v.	18	6,46	4,36	2,10	**0,0079**	2,50	14,50	12,00	**0,0051**	40	**0,0375**
6B Finland12 H [clade II]	1,2E+08	i.v.	20	5,64	3,73	1,90	**0,0001**	4,50	8,50	4,00	**< 0.0001**	32	**0,0218**
6B Finland12 L [clade II]	1,1E+08	i.v.	20	5,44	4,34	1,10	**0,0347**	6,50	8,50	2,00	**0,0131**	6	0,5000
35B SME15 H [clade III]	4,3E+07	i.v.	8	3,15	1,70	1,45	**0,0464**	6,50	15,50	9,00	**0,0171**	80	0,0594
35B SME15 L [clade III]	4,8E+07	i.v.	8	3,35	2,48	0,87	**0,0422**	9,00	13,00	4,00	0,3293	20	0,5000
TIGR4 H [clade I]	3,7E+06	i.n.	8	4,52	1,70	2,82	**0,0009**	5,50	10,50	5,00	**0,0009**	100	**0,0007**
TIGR4 L [clade I]	3,0E+06	i.n.	8	6,44	3,26	3,18	**0,0068**	2,50	8,00	5,50	**0,0123**	43	0,1410
PASSIVE IMMUNIZATION													
TIGR4 wild type [clade I]	3,8E+05	i.v.	8	6,43	3,74	2,69	**0,0041**	5,00	10,50	5,50	**0,0225**	57	0,0594
TIGR4 H [clade I]	4,4E+05	i.v.	8	6,53	3,25	3,28	**0,0027**	3,50	10,50	7,00	**0,0006**	75	**0,0035**
TIGR4 L [clade I]	3,6E+05	i.v.	8	5,73	3,15	2,58	**0,0041**	3,50	10,50	7,00	**0,0492**	50	0,1573
TIGR4Δ*PI-1* [no pilus]	4,2E+05	i.v.	8	6,86	6,77	0,09	0,4790	3,00	5,00	2,00	0,1931	14	0,5000

(a) i.v. = intravenous; i.n. = intranasal

(b) Mann-Whitney U-test

(c) survival rate = [1 - (% dead vaccinated / % dead controls)] x 100

(d) Fisher's exact test

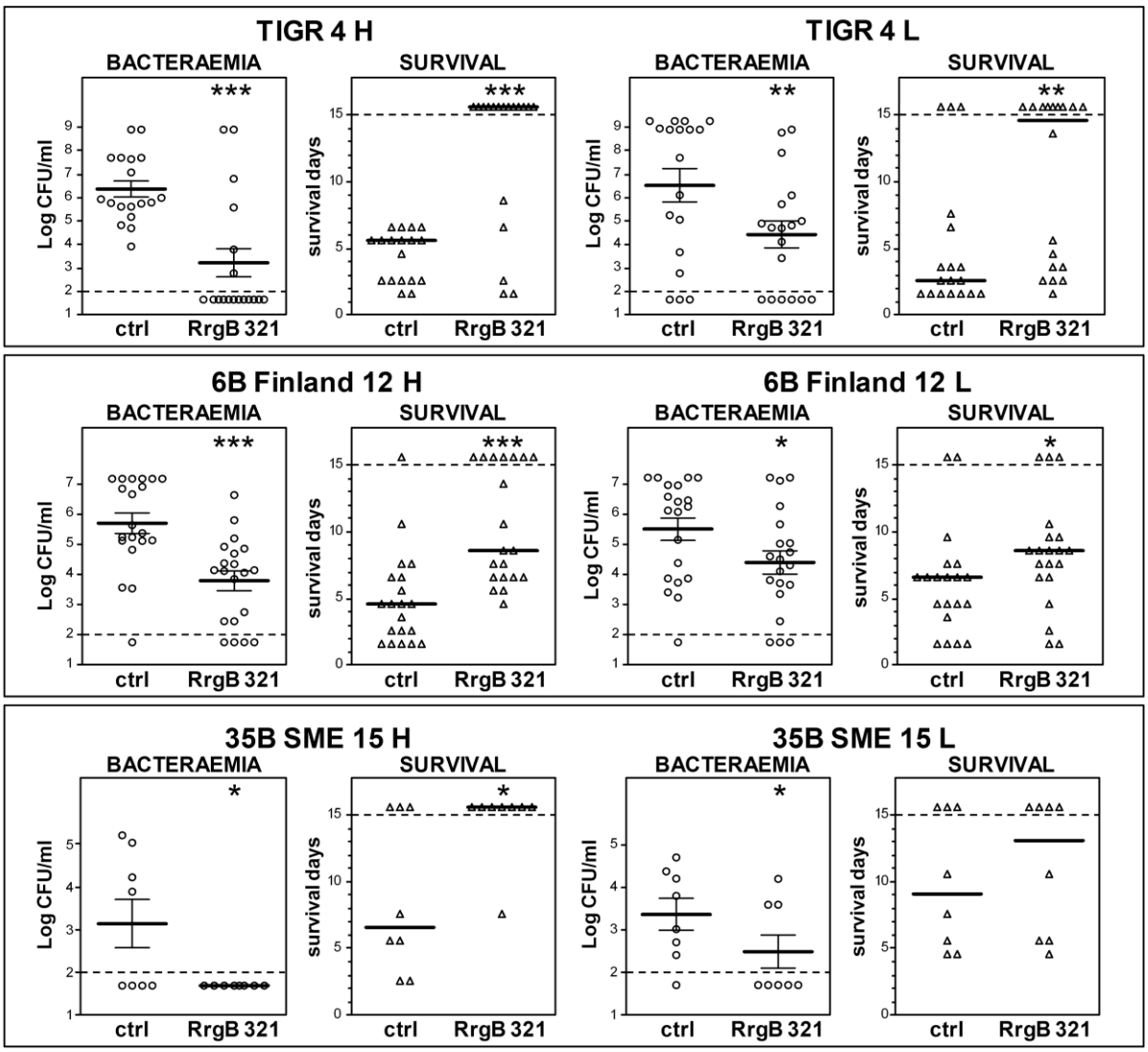

Figure 2.6. CD1 mice immunized with RrgB321 are protected when challenged i.v. with either the H (left panels) or the L (right panels) pilus-expressing bacterial populations of the indicated strains. Challenge doses and detailed statistical analyses are reported in Table 2.1. In the bacteraemia panels circles represent values of Log CFU/ml for the blood of single animals, horizontal bars represent the mean ± SEM for each group, and the dashed line indicates the detection limit (*i.e.* no CFU were detected in samples positioned below dashed line). In the survival panels the triangles represent survival days for single animals, the horizontal bars represent the median survival time for each group, and the dashed line indicates the endpoint of observation (animals whose survival time is above the dashed line were alive at the end of the experiment). Values of $P \leq 0.05$, ≤ 0.01, and ≤ 0.001 are indicated by *, **, and ***, respectively. Ctrl = control.

Interestingly, significant decrease in bacteraemia (from about 1 to 2 Logs) was also observed upon challenge with the L populations of all the three *S. pneumoniae* strains, and a significant increase in median survival time was obtained with TIGR4 L and 6B Finland 12 L (Table 2.1 and Figure 2.6, right panels). However, a significant survival rate was achieved only with TIGR4 L (Table 2.1).
In the bacteraemic pneumonia model, following i.p. immunization with RrgB321, mice were infected intranasally (i.n). to establish lung infection. Upon challenge with either

TIGR4 H or TIGR4 L, bactaeremia was significantly lower and median survival significantly increased in mice immunized with RrgB321 with respect to the corresponding controls, even though a significant survival rate was obtained only in mice challenged with TIGR4 H (Table 2.1 and Figure 2.7).
Noteworthy, no significant difference was observed between the infectivity exerted by the H and L populations of each of the three strains, indicating that the pilus expression status does not dramatically affect virulence (*P* values ranging from 0.3723 to 0.9027, 0.2415 to 0.7209, 0.2286 to 1.0000 in the i.v. model and *P* = 0.0838, = 0.1304, = 1.0000 in the i.n. model for bacteraemia, survival course and survival rate, respectively) (Table 2.2).

Table 2.2 Comparison of virulence of pneumococcal strains with different pilus status.

strain [RrgB clade]	challenge route [(a)]	*P* [(b)] bacteremia	survival course	*P* [(c)] survival rate
TIGR4 [clade I] H *vs.* L	i.v.	0,3723	0,3081	0,2286
6B-Finland12 [clade II] H *vs.* L	i.v.	0,9027	0,2415	1,0000
35B-SME15 [clade III] H *vs.* L	i.v.	0,7984	0,7209	1,0000
TIGR4 [clade I] H *vs.* L	i.n.	0,0838	0,1304	1,0000
TIGR4 [clade I] H *vs.* wild type	i.v.	0,6355	0,1239	1,0000
TIGR4 [clade I] L *vs.* wild type	i.v.	0,1267	0,8313	1,0000
TIGR4 [clade I] ΔPI-1 *vs.* wild type	i.v.	0,3170	0,4916	1,0000

(a) i.v. = intravenous; i.n. = intranasal
(b) two-tailed Mann-Whitney U-test
(c) two-tailed Fisher's exact test

To assess the relevance of antibodies in the mechanism of protection elicited by RrgB321, an experiment of passive serum transfer was performed. Groups of mice administered with either RrgB321 antisera or control sera were challenged i.v. with TIGR4 wild type (w.t.), TIGR4 H, TIGR4 L, or a TIGR4Δ*PI-1* isogenic mutant. As shown in Figure 2.8 and Table 2.1, RrgB321 antiserum was able to significantly protect mice, against each of the PI-1 positive TIGR4 strains; in the vaccinated groups as compared with the control group bacteraemia was significantly reduced by over 2 Logs, the median survival was significantly increased by over 5 days, and survival rates ≥ 50% were achieved. No protection was observed against TIGR4Δ*PI-1*, as expected.
All the TIGR4 strains tested displayed a level of infectivity comparable to that of TIGR4 wt (*P* values ranging from 0.1267 to 0.6355, 0.1239 to 0.8313, and 1.0000 for bacteraemia, survival course and survival rate, respectively) (Table 2.2), confirming the results obtained with the H and L populations described above. This is consistent with a previous report showing that only experiments of competition between the wild-type and pilus-defective mutant strain could demonstrate a difference in virulence, otherwise inappreciable [46].

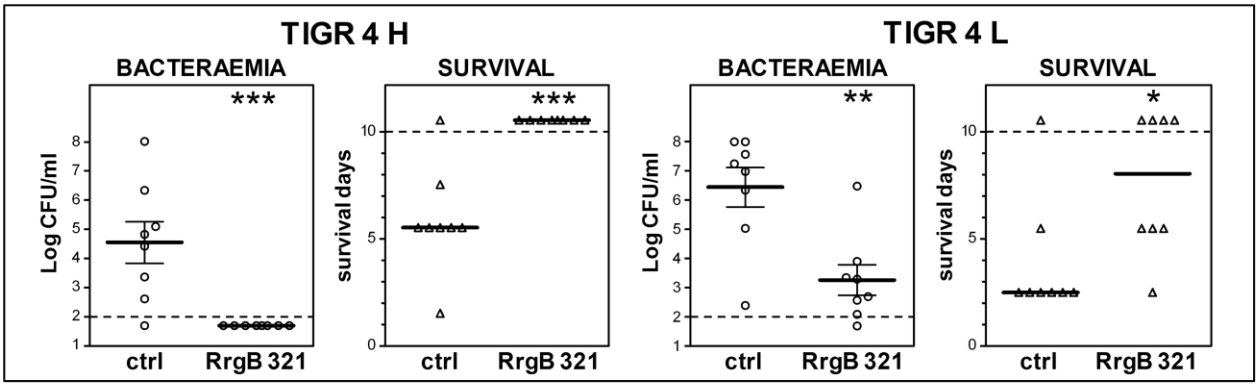

Figure 2.7. BALB/c mice immunized with RrgB321 are protected when challenged i.n. with either the H (left panels) or the L (right panels) pilus-expressing bacterial populations of TIGR4. Challenge doses and detailed statistical analyses are reported in Table 2.1. Symbols are as described in Figure 2.6.

The results presented here indicate that RrgB321 is able to induce an immune response that is efficacious when almost all pneumococci express pili, but also that it is possible to achieve protection, both by active and passive immunization, even when a low proportion of the bacteria express the pilus at the time of the experimental infection. This latter observation is in agreement with the biphasic regulation of the pilus reported [111,112]. In fact, the data presented here reinforce the hypothesis that, once in the host, pilus expression could be switched on by undefined mechanisms in the context of the host-pathogen interaction. One possible hypothesis is that, during infection of RrgB321-immunized mice, the killing of pilus-positive bacteria induces other pneumococci to activate pilus expression, establishing a balance between the on-state of pilus expression and bacterial killing, which results in protection. However, to explain the protection obtained against the L populations, the contribution of further, antibody-independent, protective mechanisms cannot be excluded. To investigate possible changes of pilus expression *in vivo*, bacteria from blood samples taken from i.v.-infected mice 48h post-challenge were analyzed by flow cytometry. For the three strains tested (TIGR4, 6B Finland 12 and 35B SME 15) we observed that the bacteria recovered from the mice challenged with the H population showed a slight decrease (~10%) of the pilus expression ratio with respect to the input strain.
Similarly, pilus expression ratio in mice challenged with the L populations slightly increased (~about 10%) (data not shown). These data suggest that *S. pneumoniae* pilus expression can be modulated once in the host. However, we did not observe a significant difference in the percentage of piliated pneumococci in the immunized versus the non-immunized animals, indicating that such a modulation is independent from the immune response. Notably, the 10% increase in pilus expression observed at 48h in the L subpopulation is not sufficient to explain the significant levels of protection observed. One possible hypothesis could be that, for PI-1-positive strains, pilus represents a fitness factor, important during the early stages of infection, and that the switch towards the on-state of pilus expression happens at time points earlier than that analyzed.

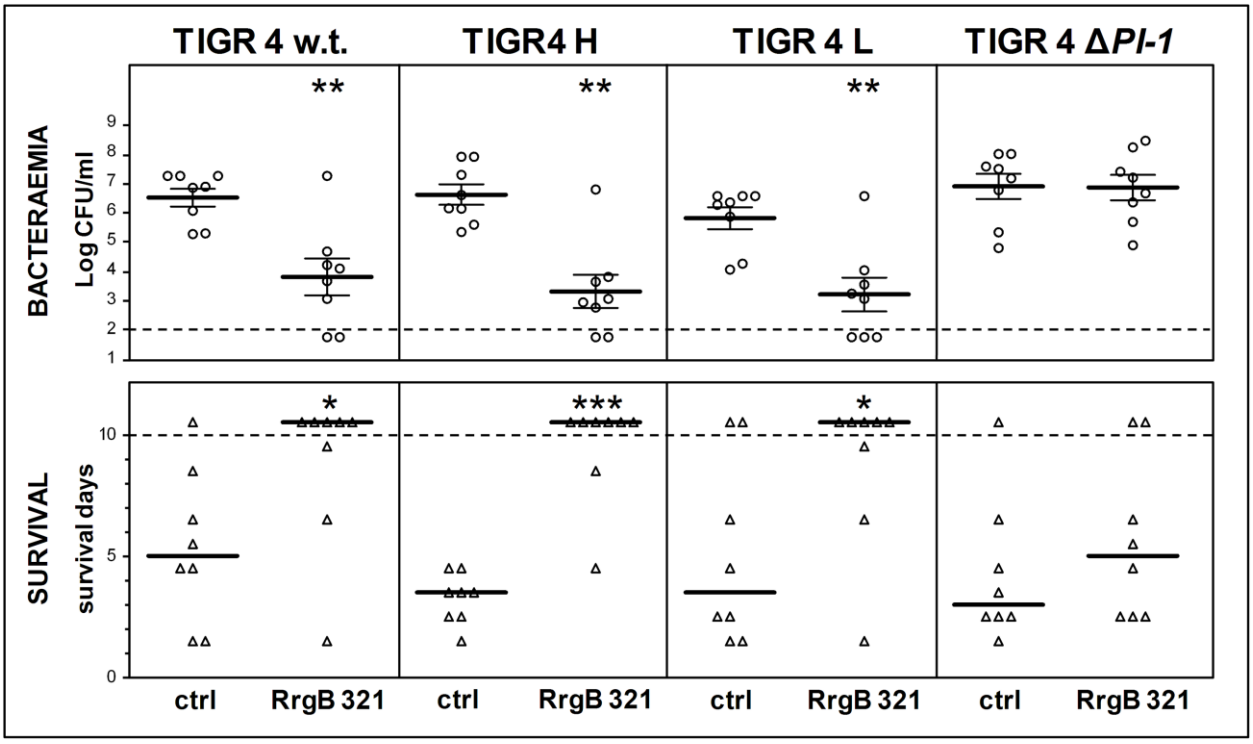

Figure 2.8. CD1 mice passively immunized with RrgB321 antisera are protected when challenged i.v. with wild-type (w.t.) TIGR4, or with TIGR4 High (H) or Low (L) pilus-expressing populations. Mice challenged with TIGR4Δ*PI-1* (TIGR4 isogenic PI-1 knock-out mutant) were not protected by anti-RrgB321 antibodies. Immunization control groups were treated with control sera. Challenge doses and detailed statistical analyses are reported in Table 2.1. Symbols are as described in Figure 2.6.

This would also explain why the protective efficacy of RrgB321 against L populations was more evident in terms of bacteraemia at 48h, and less marked in terms of survival courses and rates. With this respect, further analyses should be needed to achieve a better understanding of the kinetics of pilus expression during pneumococcal infection.

Materials and methods

Bacterial culture

S. pneumoniae strains were grown at 37°C in 5% CO_2 on Tryptic Soy Agar plates (TSA, Becton Dickinson) supplemented with colistine 10 mg/L, oxolinic acid 5 mg/L and 5% defibrinated sheep blood (vol/vol). Liquid cultures were performed in Tryptic

Soy Broth (TSB, Difco) or in Todd Hewitt Broth supplemented with 0.5% (w/w) yeast extract (THYE) (Becton Dickinson). The *S. pneumoniae* High (H) and Low (L) pilus-expressing populations used in this study were obtained as reported in chapter 1 and in *De Angelis et al*. [111].
For the OPK experiments, bacteria grown on the plates over night (o.n.) were inoculated in THYE and grown until A_{600} = 0.25. Bacteria were then harvested by centrifugation, resuspended in THYE, 20% glycerol (vol/vol), 10% Fetal Bovine Serum (vol/vol), and frozen in aliquots at -80°C. The frozen stock was titrated by plating culture aliquots at serial dilutions and counting CFUs. For intranasal (i.n.) challenge and intravenous (i.v.) challenge, bacteria were freshly harvested from TSB liquid cultures at A_{600} = 0.2 and A_{600} = 0.5, respectively, and then brought to the working concentration before administration. The challenge input was titrated by plating bacterial suspensions immediately after challenge.

RrgB321 recombinant protein expression and purification
Standard recombinant DNA techniques were used to construct plasmids expressing the RrgB321 chimera, consisting of the three full length RrgB variants in a head to tail organization and separated by a six aminoacid linker (Gly-Ser-Gly-Gly-Gly-Gly). Briefly, *rrgB* open reading frames (nucleotides corresponding to the N-terminal signal sequence and C-terminal cell wall sorting signal motif were excluded from the cloning) were amplified by PCR from chromosomal DNAs of *S. pneumoniae* TIGR4 (*rrgB* clade I), 6B SPEC (*rrgB* clade II) and 35 SME 15 (*rrgB* clade III) by using specific primers listed in Table 2.3. The obtained PCR fragments were digested with the appropriated restriction enzymes and ligated into the C-terminal 6xHis-tag expression vector pET21b+ (Novagen). The resulting plasmids were confirmed by DNA sequencing and then transformed into competent *E. coli* BL21 DE3 star (Invitrogen). Protein expression was induced by the addition of IPTG (isopropyl-β-d-thiogalactopyranoside, Sigma®) 1mM final concentration to a bacterial culture with an A_{600} of 0.4-0.5 (LB medium supplemented with ampicillin 100 µg/mL). The proteins were purified by metal chelate affinity chromatography on His-Trap HP columns (GE Healthcare). Pooled fractions containing the purified protein were dialyzed o.n. against phosphate-buffered saline (PBS) and stored at -80°C until further use.

Table 2.3 List of the primers used to create the *rrgB321* construct in pET21b+. Underlined sequences correspond to the restriction enzyme recognition sites used for cloning. Sequences in bold italic encode the 6 AA linker (Gly-Ser-Gly-Gly-Gly-Gly) introduced as a spacer before and after the central RrgB clade II subunit.

Protein Name	Oligonucleotides (5'-3')
rrgB clade III	For GTGCGT GCTAGC GCGGAACAAAAAACTAAGACACTT Rev CAGCGT GGATCC CGTGATTTTTTTGTTGACTACTTT
rrgB clade II	For GTGCGT GGATCC ***GGCAGCGGTGGCGGTGGC*** GCTGCAACAGTTTTTGCGGCGGAC Rev CAGCGT CTCGAG AGTGATTTTTTTGTTGACTACTTTTGT
rrgB clade I	For GTGCGT CTCGAG ***GGCAGCGGTGGCGGTGGC*** GCTGCAACAGTTTTTGCGGCTGGG Rev CAGCGT CTCGAG AGTGATTTTTTTGTTGACTACTTT

Antisera

To generate sera against the specific proteins, purified recombinant proteins were used to immunize New Zealand rabbits (Charles River Laboratory) of around 2.5 kg body weight. Rabbits received three doses of 100 µg protein along with Freund's adjuvant, administered subcutaneously on day 0, 21 and 35, and serum was obtained on day 49. Omniserum, the rabbit polysaccharide multivalent antiserum, was purchased from Statens Serum Institute (Copenhagen).

Generation of TIGR4 PI-1 deletion mutant

TIGR4Δ*PI-1* isogenic mutant was generated by allelic exchange, as briefly described below. Fragments of approximately 500 bp upstream and downstream the target gene were amplified by PCR (oligo listed in Table 2.4) and spliced to a kanamycin antibiotic cassette by using overlap extension PCR; the obtained PCR fragment was cloned into pGEMt (Promega) and the obtained plasmid transformed in TIGR4 with conventional methods [100]. Bacteria were plated on selective blood-agar plates (kanamycin 500 µg/mL). The presence of the isogenic mutation was confirmed by PCR and the absence of pilus-1 expression confirmed by western blot analysis.

Table 2.4 Primers used to generate the TIGR4Δ*PI-1* isogenic deletion mutant

	Oligonucleotides (5'-3')
PI-1_up	For AATTGTCGACTATAATCTCCACAGTGGGATTTAC Rev GTTGGCCACTTAGGCCATCATGACCAGATGTAAACTTAATAAAGTCCA
PI-1_down	For CTAGCCGGCATTTAAATTTGCATCGCAGGGATTCGCTCAGTGATTGCTG Rev TTTAGCGGCCGCACAAAGAGCCGGAAAAAGGAACAG
Kan	For GTCATGATGGCCAAAGTGGCCAACATACTGTAGAAAAGAGGAAGGAAAT Rev CGATGCAAATTTTAATGCCGGCTAGATCTAGGTACTAAAACAATTCATC

Animal experiments

Animal studies were done in compliance with the current law, approved by the local Animal Ethics Committee and authorized by the Italian Ministry of Health.

Female, specific pathogen-free 6-week-old BALB/c or 5-week-old CD1 mice (Charles River) received three intraperitoneal (i.p.) immunizations, two weeks apart. Each dose was composed of 20 µg of recombinant protein, along with 400 µg of aluminium hydroxide as adjuvant, in a final volume of 200 µl of saline. Negative controls received the same course of saline plus the adjuvant. Seven days after the last immunization mice were bled to obtain immune serum to be used in immunoassays and passive protection studies. Two weeks after the third immunization, BALB/c mice were challenged intranasally (i.n.), while CD1 mice were challenged intravenously (i.v.), via the tail vein. For i.n. challenge, mice anesthetized by intraperitoneal injection of xylazine and ketamine (0.1 and 0.01 mg/g of body weight, respectively), received into the nostrils 50 µl of bacterial suspension. Bacteraemia was evaluated in blood samples taken 48 hrs post challenge and plated on blood-agar plates at serial dilutions. After 24 hrs of culture, CFUs were counted and the CFUs/mL of blood calculated. Bacteraemia was expressed as $\log_{10}$ (Log) of the CFUs/mL value. After challenge, the animals were monitored for 10 (i.n. challenge) or 15 (i.v. challenge)

days. Mice were euthanized when they exhibited defined humane endpoints that had been pre-established for the study in agreement with Novartis Animal Welfare Policies, and the day of sacrifice was recorded. Survival rates were calculated according to the following formula: survival rate (%) = [1 – (% dead vaccinated / % dead controls)] x 100.
For the passive protection experiment, each female 8-week-old CD1 mouse received i.v. 50 µL of pooled serum from RrgB321-immunized or negative control mice. Six hours later mice were challenged i.v., and bacteraemia and survival (10 days) monitored as above.
The challenge strains and doses are reported in Table 2.1.

Statistical analysis
GraphPad Prism Software (version 5.0) was used for statistical analyses. For the *in vivo* experiments the following tests were applied: Mann-Whitney U test to analyze data of bacteraemia and survival course, and Fisher's exact test for survival rates. One-tailed tests were applied for comparison of vaccinated versus control groups, while two-tailed tests were used when comparing control groups each other. Values of $P \leq 0.05$ were considered and referred to as significant.

Opsonophagocytosis Killing (OPK) assay
Human proleukemiae cells HL-60 (ATCC CCL240) were maintained in enriched medium (RPMI 1640+ Glutamax, Invitrogen; 10% Fetal Bovine Serum, Hyclone; 1% Penicillin/streptomycin, Gibco), and differentiated into phagocytes using 0.8% N,N-Dimethylformamide (DMF, Sigma). After five days treatment with DMF, cells were ready to be used in OPK assay [113]. Following heat inactivation (30 min 56°C) rabbit antisera were 1:3 pre-diluted in Opsonization Buffer (OPB: Hanks' Balanced Salt Solution [HBSS] with Ca2+ e Mg2+ [Invitrogen], supplemented with 0.1% gelatine and 10% inactivated FC1 [Hyclone]) and subsequently 3 fold serially diluted in a 96-wells plate (BD corning). Frozen bacteria were thawed, washed once in OPB (3000 rpm for 5 min), and then incubated with sera (1200 CFU/well) at RT for 30 min. Baby rabbit complement (BRC) was added at 12% and differentiated HL-60 cells were distributed at $4x10^5$ per well (HL-60:bacteria ratio 400:1). Plates with reaction mixtures (final volume 80µl) were incubated at 37°C, 5% CO_2 for 1h, onto a shaking platform (400 rpm, LabNet Shaker, ORBIT 300). Phagocytosis was stopped resting plates on ice for 15 min. Five microliters of the reaction mixture were tilt plated onto THYE Agar for colony count, and the remaining mixture was plated onto TSA/blood plates for subsequent flow cytometric analysis of pilus-1 expression. The bacteria plated to evaluate bacterial survival were let dry, embedded in THYE Agar supplemented with Triphenyl Tetrazolium Chloride dye 100 mg/L (TTC, Sigma), and incubated overnight at 37°C, 5% CO_2. Colony counts were evaluated by using the colony counter ProtoCOL (Synbiosis). Results were expressed as percentage of killing, meaning the percentage of bacteria that were killed in samples containing bacteria + phagocytes + active complement + sera (BPC'+S), compared to bacteria + phagocytes + active complement (BPC'): [(BPC'+S)/BPC'] x 100.

Flow Cytometry on whole *S. pneumoniae* bacterial cells.
Bacteria surviving the OPK assay, from a frozen glycerol stock, or from frozen blood samples obtained from the mice 48h post-challenge were grown o.n. on TSA/blood plates, harvested, stained with rabbit primary antibodies (final dilution 1:300), and then with FITC-conjugated secondary anti rabbit antibodies (final dilution 1:100)

(Jackson Laboratories). Bacteria were then fixed with 2% formaldehyde and staining was analyzed with a FACS-Calibur cytometer (Becton Dickinson). For each sample 10,000 events were recorded and the percentage of pilus-positive bacteria within each sample was estimated with the CellQuest software (Becton Dickinson).

Conclusions

The use of pilus proteins as well as fimbrial components of Gram-negative bacteria as potential vaccine candidates has been extensively investigated. However, concerns were raised on the utility of these candidates because of their described susceptibility to phase and antigenic variation [114-116]. In this work we present data indicating that, despite the bistable expression of *S. pneumoniae* pilus-1, RrgB321 immunization confers *in vivo* protection against both H and L pneumococcal populations, and that the presence of anti-pilus antibodies does not induce a switch towards the pilus non-expressing state. In addition, the different results obtained *in vitro* and *in vivo* with the L populations indicate that in this case the OPK assay, although a valuable method to establish the functionality of antibodies, does not directly predict *in vivo* results. Different aspects, including the *in vivo* regulation of pilus expression, most likely determine the protection level observed with the L populations.
Therefore, immunization with the RrgB321 fusion protein can be effective to protect against the disease caused by all PI-1 positive isolates. Our results support the inclusion of this fusion protein in a multi-component protein vaccine against *S. pneumoniae*.

Reference List

1. Austrian R: The pneumococcus at the millennium: not down, not out. *J Infect Dis* 1999, 179 Suppl 2: S338-S341.

2. E.Klebs: Beitrage zur Kentnis der pathogenen Schistomyceten. *Die Monadinen Arch exp Pathol Pharmakol* 1875, 4 : 125-139.

3. Hilleringmann M, Ringler P, Muller SA, De Angelis G, Rappuoli R, Ferlenghi I *et al*.: Molecular architecture of *Streptococcus pneumoniae* TIGR4 pili. *EMBO J* 2009, 28: 3921-3930.

4. Pneumococcal vaccines. WHO position paper. *Wkly Epidemiol Rec* 1999, 74: 177-183.

5. Lexau CA, Lynfield R, Danila R, Pilishvili T, Facklam R, Farley MM *et al*.: Changing epidemiology of invasive pneumococcal disease among older adults in the era of pediatric pneumococcal conjugate vaccine. *JAMA* 2005, 294: 2043-2051.

6. O'Brien KL, Wolfson LJ, Watt JP, Henkle E, Deloria-Knoll M, McCall N *et al*.: Burden of disease caused by *Streptococcus pneumoniae* in children younger than 5 years: global estimates. *Lancet* 2009, 374: 893-902.

7. Lynch JP, III, Zhanel GG: *Streptococcus pneumoniae*: epidemiology and risk factors, evolution of antimicrobial resistance, and impact of vaccines. *Curr Opin Pulm Med* 2010, 16: 217-225.

8. Obaro S: Seven-valent pneumococcal conjugate vaccines for developing countries. *Expert Rev Vaccines* 2009, 8: 1051-1061.

9. Nelson AL, Roche AM, Gould JM, Chim K, Ratner AJ, Weiser JN: Capsule enhances pneumococcal colonization by limiting mucus-mediated clearance. *Infect Immun* 2007, 75: 83-90.

10. van der PT, Opal SM: Pathogenesis, treatment, and prevention of pneumococcal pneumonia. *Lancet* 2009, 374: 1543-1556.

11. Bratcher PE, Kim KH, Kang JH, Hong JY, Nahm MH: Identification of natural pneumococcal isolates expressing serotype 6D by genetic, biochemical and serological characterization. *Microbiology* 2010, 156: 555-560.

12. Calix JJ, Nahm MH: A new pneumococcal serotype, 11E, has a variably inactivated wcjE gene. *J Infect Dis* 2010, 202: 29-38.

13. Park IH, Pritchard DG, Cartee R, Brandao A, Brandileone MC, Nahm MH: Discovery of a new capsular serotype (6C) within serogroup 6 of *Streptococcus pneumoniae. J Clin Microbiol* 2007, 45: 1225-1233.

14. Chan MS, Maiden MC, Spratt BG: Database-driven multi locus sequence typing (MLST) of bacterial pathogens. *Bioinformatics* 2001, 17: 1077-1083.

15. Spratt BG, Hanage WP, Li B, Aanensen DM, Feil EJ: Displaying the relatedness among isolates of bacterial species -- the eBURST approach. *FEMS Microbiol Lett* 2004, 241: 129-134.

16. Feil EJ, Li BC, Aanensen DM, Hanage WP, Spratt BG: eBURST: inferring patterns of evolutionary descent among clusters of related bacterial genotypes from multilocus sequence typing data. *J Bacteriol* 2004, 186: 1518-1530.

17. Kadioglu A, Weiser JN, Paton JC, Andrew PW: The role of *Streptococcus pneumoniae* virulence factors in host respiratory colonization and disease. *Nat Rev Microbiol* 2008, 6: 288-301.

18. Cadoz M, Armand J, Arminjon F, Michel JP, Michel M, Denis F *et al*.: A new 23 valent pneumococcal vaccine: immunogenicity and reactogenicity in adults. *J Biol Stand* 1985, 13: 261-265.

19. Prevention of pneumococcal disease: recommendations of the Advisory Committee on Immunization Practices (ACIP). *MMWR Recomm Rep* 1997, 46: 1-24.

20. Mangtani P, Cutts F, Hall AJ: Efficacy of polysaccharide pneumococcal vaccine in adults in more developed countries: the state of the evidence. *Lancet Infect Dis* 2003, 3: 71-78.

21. Jackson LA, Neuzil KM, Yu O, Benson P, Barlow WE, Adams AL *et al*.: Effectiveness of pneumococcal polysaccharide vaccine in older adults. *N Engl J Med* 2003, 348: 1747-1755.

22. Wadwa RP, Feigin RD: Pneumococcal vaccine: an update. *Pediatrics* 1999, 103: 1035-1037.

23. Poland GA: The burden of pneumococcal disease: the role of conjugate vaccines. *Vaccine* 1999, 17: 1674-1679.

24. O'Brien KL, Millar EV, Zell ER, Bronsdon M, Weatherholtz R, Reid R *et al*.: Effect of pneumococcal conjugate vaccine on nasopharyngeal colonization among immunized and unimmunized children in a community-randomized trial. *J Infect Dis* 2007, 196: 1211-1220.

25. Kieninger DM, Kueper K, Steul K, Juergens C, Ahlers N, Baker S *et al*.: Safety, tolerability, and immunologic noninferiority of a 13-valent pneumococcal conjugate vaccine compared to a 7-valent pneumococcal conjugate vaccine given with routine pediatric vaccinations in Germany. *Vaccine* 2010, 28: 4192-4203.

26. Giefing C, Meinke AL, Hanner M, Henics T, Bui MD, Gelbmann D *et al*.: Discovery of a novel class of highly conserved vaccine antigens using genomic scale antigenic fingerprinting of pneumococcus with human antibodies. *J Exp Med* 2008, 205: 117-131.

27. Esposito S, Tansey S, Thompson A, Razmpour A, Liang J, Jones TR *et al*.: Safety and immunogenicity of a 13-valent pneumococcal conjugate vaccine compared to those of a 7-valent pneumococcal conjugate vaccine given as a three-dose series with routine vaccines in healthy infants and toddlers. *Clin Vaccine Immunol* 2010, 17: 1017-1026.

28. Licensure of a 13-valent pneumococcal conjugate vaccine (PCV13) and recommendations for use among children - Advisory Committee on Immunization Practices (ACIP), 2010. *MMWR Morb Mortal Wkly Rep* 2010, 59: 258-261.

29. Pai R, Moore MR, Pilishvili T, Gertz RE, Whitney CG, Beall B: Postvaccine genetic structure of *Streptococcus pneumoniae* serotype 19A from children in the United States. *J Infect Dis* 2005, 192: 1988-1995.

30. Gonzalez BE, Hulten KG, Lamberth L, Kaplan SL, Mason EO, Jr.: *Streptococcus pneumoniae* serogroups 15 and 33: an increasing cause of pneumococcal infections in children in the United States after the introduction of the pneumococcal 7-valent conjugate vaccine. *Pediatr Infect Dis J* 2006, 25: 301-305.

31. Bogaert D, Hermans PW, Adrian PV, Rumke HC, De GR: Pneumococcal vaccines: an update on current strategies. *Vaccine* 2004, 22: 2209-2220.

32. Chen Q, Cannons JL, Paton JC, Akiba H, Schwartzberg PL, Snapper CM: A novel ICOS-independent, but CD28- and SAP-dependent, pathway of T cell-dependent, polysaccharide-specific humoral immunity in response to intact *Streptococcus pneumoniae* versus pneumococcal conjugate vaccine. *J Immunol* 2008, 181: 8258-8266.

33. Wizemann TM, Heinrichs JH, Adamou JE, Erwin AL, Kunsch C, Choi GH *et al*.: Use of a whole genome approach to identify vaccine molecules affording protection against *Streptococcus pneumoniae* infection. *Infect Immun* 2001, 69: 1593-1598.

34. Kadioglu A, Weiser JN, Paton JC, Andrew PW: The role of *Streptococcus pneumoniae* virulence factors in host respiratory colonization and disease. *Nat Rev Microbiol* 2008, 6: 288-301.

35. Tilley SJ, Orlova EV, Gilbert RJ, Andrew PW, Saibil HR: Structural basis of pore formation by the bacterial toxin pneumolysin. *Cell* 2005, 121: 247-256.

36. Briles DE, Hollingshead S, Brooks-Walter A, Nabors GS, Ferguson L, Schilling M *et al*.: The potential to use PspA and other pneumococcal proteins to elicit protection against pneumococcal infection. *Vaccine* 2000, 18: 1707-1711.

37. Hoskins J, Alborn WE, Jr., Arnold J, Blaszczak LC, Burgett S, DeHoff BS *et al*.: Genome of the bacterium *Streptococcus pneumoniae* strain R6. *J Bacteriol* 2001, 183: 5709-5717.

38. Tettelin H, Nelson KE, Paulsen IT, Eisen JA, Read TD, Peterson S *et al*.: Complete genome sequence of a virulent isolate of *Streptococcus pneumoniae*. *Science* 2001, 293: 498-506.

39. Berry AM, Paton JC: Additive attenuation of virulence of *Streptococcus pneumoniae* by mutation of the genes encoding pneumolysin and other putative pneumococcal virulence proteins. *Infect Immun* 2000, 68: 133-140.

40. Ogunniyi AD, Woodrow MC, Poolman JT, Paton JC: Protection against *Streptococcus pneumoniae* elicited by immunization with pneumolysin and CbpA. *Infect Immun* 2001, 69: 5997-6003.

41. Coats MT, Benjamin WH, Hollingshead SK, Briles DE: Antibodies to the pneumococcal surface protein A, PspA, can be produced in splenectomized and can protect splenectomized mice from infection with *Streptococcus pneumoniae*. *Vaccine* 2005, 23: 4257-4262.

42. Uchiyama S, Carlin AF, Khosravi A, Weiman S, Banerjee A, Quach D *et al*.: The surface-anchored NanA protein promotes pneumococcal brain endothelial cell invasion. *J Exp Med* 2009, 206: 1845-1852.

43. Noske N, Kammerer U, Rohde M, Hammerschmidt S: Pneumococcal interaction with human dendritic cells: phagocytosis, survival, and induced adaptive immune response are manipulated by PavA. *J Immunol* 2009, 183: 1952-1963.

44. Eldholm V, Johnsborg O, Haugen K, Ohnstad HS, Havarstein LS: Fratricide in *Streptococcus pneumoniae*: contributions and role of the cell wall hydrolases CbpD, LytA and LytC. *Microbiology* 2009, 155: 2223-2234.

45. Anderton JM, Rajam G, Romero-Steiner S, Summer S, Kowalczyk AP, Carlone GM *et al*.: E-cadherin is a receptor for the common protein pneumococcal surface adhesin A (PsaA) of *Streptococcus pneumoniae*. *Microb Pathog* 2007, 42: 225-236.

46. Barocchi MA, Ries J, Zogaj X, Hemsley C, Albiger B, Kanth A *et al*.: A pneumococcal pilus influences virulence and host inflammatory responses. *Proc Natl Acad Sci U S A* 2006, 103: 2857-2862.

47. Papasergi S, Garibaldi M, Tuscano G, Signorino G, Ricci S, Peppoloni S *et al*.: Plasminogen- and fibronectin-binding protein B is involved in the adherence of *Streptococcus pneumoniae* to human epithelial cells. *J Biol Chem* 2010, 285: 7517-7524.

48. Sanchez CJ, Shivshankar P, Stol K, Trakhtenbroit S, Sullam PM, Sauer K *et al*.: The pneumococcal serine-rich repeat protein is an intra-species bacterial adhesin that promotes bacterial aggregation in vivo and in biofilms. *PLoS Pathog* 2010, 6: e1001044.

49. Telford JL, Barocchi MA, Margarit I, Rappuoli R, Grandi G: Pili in gram-positive pathogens. *Nat Rev Microbiol* 2006, 4: 509-519.

50. Ton-That H, Schneewind O: Assembly of pili in Gram-positive bacteria. *Trends Microbiol* 2004, 12: 228-234.

51. Bagnoli F, Moschioni M, Donati C, Dimitrovska V, Ferlenghi I, Facciotti C *et al*.: A second pilus type in *Streptococcus pneumoniae* is prevalent in emerging serotypes and mediates adhesion to host cells. *J Bacteriol* 2008, 190: 5480-5492.

52. LeMieux J, Hava DL, Basset A, Camilli A: RrgA and RrgB are components of a multisubunit pilus encoded by the *Streptococcus pneumoniae rlrA* pathogenicity islet. *Infect Immun* 2006, 74: 2453-2456.

53. Proft T, Baker EN: Pili in Gram-negative and Gram-positive bacteria - structure, assembly and their role in disease. *Cell Mol Life Sci* 2009, 66: 613-635.

54. Kang HJ, Coulibaly F, Clow F, Proft T, Baker EN: Stabilizing isopeptide bonds revealed in gram-positive bacterial pilus structure. *Science* 2007, 318: 1625-1628.

55. Zahner D, Gudlavalleti A, Stephens DS: Increase in pilus islet 2-encoded pili among *Streptococcus pneumoniae* isolates, Atlanta, Georgia, USA. *Emerg Infect Dis* 2010, 16: 955-962.

56. Hava DL, Hemsley CJ, Camilli A: Transcriptional regulation in the *Streptococcus pneumoniae rlrA* pathogenicity islet by RlrA. *J Bacteriol* 2003, 185: 413-421.

57. Falker S, Nelson AL, Morfeldt E, Jonas K, Hultenby K, Ries J *et al*.: Sortase-mediated assembly and surface topology of adhesive pneumococcal pili. *Mol Microbiol* 2008, 70: 595-607.

58. LeMieux J, Woody S, Camilli A: Roles of the sortases of *Streptococcus pneumoniae* in assembly of the *rlrA* pilus. *J Bacteriol* 2008, 190: 6002-6013.

59. Manzano C, Contreras-Martel C, El ML, Izore T, Fenel D, Vernet T *et al*.: Sortase-mediated pilus fiber biogenesis in *Streptococcus pneumoniae. Structure* 2008, 16: 1838-1848.

60. Hilleringmann M, Giusti F, Baudner BC, Masignani V, Covacci A, Rappuoli R *et al*.: Pneumococcal pili are composed of protofilaments exposing adhesive clusters of Rrg A. *PLoS Pathog* 2008, 4: e1000026.

61. Nelson AL, Ries J, Bagnoli F, Dahlberg S, Falker S, Rounioja S *et al*.: RrgA is a pilus-associated adhesin in Streptococcus pneumoniae. *Mol Microbiol* 2007, 66: 329-340.

62. Moschioni M, Donati C, Muzzi A, Masignani V, Censini S, Hanage WP *et al*.: *Streptococcus pneumoniae* contains 3 *rlrA* pilus variants that are clonally related. *J Infect Dis* 2008, 197: 888-896.

63. Izore T, Contreras-Martel C, El ML, Manzano C, Terrasse R, Vernet T *et al*.: Structural basis of host cell recognition by the pilus adhesin from *Streptococcus pneumoniae*. *Structure* 2010, 18: 106-115.

64. Paterson NG, Baker EN: Structure of the full-length major pilin from *Streptococcus pneumoniae:* implications for isopeptide bond formation in gram-positive bacterial pili. *PLoS One* 2011, 6: e22095.

65. Aguiar SI, Serrano I, Pinto FR, Melo-Cristino J, Ramirez M: The presence of the pilus locus is a clonal property among pneumococcal invasive isolates. *BMC Microbiol* 2008, 8: 41.

66. Basset A, Trzcinski K, Hermos C, O'Brien KL, Reid R, Santosham M *et al*.: Association of the pneumococcal pilus with certain capsular serotypes but not with increased virulence. *J Clin Microbiol* 2007, 45: 1684-1689.

67. Hemsley C, Joyce E, Hava DL, Kawale A, Camilli A: MgrA, an orthologue of Mga, Acts as a transcriptional repressor of the genes within the *rlrA* pathogenicity islet in *Streptococcus pneumoniae*. *J Bacteriol* 2003, 185: 6640-6647.

68. Gianfaldoni C, Censini S, Hilleringmann M, Moschioni M, Facciotti C, Pansegrau W *et al*.: *Streptococcus pneumoniae* pilus subunits protect mice against lethal challenge. *Infect Immun* 2007, 75: 1059-1062.

69. Rosch JW, Mann B, Thornton J, Sublett J, Tuomanen E: Convergence of regulatory networks on the pilus locus of *Streptococcus pneumoniae*. *Infect Immun* 2008, 76: 3187-3196.

70. Rosch JW, Gao G, Ridout G, Wang YD, Tuomanen EI: Role of the manganese efflux system *mntE* for signalling and pathogenesis in *Streptococcus pneumoniae*. *Mol Microbiol* 2009, 72: 12-25.

71. Song XM, Connor W, Hokamp K, Babiuk LA, Potter AA: The growth phase-dependent regulation of the pilus locus genes by two-component system TCS08 in *Streptococcus pneumoniae*. *Microb Pathog* 2009, 46: 28-35.

72. Regev-Yochay G, Hanage WP, Trzcinski K, Rifas-Shiman SL, Lee G, Bessolo A *et al*.: Re-emergence of the type 1 pilus among *Streptococcus pneumoniae* isolates in Massachusetts, USA. *Vaccine* 2010, 28: 4842-4846.

73. Hallet B: Playing Dr Jekyll and Mr Hyde: combined mechanisms of phase variation in bacteria. *Curr Opin Microbiol* 2001, 4: 570-581.

74. Van der Woude MW, Baumler AJ: Phase and antigenic variation in bacteria. *Clin Microbiol Rev* 2004, 17: 581-611, table.

75. Waite RD, Penfold DW, Struthers JK, Dowson CG: Spontaneous sequence duplications within capsule genes *cap8E* and tts control phase variation in *Streptococcus pneumoniae* serotypes 8 and 37. *Microbiology* 2003, 149: 497-504.

76. Smits WK, Kuipers OP, Veening JW: Phenotypic variation in bacteria: the role of feedback regulation. *Nat Rev Microbiol* 2006, 4: 259-271.

77. Dubnau D, Losick R: Bistability in bacteria. *Mol Microbiol* 2006, 61: 564-572.

78. Steinmoen H, Knutsen E, Havarstein LS: Induction of natural competence in *Streptococcus pneumoniae* triggers lysis and DNA release from a subfraction of the cell population. *Proc Natl Acad Sci U S A* 2002, 99: 7681-7686.

79. Nallapareddy SR, Sillanpaa J, Mitchell J, Singh KV, Chowdhury SA, Weinstock GM *et al*.: Conservation of Ebp-type pilus genes among Enterococci and demonstration of their role in adherence of *Enterococcus faecalis* to human platelets. *Infect Immun* 2011, 79: 2911-2920.

80. Nakata M, Koller T, Moritz K, Ribardo D, Jonas L, McIver KS *et al*.: Mode of expression and functional characterization of FCT-3 pilus region-encoded proteins in *Streptococcus pyogenes* serotype M49. *Infect Immun* 2009, 77: 32-44.

81. Serkin CD, Seifert HS: Iron availability regulates DNA recombination in *Neisseria gonorrhoeae*. *Mol Microbiol* 2000, 37: 1075-1086.

82. Blomfield IaMVdW: Regulation and function of phase variation in *Escherichia coli*. In *Bacterial adhesion to host tissues: mechanisms and consequences*. Edited by M.Wilson. Cambridge, England: Cambridge University Press ; 2002:89-113.

83. Krabbe M. NWaDL: Environmental control of pilus gene expression. In *Bacterial stress responses*. Edited by G.Storz and R.Hengge-Aronis. Washington D.C.: ASM Press; 2000:305-321.

84. Zahner D, Hakenbeck R: The *Streptococcus pneumoniae* beta-galactosidase is a surface protein. *J Bacteriol* 2000, 182: 5919-5921.

85. Garcia-Suarez MM, Vazquez F, Mendez FJ: *Streptococcus pneumoniae* virulence factors and their clinical impact: An update. *Enferm Infecc Microbiol Clin* 2006, 24: 512-517.

86. Rioux S, Neyt C, Di PE, Turpin L, Charland N, Labbe S *et al*.: Transcriptional regulation, occurrence and putative role of the Pht Family of *Streptococcus pneumoniae*. *Microbiology* 2010.

87. Dave S, Brooks-Walter A, Pangburn MK, McDaniel LS: PspC, a pneumococcal surface protein, binds human factor H. *Infect Immun* 2001, 69: 3435-3437.

88. Janulczyk R, Masignani V, Maione D, Tettelin H, Grandi G, Telford JL: Simple sequence repeats and genome plasticity in *Streptococcus agalactiae*. *J Bacteriol* 2010, 192: 3990-4000.

89. Puopolo KM, Madoff LC: Upstream short sequence repeats regulate expression of the alpha C protein of group B Streptococcus. *Mol Microbiol* 2003, 50: 977-991.

90. Van Ham SM, Van AL, Mooi FR, Van Putten JP: Phase variation of *H. influenzae* fimbriae: transcriptional control of two divergent genes through a variable combined promoter region. *Cell* 1993, 73: 1187-1196.

91. Muzzi A, Moschioni M, Covacci A, Rappuoli R, Donati C: Pilus operon evolution in *Streptococcus pneumoniae* is driven by positive selection and recombination. *PLoS One* 2008, 3: e3660.

92. Kloosterman TG, Bijlsma JJ, Kok J, Kuipers OP: To have neighbour's fare: extending the molecular toolbox for *Streptococcus pneumoniae*. *Microbiology* 2006, 152: 351-359.

93. El Mortajl L, Terrasse R, Dessen A, Vernet T, Di Guilmi AM: Stability and assembly of pilus subunits of *Streptococcus pneumoniae. J Biol Chem* 2010, 285: 12405-12415.

94. Neiers F, Madhurantakam C, Falker S, Manzano C, Dessen A, Normark S *et al*.: Two crystal structures of pneumococcal pilus sortase C provide novel insights into catalysis and substrate specificity. *J Mol Biol* 2009, 393: 704-716.

95. Achen MG, Davidson BE, Hillier AJ: Construction of plasmid vectors for the detection of streptococcal promoters. *Gene* 1986, 45: 45-49.

96. Rozen S, Skaletsky H: Primer3 on the WWW for general users and for biologist programmers. *Methods Mol Biol* 2000, 132: 365-386.

97. Vallon-Christersson J, Nordborg N, Svensson M, Hakkinen J: BASE--2nd generation software for microarray data management and analysis. *BMC Bioinformatics* 2009, 10: 330.

98. Storey JD, Tibshirani R: Statistical significance for genomewide studies. *Proc Natl Acad Sci U S A* 2003, 100: 9440-9445.

99. Saeed AI, Bhagabati NK, Braisted JC, Liang W, Sharov V, Howe EA *et al*.: TM4 microarray software suite. *Methods Enzymol* 2006, 411: 134-193.

100. Alloing G, Martin B, Granadel C, Claverys JP: Development of competence in *Streptococcus pneumonaie*: pheromone autoinduction and control of quorum sensing by the oligopeptide permease. *Mol Microbiol* 1998, 29: 75-83.

101. Moschioni M, De Angelis G, Melchiorre S, Masignani V, Leibovitz E, Barocchi MA *et al*.: Prevalence of pilus encoding islets among acute otitis media *Streptococcus pneumoniae* isolates from Israel. *Clin Microbiol Infect* 2009.

102. Spraggon G, Koesema E, Scarselli M, Malito E, Biagini M, Norais N *et al*.: Supramolecular organization of the repetitive backbone unit of the *Streptococcus pneumoniae* pilus. *PLoS One* 2010, 5: e10919.

103. Turner KH, Vallet-Gely I, Dove SL: Epigenetic control of virulence gene expression in *Pseudomonas aeruginosa* by a LysR-type transcription regulator. *PLoS Genet* 2009, 5: e1000779.

104. Godfroid F, Hermand P, Verlant V, Denoel P, Poolman JT: Preclinical evaluation of the Pht proteins as potential cross-protective pneumococcal vaccine antigens. *Infect Immun* 2011, 79: 238-245.

105. Harfouche C, Filippini S, Gianfaldoni C, Ruggiero P, Moschioni M, Maccari S *et al*.: RrgB321, a fusion protein of the three variants of the pneumococcal pilus backbone RrgB, is protective in vivo and elicits opsonic antibodies. *Infect Immun* 2011.

106. Buttery J, Moxon ER: Capsulate bacteria and the lung. *Br Med Bull* 2002, 61: 63-80.

107. Kaplanski G, Marin V, Montero-Julian F, Mantovani A, Farnarier C: IL-6: a regulator of the transition from neutrophil to monocyte recruitment during inflammation. *Trends Immunol* 2003, 24: 25-29.

108. Romero-Steiner S, Libutti D, Pais LB, Dykes J, Anderson P, Whitin JC *et al*.: Standardization of an opsonophagocytic assay for the measurement of functional antibody activity against *Streptococcus pneumoniae* using differentiated HL-60 cells. *Clin Diagn Lab Immunol* 1997, 4: 415-422.

109. Kim KH, Yu J, Nahm MH: Efficiency of a pneumococcal opsonophagocytic killing assay improved by multiplexing and by coloring colonies. *Clin Diagn Lab Immunol* 2003, 10: 616-621.

110. Recommendations for the production and control of pneumococcal conjugate vaccines. WHO Technical Report Series 927[Annex 2], 64-98. 2005.

111. De Angelis G., Moschioni M, Muzzi A, Pezzicoli A, Censini S, Delany I *et al*.: The *Streptococcus pneumoniae* Pilus-1 Displays a Biphasic Expression Pattern. *PLoS One* 2011, 6: e21269.

112. Basset A, Turner KH, Boush E, Sayeed S, Dove SL, Malley R: Expression of the Type 1 Pneumococcal Pilus Is Bistable and Negatively Regulated by the Structural Component RrgA. *Infect Immun* 2011, 79: 2974-2983.

113. Burton RL, Nahm MH: Development and validation of a fourfold multiplexed opsonization assay (MOPA4) for pneumococcal antibodies. *Clin Vaccine Immunol* 2006, 13: 1004-1009.

114. Kreikemeyer B, Gamez G, Margarit I, Giard JC, Hammerschmidt S, Hartke A *et al*.: Genomic organization, structure, regulation and pathogenic role of pilus constituents in major pathogenic Streptococci and Enterococci. *Int J Med Microbiol* 2011, 301: 240-251.

115. Carbonnelle E, Hill DJ, Morand P, Griffiths NJ, Bourdoulous S, Murillo I *et al*.: Meningococcal interactions with the host. *Vaccine* 2009, 27 Suppl 2: B78-B89.

116. Proft T, Baker EN: Pili in Gram-negative and Gram-positive bacteria - structure, assembly and their role in disease. *Cell Mol Life Sci* 2009, 66: 613-635.

Publications:

During my PhD program I worked at Novartis Vaccines and Diagnostics on a project aiming at the development of a protein-based vaccine against *Streptococcus pneumoniae*. In particular, I focused my research on characterization of pilus-1 components.

During my PhD I have been coauthor of the following manuscripts:

1. Moschioni M, **De Angelis G**, Harfouche C, Bizzarri E, Filippini S *et al.* (2011) Immunization with the RrgB321 fusion protein protects mice against both High and Low pilus-expressing *Streptococcus pneumoniae* populations. *Submitted to Vaccine journal.*

2. **De Angelis G**, Moschioni M, Muzzi A, Pezzicoli A, Censini S, *et al*. (2011) The *Streptococcus pneumoniae* Pilus-1 Displays a Biphasic Expression Pattern. *PLoS ONE* 6(6): e21269.

3. Hilleringmann M, Ringler P, Müller SA, **De Angelis G**, Rappuoli R, Ferlenghi I, Engel A. Molecular architecture of *Streptococcus pneumoniae* TIGR4 pili. *EMBO J. 2009 Dec 16;28(24):3921-30*

4. Moschioni M, **De Angelis G**, Melchiorre S, Masignani V, Leibovitz E, Barocchi MA, Dagan R. Prevalence of pilus encoding islets among acute otitis media *Streptococcus pneumoniae* isolates from Israel. *Clin Microbiol Infect.* 2010 Sep;16(9):1501-4

The content of publications 1 and 2 are the object of this thesis, the other publications are reported in appendix.

Communications:

- *June 23-27, 2011:* 10th European Meeting on the Molecular Biology of the Pneumococcus (EuroPneumo2011), Amsterdam, Holland

- *June 11-13, 2009:* XXVIII National Meeting, Società Italiana di Microbiologia Generale e Biotecnologie Microbiche (SIMGBM), Spoleto, Italy

Abroad experience:

April-August 2010: Internship at the Microbiology and Immunology Department (Prof. Carlos J. Orihuela), University of Texas Health Science Center – San Antonio (UTHSCSA), San Antonio (Tx), USA.

The EMBO Journal (2009) 28, 3921–3930 | © 2009 European Molecular Biology Organization | All Rights Reserved 0261-4189/09
www.embojournal.org

THE EMBO JOURNAL

Molecular architecture of *Streptococcus pneumoniae* TIGR4 pili

Markus Hilleringmann[1,3], Philippe Ringler[2,3], Shirley A Müller[2], Gabriella De Angelis[1], Rino Rappuoli[1,*], Ilaria Ferlenghi[1] and Andreas Engel[2,*]

[1]Research Center, Novartis Vaccines and Diagnostics s.r.l., Siena, Italy and [2]Maurice E Müller Institute for Structural Biology and C-CINA, Biozentrum, University of Basel, Basel, Switzerland

Although the pili of Gram-positive bacteria are putative virulence factors, little is known about their structure. Here we describe the molecular architecture of pilus-1 of *Streptococcus pneumoniae*, which is a major cause of morbidity and mortality worldwide. One major (RrgB) and two minor components (RrgA and RrgC) assemble into the pilus. Results from TEM and scanning transmission EM show that the native pili are approximately 6 nm wide, flexible filaments that can be over 1 μm long. They are formed by a single string of RrgB monomers and have a polarity defined by nose-like protrusions. These protrusions correlate to the shape of monomeric RrgB–His, which like RrgA–His and RrgC–His has an elongated, multi-domain structure. RrgA and RrgC are only present at the opposite ends of the pilus shaft, compatible with their putative roles as adhesin and anchor to the cell wall surface, respectively. Our structural analyses provide the first direct experimental evidence that the native *S. pneumoniae* pilus shaft is composed exclusively of covalently linked monomeric RrgB subunits oriented head-to-tail.

The EMBO Journal (2009) **28,** 3921–3930. doi:10.1038/emboj.2009.360; Published online 26 November 2009
Subject Categories: microbiology & pathogens; structural biology
Keywords: Gram-positive bacteria; mass measurement; pilus; STEM; *Streptococcus pneumoniae*

Introduction

Various types of filamentous surface appendages, pili, have been identified in Gram-negative and Gram-positive bacteria (Wu and Fives-Taylor, 2001). Pili fulfill manifold functions during bacterial life cycles, such as host cell invasion, biofilm formation, cell aggregation, DNA transfer and twitching motility (Proft and Baker, 2009). Their structure has to withstand both environmental stress and the activities of the host immune system. The role of pili as adhesive organelles is crucial to the survival of pathogenic bacteria, which have to attach to specific host cells for colonisation and to establish an infection. While many Gram-negative pili have been studied in detail over the last decades (Fronzes *et al*, 2008), the majority of Gram-positive pili have been discovered only recently and their study, initiated through pioneering work by Schneewind and co-workers on *Corynebacterium diphtheriae* pili (Ton-That and Schneewind, 2003; Ton-That *et al*, 2004), is in its infancy. In contrast to Gram-negative pili, which are typically formed by non-covalently linked subunits, Gram-positive pili are extended polymers assembled from covalently cross-linked pilin subunits and tethered to the cell wall peptidoglycan (reviewed by Ton-That and Schneewind, 2004; Telford *et al*, 2006; Mandlik *et al*, 2008b). As demonstrated for the major pilin subunit of *C. diphtheriae*, the conserved genetic requirements necessary for pilus formation include the pilin motif (WXXXVXVYPKN), the E-box domain (YXLXETXAPXGY) and the cell wall sorting signal (LPXTG), followed first by hydrophobic and then by charged amino acids (Ton-That and Schneewind, 2003, 2004; Ton-That *et al*, 2004). Mass spectrometric studies of pilus fragments of *Bacillus anthracis* have confirmed the existence of intermolecular amide bonds between the C-terminal threonine of cleaved sorting signals and the conserved lysine residue (YPKN) within the pilin motif (Budzik *et al*, 2008). However, the structure of the backbone pilin Spy0128 of *Streptococcus pyogenes* and mass spectrometric analysis of pilus fractions showed the isopeptide bond to link the threonine of the sorting signal EVPTG with a conserved lysine that is close to but not within the pilin-like motif (Kang *et al*, 2007). Sortases catalyse the reaction between the threonine of the LPXTG motif and the conserved lysine of the next backbone-forming protein (Marraffini *et al*, 2006; Manzano *et al*, 2008; Neiers *et al*, 2009), and also anchor pili in the cell wall, as demonstrated for several bacterial genera (Swaminathan *et al*, 2007; Budzik *et al*, 2008; Mandlik *et al*, 2008a; Nobbs *et al*, 2008; Neiers *et al*, 2009).

The Gram-positive bacterium *Streptococcus pneumoniae*, also known as pneumococcus, is a major human pathogen (Lode, 2009). The clinical serotype-4 strain *S. pneumoniae* TIGR4 (TIGR4) forms long pili (Barocchi *et al*, 2006; Hilleringmann *et al*, 2008) and its virulence depends on them (Barocchi *et al*, 2006; Rosch *et al*, 2008). However, the second pneumococcal pilus found recently (Bagnoli *et al*, 2008) has not been detected. The long *S. pneumoniae* TIGR4 pili are encoded by the *rlrA* pathogenicity islet that includes a Rof-A-like transcriptional regulator (RlrA), three sortases (SrtC-1, SrtC-2 and SrtC-3) and three structural proteins RrgA (Swiss-Prot Q97SC3), RrgB (Swiss-Prot Q97SC2) and RrgC (Swiss-Prot Q97SC1), all of which contain an LPXTG motif (or variants thereof). As pneumococcal RrgB possesses the conserved motifs necessary for pilus formation (Ton-That and Schneewind, 2003, 2004; Ton-That *et al*, 2004), it has been suspected to form the backbone of the pneumococcal

*Corresponding authors. A Engel, Maurice E Müller Institute for Structural Biology and C-CINA, University of Basel, WRO-1058.P.18, Mattenstrasse 26, Basel CH-4056, Switzerland. Tel.: +41 61 387 32 17; Fax: +41 61 387 39 86; E-mail: andreas.engel@unibas.ch or R Rappuoli, Research Center, Novartis Vaccines and Diagnostics s.r.l., Via Fiorentina 1, Siena, Italy. Tel.: +39 0577 243414; Fax: +39 0577 243564; E-mail: rino.rappuoli@novartis.com
[3]These authors contributed equally to this work

Received: 12 June 2009; accepted: 6 November 2009; published online: 26 November 2009

TIGR4 pilus, as indeed implied by immunoelectron microscopy (immuno-EM; Barocchi *et al*, 2006; LeMieux *et al*, 2006; Hilleringmann *et al*, 2008). This supposition was recently proved correct by the work of Fälker *et al* (2008), which revealed that only RrgB is required for pilus formation. Roles as ancillary proteins have been suggested for the two other components, RrgA and RrgC (Barocchi *et al*, 2006; LeMieux *et al*, 2006, 2008; Nelson *et al*, 2007; Hilleringmann *et al*, 2008).

Immuno-EM has been used to unravel the location of the various pilus proteins since the first molecular description of Gram-positive pili (Ton-That and Schneewind, 2003). Antibodies targeted to RrgB, the major pilus building block of pneumococcal TIGR4 pili, were consistently found to bind along the filaments (Barocchi *et al*, 2006; LeMieux *et al*, 2006; Hilleringmann *et al*, 2008). Results concerning the location of the ancillary proteins RrgA and RrgC are less consistent: anti-RrgA is reported to bind in regularly spaced clusters along the pili (LeMieux *et al*, 2006) and close to the cell surface in the absence of both RrgB and RrgC (LeMieux *et al*, 2006; Nelson *et al*, 2007). Triple labelling has shown RrgA clusters to decorate pilus assemblies randomly and independent of RrgC distribution (Nelson *et al*, 2007; Hilleringmann *et al*, 2008), whereas a colocalisation of RrgA and RrgC in clusters has been observed by double-labelling experiments (Fälker *et al*, 2008). In addition, surface topographs acquired by atomic-force microscopy allowed identification of RrgC at the ends of detached pili (Fälker *et al*, 2008). Given these, in part contradictory, data the localisation of the three proteins in the pilus is still uncertain. In fact, both local association of RrgA and RrgC to the pilus shaft and their incorporation within it have been proposed (LeMieux *et al*, 2006; Nelson *et al*, 2007; Fälker *et al*, 2008; Hilleringmann *et al*, 2008).

The pilus-specific TIGR4 sortases, SrtC-1, SrtC-2 and SrtC-3 (formerly SrtB, SrtC and SrtD) diverge in sequence from the housekeeping sortase, SrtA, the latter being dispensable for pilus assembly and localisation to the cell wall (LeMieux *et al*, 2008). Class-C sortases exhibit functional redundancy concerning pilus assembly and cell wall localisation (LeMieux *et al*, 2008; Manzano *et al*, 2008; Neiers *et al*, 2009). One study showed SrtC-1 and SrtC-3 to be required for incorporation of the ancillary subunits (LeMieux *et al*, 2008), while another report suggested SrtC-1 and SrtC-2 to differ only in their ability to incorporate RrgC (Neiers *et al*, 2009). Manzano *et al* (2008) demonstrated that SrtC-1 assembles RrgB fibres with high efficiency *in vitro*, whereas SrtC-3 has a much smaller fibre-assembling capacity and SrtC-2 has none at all. Negative-stain EM showed that these *in vitro* fibres mimic the pneumococcal pilus backbone with its beaded appearance. The structures of SrtC-1 and SrtC-3 both exhibit a flexible lid that shields the active site (Manzano *et al*, 2008). Based on this information a universal mechanism for pilus biogenesis was proposed, where class-C sortases with encapsulated active sites require activation by their specific substrate for pilus assembly (Manzano *et al*, 2008). Most recently, the structure of SrtC-2, showing the lid for this sortase as well, corroborated this hypothesis (Neiers *et al*, 2009).

Although genetically based functional and epidemiological studies have substantially increased our understanding of Gram-positive pili (Telford *et al*, 2006), information on their native structure is lacking. Crystal structures of single pilus subunits of *Streptococcus agalactiae* (GBS) and *S. pyogenes* (GAS) have given novel insights into Gram-positive pilus structure: Krishnan *et al* (2007) describe the ancillary protein GBS52 as having a typical adhesin fold with two immunoglobulin-like domains. The first crystal structure of a Gram-positive pilus backbone protein showed the GAS shaft subunit, Spy0128, as an extended protein comprising two Ig-like domains and two intramolecular isopeptide bonds (Kang *et al*, 2007). These intramolecular bonds are likely to dictate pilus integrity, and a model based on Spy0128 describes the pilus fibre as a chain of individual subunits covalently linked head-to-tail by intermolecular peptide bonds (Kang *et al*, 2007; Kang and Baker, 2009).

Given the fundamental structural difference between Gram-positive pili and their Gram-negative counterparts, and the significance these pili have during the bacterial life cycle, the elucidation of their native structure is of importance, not only to increase our understanding of the biology of Gram-positive bacteria, but also of related human disease. Here we study the molecular architecture of a Gram-positive pilus. We visualise native pneumococcal TIGR4 pili using a combination of electron microscopic techniques and show the pilus as a chain of RrgB proteins covalently linked head-to-tail, with the ancillary proteins RrgA and RrgC at its distal and proximal ends, respectively. Our results provide the first direct electron microscopic evidence for a simple Gram-positive pilus architecture, and resolve some of the open questions concerning the location and function of RrgA and RrgC.

Results

Overall morphology of native pneumococcal TIGR4 pili

As documented earlier, the surface of the *S. pneumoniae* TIGR4 bacteria examined was covered by a non-homogenous distribution of pili (Barocchi *et al*, 2006). Different phenotypes of varying complexity have been described for these long structures (Barocchi *et al*, 2006; LeMieux *et al*, 2006; Hilleringmann *et al*, 2008). When TIGR4 bacteria were imaged by negative-stain EM after minimum perturbation (see section Materials and methods), the pili were seen as

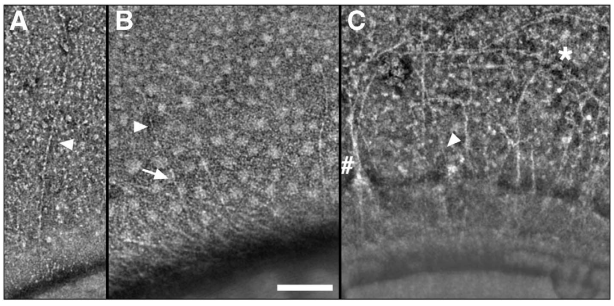

Figure 1 The pili of *S. pneumoniae* TIGR4 bacteria imaged by negative-stain TEM. (**A**) Fine pili protruding from the bacterial surface (arrowheads). (**B**) Second example illustrating the variability in pilus number. Note that the individual pili (arrowhead) appear wider close the cell surface (arrow) due to different negative staining. (**C**) Third example illustrating the pilus bundles (#) and tangles (*) that can form. Some individual pili can also be detected (arrowhead). Pili can be followed back to the bacterial surface. Negative stain: 2% phosphotungstic acid (PTA). A high-pass filter was applied to increase pilus visibility. Scale bar: 100 nm.

fine flexible filaments ~6 nm in diameter (Figure 1A–C, arrowheads) that could be at least 1.5 μm long. In some cases changes in the degree of negative staining caused them to appear wider close to the bacterial surface (Figure 1B, arrow). A distinct tendency of the pili to associate into bundles of various diameters (Figure 1C, #) or, at larger distances from the bacterium, to intertwine to form tangles was also detected (Figure 1C, *). Both types of association were random and probably dependent on the bacterium, the negative-staining agent and grid handling. The resulting aggregates correlate well with the phenotypes of varying complexity detected previously primarily by immuno-EM (Barocchi *et al*, 2006; Hilleringmann *et al*, 2008), a technique that cannot match the structural resolution obtained by negative-stain transmission EM (TEM). Our results suggest that pneumococcal TIGR4 pili are single filaments and that the aggregates and super-helical assemblies previously observed are sample preparation artefacts. The degree to which the bacterial capsule and attached filaments could be visualised in the present experiments depended on the negative stain used. Under optimum staining conditions the fine ~6-nm-wide pili could be followed all the way to the cell boundary (Figure 1C).

The pilus shaft is formed by RrgB and has RrgA and RrgC at its ends

TIGR4 bacteria were treated with the murein-hydrolysing enzyme mutanolysin to release their peptidoglycan-anchored pili into the supernatant. Using a modified procedure of Hilleringmann *et al* (2008), the liberated pili were then isolated in 10 mM Tris–HCl (pH 8), 1 mM EDTA and 1 mM DTT (see section Materials and methods). Under the transmission electron microscope TIGR4 pili appeared as long, flexible, ~6-nm-wide filaments (Figure 2A), with the general morphology observed *in situ* (Figure 1). The structure revealed in enlarged views (Figure 2A, inset) bears some similarity to that of RrgB filaments assembled *in vitro* (Manzano *et al*, 2008). Analysis of the same high-molecular-weight (HMW) fractions by SDS–PAGE and Western blotting documented the presence of all three pilus proteins, RrgA, RrgB and RrgC (Figure 2B). In agreement with previous reports (LeMieux *et al*, 2006, 2008; Fälker *et al*, 2008; Hilleringmann *et al*, 2008) RrgB was found to be the major constituent and RrgA and RrgC only accounted for a minor fraction of the total protein present. The HMW fractions observed for RrgB confirm the covalent association of Gram-positive pilus subunits previously reported (Telford *et al*, 2006).

Immunolabelling was used to localise all three proteins within the pilus structure. In contrast to previous reports, we directly visualised primary antibodies to overcome the resolution limit imposed by the size of the primary and secondary gold-bearing antibody complex (Barocchi *et al*, 2006; LeMieux *et al*, 2006; Fälker *et al*, 2008; Hilleringmann *et al*, 2008). The polyclonal antibodies generally used for Western blots were purified further according to the protocol of Mueller *et al* (2005), were highly specific and did not show cross-reactivity (Supplementary Figure S1). Their concentrations were adjusted to show binding but minimise the number of free antibodies in the solutions. Anti-RrgB–His antibodies decorated the pilus shaft at irregular intervals and, having two binding sites, often linked pili together forming ladder- and net-like assemblies depending on the degree of lateral cross-linking (Figure 2C and Supplementary Figure S2). Views of single antibodies are shown in the inset of Figure 2D for comparison. In contrast to anti-RrgB–His antibodies, antibodies against RrgA–His only bound at the end of pili, generally clustering and, as they are divalent, frequently linking two pili together in typical v-shaped assemblies not otherwise observed (Figure 2D and Supplementary Figure S3). Anti-RrgC–His also bound at the end of the pilus shaft and sometimes clustered there (Figure 2E and Supplementary Figure S4). As RrgC is two times smaller than RrgA (see below and Figure 3), the capacity of anti-RrgC–His to link two fibres appears to be much diminished. As polyclonal antibodies were used, the formation of antibody clusters does not necessarily mean that there is more than one copy of the labelled protein present. Neither anti-RrgA–His nor anti-RrgC–His decorated the pilus shaft, and the ladder-like assemblies typical of anti-RrgB–His were not formed. Occasionally an antibody was extremely close to the side of a pilus, but this was a chance occurrence rather than specific binding as it was rare and reflected the free antibody concentration and distribution on the grid. Accordingly, the results show that RrgA and RrgC are present at the ends of the pilus shaft formed by RrgB, and strongly imply that these two ancillary proteins are neither incorporated in nor associated with it. In confirmation, mutant bacteria lacking either RrgA or, RrgC or both (Supplementary Figure S5) still form long pili with the shaft morphology of the wild type (see below; Supplementary Figure S6 and reference Fälker *et al*, 2008).

All three pilus components have an elongated structure with several domains

To acquire further structural information, the three pilus components were expressed in *Escherichia coli* with an engineered C-terminal His_6 tag but otherwise mimicking the predicted processed forms, which are lacking the N-terminal signal sequence and the C-terminal region starting from the respective LPXTG sorting motif (Supplementary Figure S7). The affinity purified RrgA–His (93.37 kDa), RrgB–His (66.29 kDa) and RrgC–His (40.26 kDa) proteins were examined by EM. First, the oligomeric state of RrgA–His was defined by scanning TEM (STEM) mass measurements. The measured mass of 108 (±42)kDa ($n = 319$) clearly showed the large majority of the protein to be monomeric (Supplementary Figure S8A). Also, all three proteins were imaged by negative-stain TEM. The average projections calculated by single-particle analysis of TEM electron micrographs and STEM single-shot images are shown in Figure 3. RrgA–His is a flexible, ~18-nm-long, elongated macromolecule with four domains of unequal size. These domains give the structure a distinct taper, one end being ~5 nm wide and the other ~3 nm wide (Figure 3A). RrgB–His is an ~12-nm-long, elongated particle (Figure 3B). Up to three domains can be detected and, depending on the orientation, a lateral protrusion is sometimes discernible. The domains are almost 5 nm wide without and ~6.5 nm wide with the protrusion. Being of about 2/3 the length of RrgA–His and roughly the same width, the imaged RrgB–His was monomeric. The overall shape of the RrgB–His particles is compatible with the partial 2.2-Å X-ray structure of Spy0128 (aa 18–308), the major pilin subunit of the Gram-positive human pathogen

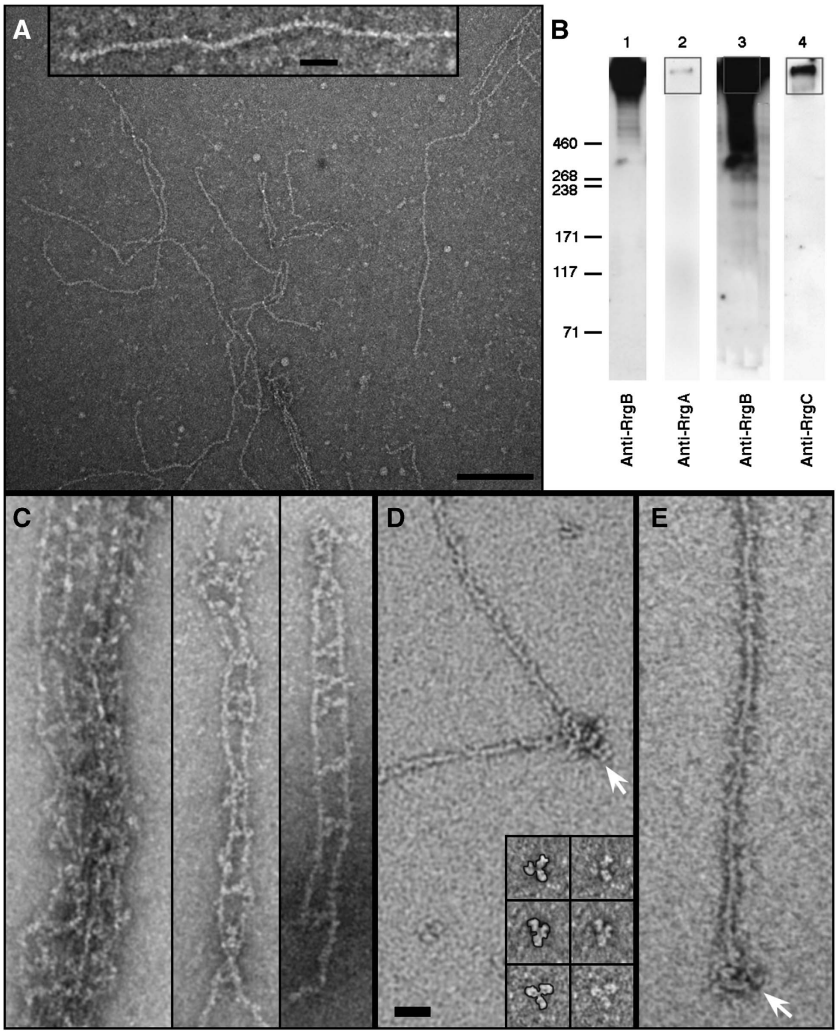

Figure 2 Constituents of isolated TIGR4 pili and their structural significance. (**A**) TEM image of TIGR4 pili isolated in Tris buffer and negatively stained with 2% UAc. A beaded structure is evident in an enlarged view (inset). (**B**) Western blot analysis of the HMW pilus fractions. RrgB forms a ladder of HMW polymers (lane 1, anti-RrgB-His antibody). Loading equal volumes showed the HMW pilus material to contain different amounts of RrgA (lane 2), RrgB (lane 3) and RrgC (lane 4) as measured by Western blotting with anti-RrgA–His, anti-RrgB–His and anti-RrgC–His antibodies, respectively. (**C**) TEM images of TIGR4 pili after incubation with antibodies to RrgB–His. Single antibodies link the pili laterally to form ladder-like structures. (**D**) TEM image of TIGR4 pili after incubation with antibodies to RrgA–His. A cluster of antibodies (white arrow) links the pili together at their ends; the individual antibodies are difficult to distinguish. Such v-shaped pilus assemblies were typical. Inset: various orientations of individual antibodies and traces indicating their outer contours. (**E**) TEM image of a TIGR4 pilus after incubation with antibodies to RrgC-His. A single antibody is attached to the end of the pilus (white arrow). Note the absence of antibodies along the pilus shafts in panels D and E. Scale bars: panel A, 100 nm, inset 20 nm; panels C–E and inset in panel D, 20 nm.

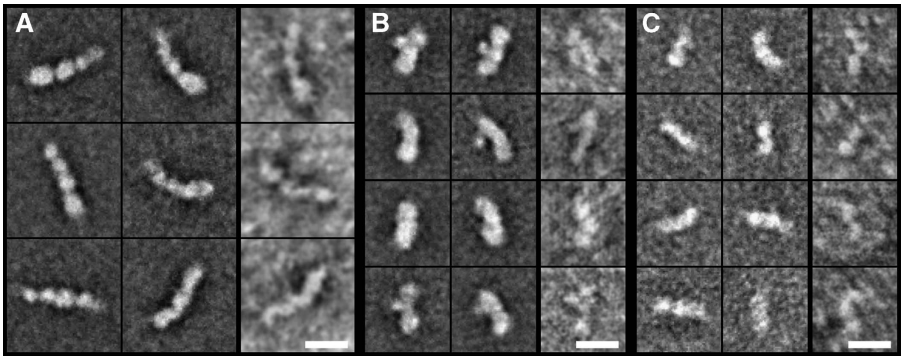

Figure 3 EM of the purified pilus constituents. Representative negative stain (2% UAc) TEM averages (left gallery) and contrast reversed STEM single-shot, dark-field images (right gallery) are shown. (**A**) RrgA–His. The averages were calculated by sorting 592 single projections into 19 classes. (**B**) RrgB–His. The averages were calculated by sorting 706 single projections into 14 classes. (**C**) RrgC–His. The averages were calculated by sorting 256 single projections into 12 classes. Scale bar: 10 nm.

S. pyogenes (Kang *et al*, 2007). With 291 residues this construct is much smaller than RrgB, which comprises 608 residues in its predicted processed form. This explains the different dimensions of the two structures, the Spy0128 construct being 2–3 nm wide and 9.8 nm long, that is, half as wide and 20% shorter than the RrgB–His class averages. Images of RrgC–His, the smallest of the three pilus proteins, revealed up to 4-nm-wide and 10-nm-long elongated particles with 2–3 domains (Figure 3C). From these dimensions the protein was also monomeric, as confirmed by size-exclusion chromatography (data not shown).

The shaft subunits are RrgB monomers and these give the pilus a distinct polarity

The mass-per-length of freeze-dried, unstained, isolated TIGR4 wt pili (Figure 4A) was measured by STEM to determine the stoichiometry of their RrgB subunits. The 395 segments evaluated gave a histogram with a single peak at 6.4 (±1.4)kDa/nm (standard error, 0.07 kDa/nm; Figure 4B). Given the ±5% overall precision of the STEM measurement (Müller and Engel, 2006), this indicates the presence of one 65.44-kDa RrgB monomer every 10.2 (±0.5)nm on average, which is slightly shorter than the length determined for a recombinant RrgB-His monomer, ~12 nm. As expected the mass-per-length of TIGR4 Δ*rrgA* pili was comparable (Supplementary Figure S8B).

The high signal-to-noise ratio of the STEM was also exploited to examine negatively stained TIGR4 pili. These images confirmed that the pilus is formed by a single string of subunits and revealed a well-defined protrusion extending at irregular intervals from the filament shaft like a 'nose' (Figure 4C and D). Most importantly, they showed that this 'nose' points in a defined direction giving the pilus a distinct polarity. Where the boundaries of single subunits could be discerned (Figure 4C and Supplementary Figure S9, lines), their shapes correlated well to those of the RrgB–His class averages and single projections implying that the pilus 'nose' is the protrusion observed in some orientations of the macromolecule. In agreement with the measured mass-per-length, the subunit spacing (10.2 (±0.6)nm; marked by lines in Figure 4C and Supplementary Figure S9) was somewhat less than the length of an RrgB–His monomer, implying that adjacent RrgB monomers may overlap slightly, as detailed in Figure 4E and F. Close examination of the pili formed by TIGR4 Δ*rrgC*, TIGR4 Δ*rrgAC* bacteria revealed the same substructure, that is, a single string of monomeric RrgB subunits, with 'noses' protruding at irregular intervals (Supplementary Figure S6, insets).

As the 'nose' was not always visible at regular intervals along the pilus shaft under the preparation conditions used, the RrgB monomers do not appear to assemble according to a defined helical rule. In any case, the covalent bonds formed between the monomeric RrgB subunits and further possible molecular interactions not only allow the filaments to bend freely, but also permit a degree of rotation around the long filament axis under the forces encountered on adsorption to the EM grid.

The ancillary proteins RrgA and RrgC are localised at opposite ends of the pilus shaft

Knowledge of its existence allowed the fine 'nose' feature to be detected on TEM images and showed it to consistently point in one direction for longer pilus stretches, indicating that the individual RrgB pilus subunits are linked head-to-tail. Examination of the immunolabelling images with this information also clearly showed that anti-RrgA–His and anti-RrgC–His labelled opposite ends of the pilus shaft (Figure 5 and Supplementary Figure S10). The role of RrgA as a pilus-associated adhesin that is expected to locate at the distal end (Nelson *et al*, 2007; Hilleringmann *et al*, 2008), would suggest that RrgC is located at the proximal end of the pilus shaft. In accordance, the pili formed by a TIGR4 Δ*rrgC* genetic background (TIGR4 Δ*rrgC* and TIGR4 Δ*rrgAC*) detached more easily from the bacteria, resulting in the appearance of more HMW pili material in the culture supernatant (Supplementary Figure S11).

Discussion

Since Ton-That *et al*'s description of the pili of *C. diphtheriae* (Ton-That and Schneewind, 2003), many Gram-positive bacteria have been shown to possess such filamentous appendages, including group-A *Streptococci* (Mora *et al*, 2005), group-B *Streptococci* (Lauer *et al*, 2005), *S. pneumoniae* (Barocchi *et al*, 2006), *Enterococcus faecalis* (Nallapareddy *et al*, 2006), *Bacillus cereus* (Budzik *et al*, 2007) and actinomyces (Wu and Fives-Taylor, 2001; Ton-That *et al*, 2004). In addition, probable pilus loci have been identified by genome sequencing of *Streptococcus spp*. (Osaki *et al*, 2002; Xu *et al*, 2007). The adhesive function of pili (Barocchi *et al*, 2006; Dramsi *et al*, 2006) is critical for the attachment of pathogens to specific host cells during colonisation, and explains why pilus expression increases the pathogenicity of various Gram-positive bacteria in animal models (Hava and Camilli, 2002; Abbot *et al*, 2007; Maisey *et al*, 2007; Rosch *et al*, 2008). This central function has promoted several EM analyses of native pili attached to bacterial cells and after purification (LeMieux *et al*, 2006; Nelson *et al*, 2007; Fälker *et al*, 2008; Hilleringmann *et al*, 2008), as well as X-ray studies of Gram-positive pilus components (Kang *et al*, 2007; Krishnan *et al*, 2007) and of the pilus assembly machinery (Manzano *et al*, 2008; Neiers *et al*, 2009).

We have used TEM, antibody labelling and STEM to elucidate the structure of the native TIGR4 pilus. The shaft is an ~6-nm-wide, single chain of slightly overlapping, head-to-tail covalently linked, monomeric RrgB subunits and can be at least 1.5 μm long. According to the mass-per-length measurements by STEM, a 1.5-μm-long pilus comprises approximately 150 RrgB monomers. TIGR4 pili assembled in a Δ*rrgA*, Δ*rrgC* or Δ*rrgAC* genetic background were also examined after purification and exhibit the same length and morphology as the wt pilus. The two ancillary proteins RrgA and RrgC are found at opposite ends of the shaft. RrgA is distal and consequently, RrgC proximal to the bacterium, as illustrated in Figure 6.

The proposed model agrees with functional implications derived from the structures of the *S. pneumoniae* sortases SrtC-1 and SrtC-3 (Manzano *et al*, 2008), and SrtC-2 (Neiers *et al*, 2009). All of them possess an encapsulated active site that is postulated to be activated by the specific LPXTG-like motifs found in RrgA, RrgB and RrgC. These motifs are known to have profound consequences for catalysis (LeMieux *et al*, 2008), and could be indicative of a controlled sequential pilus assembly process. Although the sequence of this process remains to be unveiled, it would ensure RrgA to

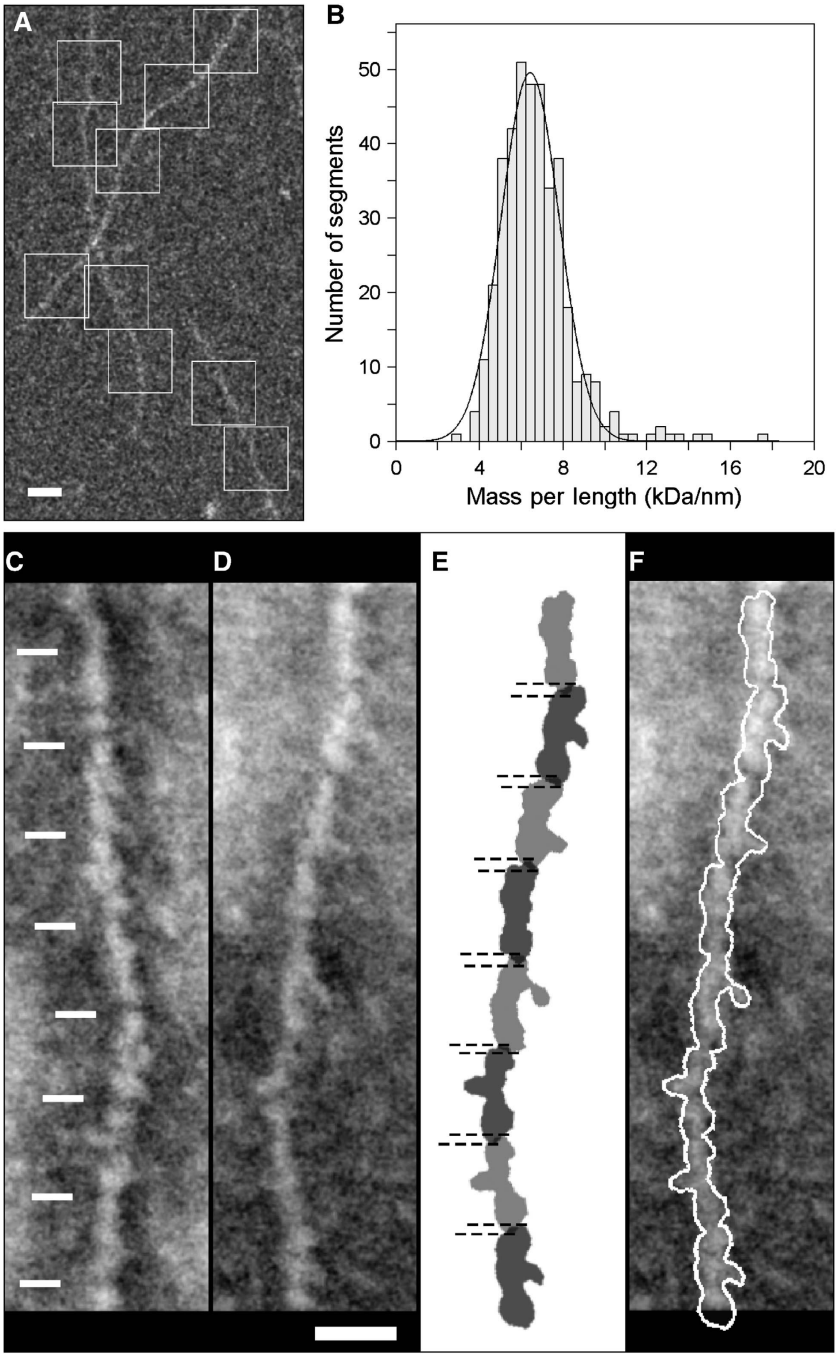

Figure 4 STEM analysis of isolated TIGR4 pili. (**A**) STEM dark-field image of unstained, freeze-dried TIGR4 pili; the regions selected for mass-per-length measurement are indicated. (**B**) The mass-per-length histogram obtained from this sample. The peak at 6.4 (±1.4)kDa/nm ($n = 395$) shows the pilus filament to be a single string of RrgB monomers and predicts the presence of one monomer every 10.2 (±0.5)nm. (**C**, **D**) Contrast-reversed STEM dark-field images recorded at a magnification of $\times 10^6$ from negatively stained TIGR4 (2% PTA). A nose-like protrusion is present at irregular intervals and gives the filaments a defined polarity. Indeed, individual pilus subunits can be distinguished and have the same shape as RrgB–His monomers; compare with Figure 3B. Subunit boundaries are indicated by white lines in panel C (analysed in Supplementary Figure S9) and for panel D by the model in panel E. (**E**) Highly contoured TEM images of RrgB–His monomers (average length 12.2 (±0.5)nm) matched, without straightening, to the subunits of pilus (D), illustrating that its RrgB subunits overlap; the RrgB monomers are shown in alternating shades of grey and their ends are marked by dotted lines to facilitate visualisation. (**F**) Outline of the outer contours of panel E superimposed on panel D. Scale bar: panel A, 30 nm and panels C–F, 10 nm.

be at the distal tip of the pilus shaft assembled from RrgB, which is the only one of the three pilins to have both the pilin and the LPXTG domain (Supplementary Figure S7B). Incorporation of the RrgC protein at the proximal end would then terminate the pilus assembly process and induce cell wall linkage similar to that observed for SpaB in *C. diphtheriae* (Mandlik *et al*, 2008a) or GBS150 in *S. agalactiae* (Nobbs *et al*, 2008).

In spite of this agreement our model is in contrast to other reports, which state that ancillary proteins RrgA and RrgC are

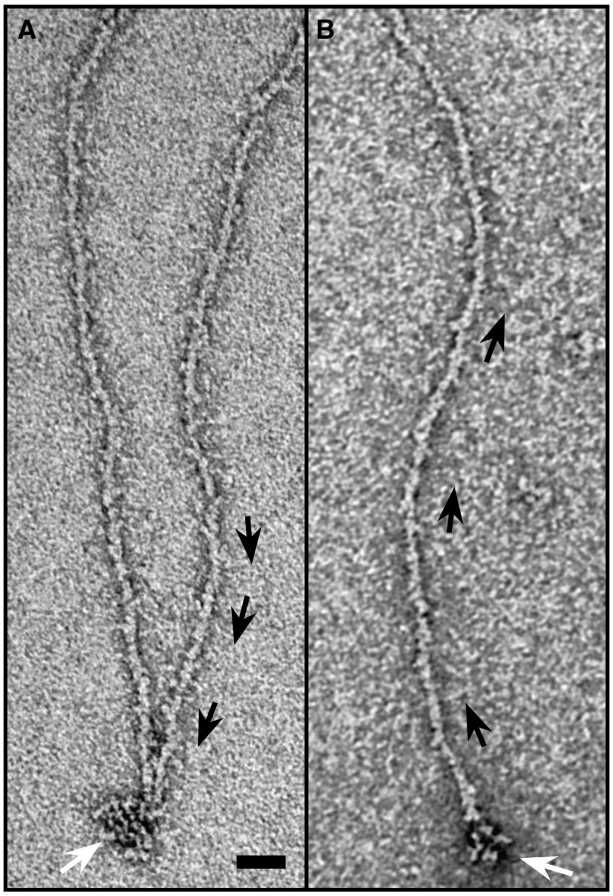

Figure 5 Localisation of the ancillary proteins, RrgA and RrgC. TEM of negatively stained (2% UAc) immunolabelled TIGR4 pili, enlarged to show pilus polarity. (**A**) Pili labelled with anti-RrgA-His; the noses point away from the antibody cluster. The antibody cluster is indicated by a white arrow. (**B**) Pilus labelled with anti-RrgC–His; the noses point towards the antibody. The antibody is indicated by a white arrow. As RrgC anchors the pilus to the cell wall, as suggested by the release of pili in the absence of RrgC (Supplementary Figure S11), the black arrows in panels A and B point away from the bacterium. Scale bar: panels A and B, 20 nm.

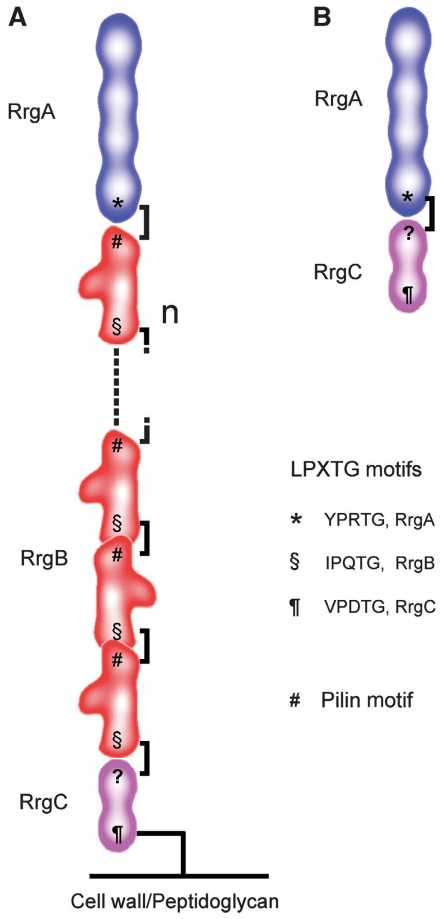

Figure 6 Model of *S. pneumoniae* pilus. (**A**) The TIGR4 pilus consists of a shaft composed of RrgB, with RrgA at its distal and RrgC at its proximal end. Sortase SrtC-1 mediates the polymerisation of RrgB (red) via the LPXTG motif (*, IPQTG) and pilin motif (#) (Manzano *et al*, 2008) into a single string of monomers, covalently linked head-to-tail. The nose-like feature of RrgB gives the pilus a clear polarity. C-type sortases also control the addition of the ancillary proteins RrgA and RrgC, and anchor RrgC to the peptidoglycan cell wall, depending on the recognition of the respective LPXTG motifs YPRTG (RrgA) and VPDTG (RrgC; LeMieux *et al*, 2008; Neiers *et al*, 2009). RrgA is located at the distal end of the pilus, while RrgC is proximal to the bacterium. This is in agreement with the proposed role of RrgA as adhesin (Nelson *et al*, 2007; Hilleringmann *et al*, 2008) and the release of pili into the supernatant when RrgC is not present. RrgA and RrgC do not localise together in these single pili and are neither incorporated into the pilus shaft nor present along its length as proposed earlier (LeMieux *et al*, 2006; Fälker *et al*, 2008; Hilleringmann *et al*, 2008). (**B**) The ability of RrgA and RrgC to form a heterodimer (LeMieux *et al*, 2008) suggests a site in RrgC that can be covalently linked to an LPXTG motif from either RrgA or RrgB. The inability of RrgA and/or RrgC to form polymers may indicate that (i) RrgA has no site to interact with an LPXTG motif and (ii) RrgC has an LPXTG motif that activates only the C-type sortase, which links it to the cell wall.

either incorporated in or associated with the pilus shaft (LeMieux *et al*, 2006; Nelson *et al*, 2007; Fälker *et al*, 2008; Hilleringmann *et al*, 2008). Immuno-EM showed RrgC and RrgA to be in clusters along the length of the pilus shaft (LeMieux *et al*, 2006; Hilleringmann *et al*, 2008), sometimes together as indicated by double-labelling studies (Fälker *et al*, 2008). The discrepancy to the observations presented here is explained by the lower resolution of the previous immuno-EM studies, which could not resolve single pili with certainty, but rather visualised immunogold-labelled pilus bundles. LeMieux *et al* (2008) came to a similar conclusion speculating that the observed clustering of RrgA simply manifests the bundling of different-length pili with RrgA at their tips. Immunogold labelling cannot prove this hypothesis because single pili within a bundle cannot be resolved. Negative-stain EM can achieve higher resolution. Using this technique we first demonstrate that pili emerge from the cell surface as single, ~6-nm-wide filaments, which then form bundles or tangle at random (Figure 1). Second, by isolation of native pili using a modified protocol we obtain a higher-resolution definition of the pilus shaft by STEM dark-field imaging of single pili, and show their previously observed beaded structure (Manzano *et al*, 2008) to arise from single RrgB monomers linked head-to-tail with a periodicity of about 10 nm (Figure 4C–F and Supplementary Figure S9). This periodicity is compatible with STEM mass-per-length measurements; 6.4 ± 1.4 kDa/nm (Figure 4B) also translates to about 1 RrgB monomer/10 nm. Third, the well-defined protrusions on the filaments, the 'noses', result in clear polarity and indicate a head-to-tail subunit assembly (Figure 4C–F).

These 'noses' relate to lateral protrusions on images of negatively stained, recombinantly expressed RrgB–His monomers (Figure 3B). In agreement, antibody labelling demonstrated the pilus shaft to be exclusively comprised of RrgB proteins (Figure 2C–E and Supplementary Figure S2–4). Fourth, once these basic simple features of the TIGR4 pilus had been defined by high-resolution STEM, we could also recognise them on close inspection of TEM images recorded at lower magnification. Based on the polarity imposed by the 'noses' and primary antibody labelling it can be said that RrgA and RrgC are located at opposite ends of the pilus shaft (Figure 5 and Supplementary Figure S10). In contrast to immuno-EM, where a secondary, gold-labelled antibody is necessary, direct visualisation of the primary antibody provides the resolution required to locate a specific protein associated with a single pilus shaft. With the new higher resolution data obtained, the previously reported clusters of surface-located RrgA can be interpreted as the distal ends of several interacting individual pili that may emerge from different sites of the cell wall or have different length.

The location of RrgA is assigned as distal as this protein has recently been described as an adhesin (Nelson *et al*, 2007; Hilleringmann *et al*, 2008). This implies that RrgC is at the proximal end of the pilus, which must be anchored in the bacterial cell wall. In *C. diphtheriae* the protein SpaB is proposed to act as the terminal subunit and cell wall anchor in pilus assembly, and in its absence the pili formed are largely found in the medium (Mandlik *et al*, 2008a). In *S. agalactiae* the pilus is covalently linked to the cell wall via the ancillary pilus subunit GBS150, and its absence provokes the release of pili into the culture supernatant (Nobbs *et al*, 2008). Similarly, less HMW pneumococcal TIGR4 pili are found in the supernatant of wt *S. pneumoniae* liquid cultures than in the supernatants of Δ*rrgC* and Δ*rrgAC* mutants, the apparent enhanced pilus loss of the latter over the Δ*rrgC* mutant probably resulting from the missing adhesive function of RrgA (Supplementary Figure S11). Accordingly, RrgC is likely to be the terminal pilus subunit and to warrant cell wall anchoring. The proposed pilus model (Figure 6) agrees with the fact that RrgB assembles *in vitro* in the presence of the pilus-polymerising transpeptidase SrtC-1 (Manzano *et al*, 2008) and *in vivo* in the absence of both RrgA and RrgC (Supplementary Figure S6C and Fälker *et al*, 2008; LeMieux *et al*, 2008). The observation that the accessory subunits RrgA and RrgC are found in similar quantities within each 'rung' of the ladder of bands arising from pili of different lengths on Western blots corroborates this model as well (LeMieux *et al*, 2008). Our results confirm the observation that RrgA and RrgC can form covalent heterodimers, but not higher order polymers in the Δ*rrgB* background. As indicated in our model, this implies that the IPQTG motif in the RrgB protein can be covalently linked to a critical lysine in RrgC, and that in the absence of RrgB the same site in RrgC is linked to the YPRTG motif of RrgA. Whereas RrgC must have another site to be anchored to the cell wall, RrgA appears to expose a single motif for sortase action (Figure 6 and Supplementary Figure S7).

Our model of the pilus shaft (Figure 6) extends the previous model of the *S. pyogenes* pilus created on the basis of the 2.2-Å Spy0128 structure and mass spectrometry (Kang *et al*, 2007). No overlap of subunits is proposed in the Spy0128 filament model. In contrast, we predict an overlap of about 1 nm for RrgB, in accordance with the sequence-based pneumococcal pilus assembly model (Telford *et al*, 2006). The overlap is based on pilus images recorded at $\times 10^6$ magnification, the mass-per-length values provided by STEM and the dimensions of RrgB–His monomers. A major difference in the mass of Spy0128 (aa 18–308; Kang *et al*, 2007) and the integrated RrgB monomer (608 aa) may explain this overlap, but a high-resolution structure of full-length RrgB is required to prove our hypothesis.

Using quantitative EM techniques we have visualised the molecular details of a Gram-positive pilus for the first time. Together with the sequence analysis presented by Manzano *et al* (2008), our observations suggest a pilus architecture that is likely to be valid for other Gram-positive pili. It implies a simple pilus assembly mechanism, and indicates novel sites for therapeutic intervention.

Materials and methods

Bacterial strains and culture conditions

S. pneumoniae type-4 strain TIGR4 was used (Tettelin *et al*, 2001). The TIGR4 Δ*rrgA* mutant used initially was kindly donated by B Henriques-Normark (Karolinska Institutet, Stockholm). Later TIGR4 Δ*rrgA*, TIGR4 Δ*rrgB*, TIGR4 Δ*rrgC* and TIGR4 Δ*rrgAC* mutants were created by PCR-based overlap extension (Supplementary data and Supplementary Tables S1–S2). The pneumococcal strains were stored at −80°C in 12% glycerol and routinely grown at 37°C under 5% CO_2 on Tryptic Soy Agar (Becton Dickinson) supplemented with 5% defibrinated sheep blood or in Todd–Hewitt Yeast Extract (THYE) broth. When appropriate, erythromycin and kanamycin (Sigma-Aldrich) were used as selection markers.

Expression and purification of RrgA, RrgB and RrgC

Recombinant expression and purification of His_6-tagged pilus proteins was performed as described previously (Hilleringmann *et al*, 2008). When necessary a size-exclusion chromatography step was performed after affinity purification. Purified proteins were finally dialysed against 10 mM Tris–HCl (pH 8), 1 mM EDTA and 0.5 mM DTT.

TIGR4 pilus purification

The native pili of TIGR4 wt and TIGR4 Δ*rrgA*, TIGR4 Δ*rrgC* and TIGR4 Δ*rrgAC* were purified essentially according a protocol described by Hilleringmann *et al* (2008) treating bacteria with mutanolysin, a murein-hydrolysing enzyme (Sigma M9901), to liberate covalently peptidoglycan-anchored pili into the supernatant, but using a Tris buffer (10 mM Tris–HCl (pH 8), 1 mM EDTA, 1 mM DTT)-based procedure. In addition the following modifications were applied: harvested bacteria were washed in Tris buffer and resuspended in Tris containing protoplast buffer (Tris buffer, 20% sucrose). Final sample dialysis against Tris buffer was performed using a molecular weight cut-off of 300 kDa (Spectra/Por Biotech cellulose ester).

SDS–PAGE and Western blot analysis

SDS–PAGE analysis was performed using NuPAGE 3–8% Tris Acetate Gels (Invitrogen) according to the instructions of the manufacturer. HiMark pre-stained, HMW protein standard (Invitrogen) served as the protein standard. Western blot analysis was performed using standard protocols. Unless otherwise stated, antibodies against recombinant RrgA–His and RrgB–His were used at 1:10 000 dilution, and against RrgC–His at 1:2000 dilution. Secondary goat anti-mouse HRP antibodies were diluted 30 000 ×.

Animal sera and antibodies

Polyclonal mouse antibodies against recombinant RrgA–His, RrgB–His and RrgC–His were produced in our laboratory. For immunolabelling of isolated native pili, antibodies were purified to 100% specificity against their respective proteins using the protocol described by Mueller *et al* (2005).

Immunolabelling of the isolated pili

The respective affinity-purified antibodies were individually incubated with wt or Δ*rrgA* TIGR4 pili (control experiments) overnight or during 50 min at 4°C in a series of runs covering a range of concentrations. Samples were inspected by negative-stain TEM. The conditions were optimised to yield good labelling and have the minimum number of free antibodies on the EM grids.

Transmission electron microscopy

For TEM of whole bacteria, 100–200 μl of PBS was added to the blood agar growth plate and agitated gently to delicately remove bacteria from the agar. The plate was tilted and an aliquot of the resulting bacterial suspension was removed from close to the liquid surface. Small aliquots of this stock suspension were then directly loaded onto carbon-coated Parlodion microscopy grids. The bacteria were allowed to settle (5 min) and then stabilised by addition of 2% paraformaldehyde (40 s). Grids were washed on droplets of water, negatively stained and examined. As dictated by grid quality, the stock was sometimes centrifuged gently for several minutes (3000 r.p.m. for 5–10 min), the pellet was then gently resuspended in PBS and grids were prepared; if necessary these steps were repeated.

Samples of the isolated pili were diluted in buffer as required and adsorbed for 1 min to glow discharged 400 mesh carbon-coated Parlodion or STEM grids (see below). These were washed and negatively stained with 2% (w/v) uranyl acetate (UAc) or 2% (w/v) phosphotungstic acid (PTA) and imaged with a CM 100 transmission electron microscope (Philips, Eindhoven, the Netherlands) operating at 80 kV. Electron micrographs where recorded with a 2000 by 2000 pixel, charge-coupled device camera (Veleta; Olympus soft imaging solutions GmbH, Münster, Germany) at a nominal magnification of × 130 000, yielding a final pixel size corresponding to 0.36 nm on the specimen scale. Particles were manually selected for single-particle analysis and averaged using the EMAN software (Ludtke *et al*, 1999).

Scanning TEM

Samples were prepared on glow-discharged, thin carbon films coating a perforated carbon layer on gold-coated copper grids, washed and either freeze-dried for mass measurement or negatively stained as above. Mass measurements were performed on pilus and recombinant RrgA–His samples as described (Broz *et al*, 2007), except that the grids were washed on eight drops of quartz double-distilled water. Images were recorded from the TIGR4 pili at doses ranging from 400 to 950 electrons/nm^2 and from pili of the TIGR4 Δ*rrgA* mutant at a dose of 700 ± 56 electrons/nm^2, and evaluated using the MASDET program package (Krzyžáneka *et al*, 2009). A linear regression describing the dose dependence of the mass-per-length values determined for the former sample defined beam-induced mass-loss. Both the TIGR4 data set and the Δ*rrgA* pilus data were corrected accordingly and scaled to the mass-per-length determined in the same run for tobacco mosaic virus (TMV). Images were recorded from the RrgA–His sample at a dose of 1170 ± 100 electrons/nm^2 and evaluated using MASDET (Krzyžáneka *et al*, 2009). Beam-induced mass-loss was corrected according to the behaviour of proteins in the mass range 120–190 kDa (Müller and Engel, 2001 and unpublished results) and the data were scaled according to the mass-per-length measured for TMV. The corrected data sets were binned into histograms and described by Gauss curves.

Supplementary data

Supplementary data are available at *The EMBO Journal* Online (http://www.embojournal.org).

Acknowledgements

We thank Vladislav Krzyžáneka and Rudolf Reichelt, University of Münster, for continuous help with improving the mass determination software used in this project; Françoise Erne-Brand for STEM mass measurements; Ruben Diaz-Avalos, Florida State University, for providing Tobacco Mosaic Virus samples; and Monica Moschioni and Angela H Nobbs for valuable discussions and for supplying material. Further we thank Silvana Savino and Vega Masignani for promoting the project. This work was supported by the Swiss National Science Foundation (grant 3100A0-108299 to AE), the Maurice E Müller Foundation of Switzerland and Novartis Vaccines and Diagnostics s.r.l.

Conflict of interest

MH, GD, RR and IF are employees of Novartis Vaccines and Diagnostics s.r.l.

References

Abbot EL, Smith WD, Siou GP, Chiriboga C, Smith RJ, Wilson JA, Hirst BH, Kehoe MA (2007) Pili mediate specific adhesion of *Streptococcus pyogenes* to human tonsil and skin. *Cell Microbiol* **9:** 1822–1833

Bagnoli F, Moschioni M, Donati C, Dimitrovska V, Ferlenghi I, Facciotti C, Muzzi A, Giusti F, Emolo C, Sinisi A, Hilleringmann M, Pansegrau W, Censini S, Rappuoli R, Covacci A, Masignani V, Barocchi MA (2008) A second pilus type in *Streptococcus pneumoniae* is prevalent in emerging serotypes and mediates adhesion to host cells. *J Bacteriol* **190:** 5480–5492

Barocchi MA, Ries J, Zogaj X, Hemsley C, Albiger B, Kanth A, Dahlberg S, Fernebro J, Moschioni M, Masignani V, Hultenby K, Taddei AR, Beiter K, Wartha F, von Euler A, Covacci A, Holden DW, Normark S, Rappuoli R, Henriques-Normark B (2006) A pneumococcal pilus influences virulence and host inflammatory responses. *Proc Natl Acad Sci USA* **103:** 2857–2862

Broz P, Mueller CA, Muller SA, Philippsen A, Sorg I, Engel A, Cornelis GR (2007) Function and molecular architecture of the *Yersinia* injectisome tip complex. *Mol Microbiol* **65:** 1311–1320

Budzik JM, Marraffini LA, Schneewind O (2007) Assembly of pili on the surface of *Bacillus cereus* vegetative cells. *Mol Microbiol* **66:** 495–510

Budzik JM, Oh SY, Schneewind O (2008) Cell wall anchor structure of BcpA pili in *Bacillus anthracis*. *J Biol Chem* **283:** 36676–36686

Dramsi S, Caliot E, Bonne I, Guadagnini S, Prevost MC, Kojadinovic M, Lalioui L, Poyart C, Trieu-Cuot P (2006) Assembly and role of pili in group B streptococci. *Mol Microbiol* **60:** 1401–1413

Fälker S, Nelson AL, Morfeldt E, Jonas K, Hultenby K, Ries J, Melefors Ö, Normark S, Henriques-Normark B (2008) Sortase-mediated assembly and surface topology of adhesive pneumococcal pili. *Mol Microbiol* **70:** 595–607

Fronzes R, Remaut H, Waksman G (2008) Architectures and biogenesis of non-flagellar protein appendages in Gram-negative bacteria. *EMBO J* **27:** 2271–2280

Hava DL, Camilli A (2002) Large-scale identification of serotype 4 *Streptococcus pneumoniae* virulence factors. *Mol Microbiol* **45:** 1389–1406

Hilleringmann M, Giusti F, Baudner Barbara C, Masignani V, Covacci A, Rappuoli R, Barocchi Michele A, Ferlenghi I (2008) Pneumococcal pili are composed of protofilaments exposing adhesive clusters of Rrg A. *PLoS Pathog* **4:** e1000026

Kang HJ, Baker EN (2009) Intramolecular isopeptide bonds give thermodynamic and proteolytic stability to the major pilin protein of *Streptococcus pyogenes*. *J Biol Chem* **284:** 20729–20737

Kang HJ, Coulibaly F, Clow F, Proft T, Baker EN (2007) Stabilizing isopeptide bonds revealed in Gram-positive bacterial pilus structure. *Science (Washington, DC, USA)* **318:** 1625–1628

Krishnan V, Gaspar AH, Ye N, Mandlik A, Ton-That H, Narayana SVL (2007) An IgG-like domain in the minor pilin GBS52 of *Streptococcus agalactiae* mediates lung epithelial cell adhesion. *Structure (Cambridge, MA, USA)* **15:** 893–903

Krzyžáneka V, Müller SA, Engel A, Reichelt R (2009) MASDET—a fast and user-friendly multiplatform software for mass determination by dark-field electron microscopy. *J Struct Biol* **165:** 78–87

Lauer P, Rinaudo CD, Soriani M, Margarit I, Maione D, Rosini R, Taddei AR, Mora M, Rappuoli R, Grandi G, Telford JL (2005) Genome analysis reveals pili in group B *Streptococcus*. *Science* **309:** 105

LeMieux J, Hava DL, Basset A, Camilli A (2006) RrgA and RrgB are components of a multisubunit pilus encoded by the *Streptococcus pneumoniae rlrA* pathogenicity islet. *Infect Immun* **74:** 2453–2456

LeMieux J, Woody S, Camilli A (2008) Roles of the sortases of *Streptococcus pneumoniae* in assembly of the RlrA pilus. *J Bacteriol* **190:** 6002–6013

Lode HM (2009) Clinical impact of antibiotic-resistant Gram-positive pathogens. *Clin Microbiol Infect* **15:** 212–217

Ludtke SJ, Baldwin PR, Chiu W (1999) EMAN: semiautomated software for high-resolution single-particle reconstitutions. *J Struct Biol* **128:** 82–97H

Maisey HC, Hensler M, Nizet V, Doran KS (2007) Group B streptococcal pilus proteins contribute to adherence to and invasion of brain microvascular endothelial cells. *J Bacteriol* **189:** 1464–1467

Mandlik A, Das A, Ton-That H (2008a) The molecular switch that activates the cell wall anchoring step of pilus assembly in Gram-positive bacteria. *Proc Natl Acad Sci USA* **105:** 14147–14152

Mandlik A, Swierczynski A, Das A, Ton-That H (2008b) Pili in Gram-positive bacteria: assembly, involvement in colonization and biofilm development. *Trends Microbiol* **16:** 33–40

Manzano C, Contreras-Martel C, El Mortaji L, Izore T, Fenel D, Vernet T, Schoehn G, Di Guilmi AM, Dessen A (2008) Sortase-mediated pilus fiber biogenesis in *Streptococcus pneumoniae*. *Structure* **16:** 1838–1848

Marraffini LA, Dedent AC, Schneewind O (2006) Sortases and the art of anchoring proteins to the envelopes of Gram-positive bacteria. *Microbiol Mol Biol Rev* **70:** 192–221

Mora M, Bensi G, Capo S, Falugi F, Zingaretti C, Manetti AG, Maggi T, Taddei AR, Grandi G, Telford JL (2005) Group A *Streptococcus* produce pilus-like structures containing protective antigens and Lancefield T antigens. *Proc Natl Acad Sci USA* **102:** 15641–15646

Mueller CA, Broz P, Müller SA, Ringler P, Erne-Brand F, Sorg I, Kuhn M, Engel A, Cornelis GR (2005) The V-antigen of *Yersinia* forms a distinct structure at the tip of injectisome needles. *Science* **310:** 674–676

Müller SA, Engel A (2001) Structure and mass analysis by scanning transmission electron microscopy. *Micron* **32:** 21–31

Müller SA, Engel A (2006) Biological scanning transmission electron microscopy: imaging and single molecule mass determination. *CHIMIA* **60:** 749–753

Nallapareddy SR, Singh KV, Sillanpaa J, Garsin DA, Hook M, Erlandsen SL, Murray BE (2006) Endocarditis and biofilm-associated pili of *Enterococcus faecalis*. *J Clin Invest* **116:** 2799–2807

Neiers F, Madhurantakam C, Fälker S, Manzano C, Dessen A, Normark S, Henriques-Normark B, Achour A (2009) Two crystal structures of pneumococcal pilus sortase C provide novel insights into catalysis and substrate specificity. *J Mol Biol* **393:** 704–716

Nelson AL, Ries J, Bagnoli F, Dahlberg S, Faelker S, Rounioja S, Tschoep J, Morfeldt E, Ferlenghi I, Hilleringmann M, Holden DW, Rappuoli R, Normark S, Barocchi MA, Henriques-Normark B (2007) RrgA is a pilus-associated adhesin in *Streptococcus pneumoniae*. *Mol Microbiol* **66:** 329–340

Nobbs AH, Rosini R, Rinaudo CD, Maione D, Grandi G, Telford JL (2008) Sortase A utilizes an ancillary protein anchor for efficient cell wall anchoring of pili in *Streptococcus agalactiae*. *Infect Immun* **76:** 3550–3560

Osaki M, Takamatsu D, Shimoji Y, Sekizaki T (2002) Characterization of *Streptococcus suis* genes encoding proteins homologous to sortase of gram-positive bacteria. *J Bacteriol* **184:** 971–982

Proft T, Baker EN (2009) Pili in Gram-negative and Gram-positive bacteria—structure, assembly and their role in disease. *Cell Mol Life Sci* **66:** 613–635

Rosch JW, Mann B, Thornton J, Sublett J, Tuomanen E (2008) Convergence of regulatory networks on the pilus locus of *Streptococcus pneumoniae*. *Infect Immun* **76:** 3187–3196

Swaminathan A, Mandlik A, Swierczynski A, Gaspar A, Das A, Ton-That H (2007) Housekeeping sortase facilitates the cell wall anchoring of pilus polymers in *Corynebacterium diphtheriae*. *Mol Microbiol* **66:** 961–974

Telford JL, Barocchi MA, Margarit I, Rappuoli R, Grandi G (2006) Pili in Gram-positive pathogens. *Nat Rev Microbiol* **4:** 509–519

Tettelin H, Nelson KE, Paulsen IT, Eisen JA, Read TD, Peterson S, Heidelberg J, DeBoy RT, Haft DH, Dodson RJ, Durkin AS, Gwinn M, Kolonay JF, Nelson WC, Peterson JD, Umayam LA, White O, Salzberg SL, Lewis MR, Radune D *et al* (2001) Complete genome sequence of a virulent isolate of *Streptococcus pneumoniae*. *Science* **293:** 498–506

Ton-That H, Marraffini LA, Schneewind O (2004) Sortases and pilin elements involved in pilus assembly of *Corynebacterium diphtheriae*. *Mol Microbiol* **53:** 251–261

Ton-That H, Schneewind O (2003) Assembly of pili on the surface of *Corynebacterium diphtheriae*. *Mol Microbiol* **50:** 1429–1438

Ton-That H, Schneewind O (2004) Assembly of pili in Gram-positive bacteria. *Trends Microbiol* **12:** 228–234

Wu H, Fives-Taylor PM (2001) Molecular strategies for fimbrial expression and assembly. *Crit Rev Oral Biol Med* **12:** 101–115

Xu P, Alves JM, Kitten T, Brown A, Chen Z, Ozaki LS, Manque P, Ge X, Serrano MG, Puiu D, Hendricks S, Wang Y, Chaplin MD, Akan D, Paik S, Peterson DL, Macrina FL, Buck GA (2007) Genome of the opportunistic pathogen *Streptococcus sanguinis*. *J Bacteriol* **189:** 3166–3175

Prevalence of pilus-encoding islets among acute otitis media *Streptococcus pneumoniae* isolates from Israel

M. Moschioni[1], G. De Angelis[1], S. Melchiorre[1], V. Masignani[1], E. Leibovitz[2], M. A. Barocchi[1] and R. Dagan[2,3]

1) *Novartis Vaccines and Diagnostics s.r.l., Research Center, Siena, Italy,* 2) *Faculty of Health Sciences, Ben-Gurion University of the Negev and* 3) *Pediatric Infectious Disease Unit, Soroka University Medical Center, Beer-Sheva, Israel*

Abstract

We evaluated the distribution of the two known *Streptococcus pneumoniae* pilus encoding islets (PI-1 and PI-2) among a panel of 113 acute otitis media clinical isolates from Israel. PI-1 was present in 30.1% (n = 34) of the isolates tested, and PI-2 was present in 7% (n = 8). In addition, we found that: (i) the PI positive isolates, 50% of which belong to the international clones Spain^{9V}-3 (ST156) and Taiwan^{19F}-14 (ST236), correlate with the genotype (as determined by multilocus sequence typing) but not with the serotype; (ii) PI-2 was not present in the absence of PI-1; and (iii) the frequency of PI-1 was higher among antibiotic-resistant isolates.

Keywords: Acute otitis media, antibiotic resistance, genotype, pilus-encoding islet, *Streptococcus pneumoniae*

Original Submission: 19 August 2009; **Revised Submission:** 22 October 2009; **Accepted:** 23 October 2009
Editor: J.-L. Mainardi
Article published online: 2 November 2009

Clin Microbiol Infect 2010; **16:** 1501–1504
10.1111/j.1469-0691.2010.03105.x

Corresponding author: R. Dagan, Faculty of Health Sciences, Ben-Gurion University of the Negev and Pediatric Infectious Disease Unit, Soroka University Medical Center, Beer-Sheva, Israel
E-mail: rdagan@bgu.ac.il

The human pathogen *Streptococcus pneumoniae* is commonly associated with invasive diseases such as meningitis and sepsis. In addition, pneumococci are the most frequent cause of upper respiratory infections such as sinusitis and acute otitis media (AOM), which is one of the most widespread childhood infections and a major cause of morbidity in children [1,2]. Hence, it is important to investigate the presence of pathogenic factors that may be responsible for disease outcome among AOM clinical isolates.

Recently, genetic analysis of *S. pneumoniae* clinical isolates demonstrated that they harbour pilus structures encoded by the *rlrA* pathogenicity islet (pilus islet-1, PI-1) and the pilus islet-2 (PI-2). The PI-1 pilus was shown to be involved in virulence [3,4] and antibodies raised against its protein subunits were protective in a murine model of infection [5]. However, the islets are not widely distributed in *S. pneumoniae*. Three independent studies demonstrated that, in both invasive and nasopharyngeal clinical isolates, the frequency of the PI-1 islet is approximately 30% [6–8], although the incidence was higher among antibiotic-resistant clones [8]. This suggests that the interplay between the pilus (encoded by PI-1) and antibiotic resistance may facilitate the global spread of antibiotic nonsusceptible pneumococci [9]. A recent study demonstrated that PI-2 is present in approximately 16% of invasive and nasopharyngeal clinical isolates [10], and that both islets are present in the Taiwan^{19F}-14 (ST236) clone, whose spread is responsible for the increasing incidence of antibiotic-resistant isolates in many countries [11–13].

Therefore, to evaluate a possible correlation between AOM and the presence of PIs, we aimed to assess the prevalence of the pilus encoding islets in a collection of AOM clinical isolates, for which no data are available thus far.

A total of 113 pneumococcal isolates were obtained from the middle ear fluid of 113 patients with AOM presenting at the Soroka University Medical Center Pediatric Emergency Department, from 1 January 2007 to 29 March 2007. The patients were Jewish children (n = 55) and Bedouin children (n = 58) who did not receive the heptavalent conjugate pneumococcal vaccine (PCV7) because PCV 7 vaccination was not implemented in Israel at the time of the study. The age of the children was in the range 0.8–96.9 months (mean ± SD 13.3 ± 15.5 months; median 9.7 months). Of the 113 isolates, 85 (75%) were obtained by tympanocentesis and 17 (15%) were from spontaneous drainage; it was not clear whether the remaining 11 isolates (10%) were obtained from tympanocentesis or spontaneous drainage. Of 107 isolates from which information about antibiotic treatment of the patient in the month prior to culture was available, 32 (30%) were from children receiving antibiotics in previous months. *S. pneumoniae* was isolated as a single pathogen in 62/113 (65%) cases; in 46 (41%) together with *Haemophilus*

influenzae; and in five (4%) together with other combinations of pathogens. Identification, serotyping and antimicrobial susceptibility testing was performed as described previously [14].

The most commonly isolated serotype was serotype 14, followed by 19F, 23F, 19A, 6B and 18C (Fig. 1a). All isolates were tested for the presence of PI-1 and PI-2 by PCR using a specific set of primers as described previously [8,10]. Amplifications to determine the genomic location and the presence of islets were performed directly from bacterial colonies grown overnight on blood-agar plates.

Of 113 isolates, 34 (30.1%) were positive for *S. pneumoniae* PI-1 and eight (7%) were positive for PI-2; PI-1 was found in serotypes 6A, 6B, 14, 19F, 23F, 33A and 11A, (Fig. 1a). On the other hand, PI-2 was only found in serotype 19F isolates and always associated with PI-1 (Fig. 1a). Subsequently, the isolates containing PI-1 or both PI-1 and PI-2 were typed by multilocus sequence typing [15] and grouped by E-BURST analysis (http://eburst.mlst.net/) by clonal complex (CC) (Fig. 1b), revealing that they belonged to CCs already reported to be most likely to carry the PI-1 [6–8]. Isolates that harboured both pilus islets were mainly of the CC271, single or double locus variants of the international clone Taiwan^{19F}-14. Among the isolates containing only PI-1, CC156 was the prevalent clone (international clone Spain^{9V}-3). Interestingly, out of 12 CC156 isolates, 11 (92%) were serotype 14, confirming the increasing association of this serotype with clone CC156 [9].

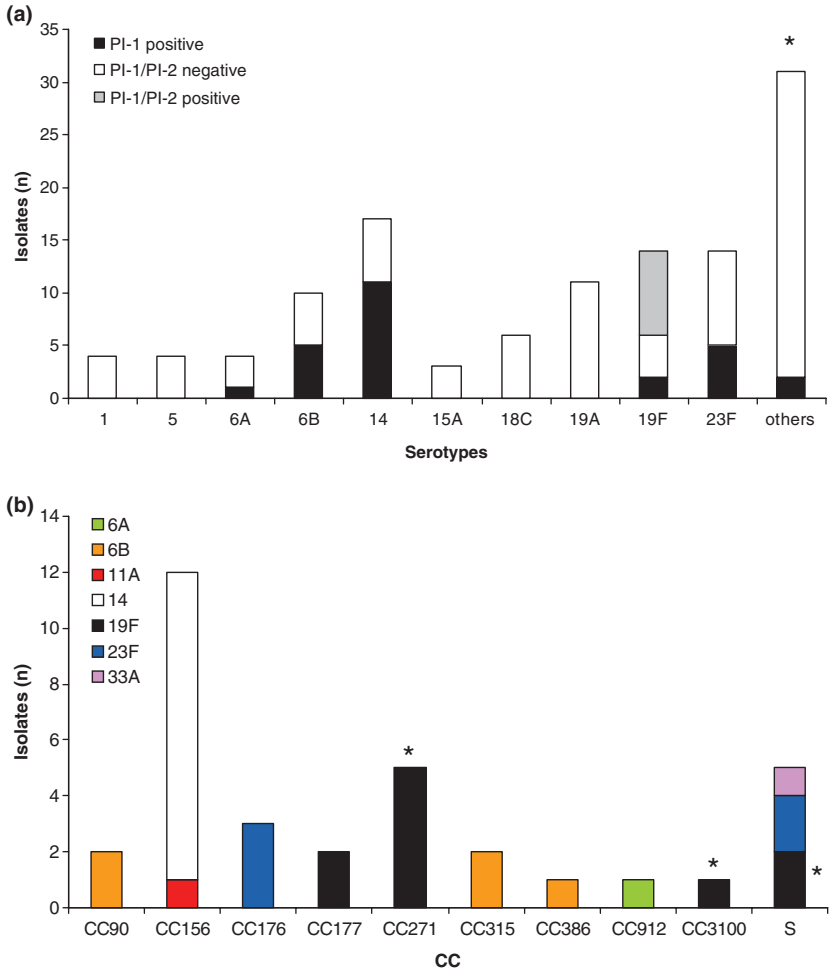

FIG. 1. Acute otitis media (AOM) isolates collection characterized for the presence of pilus islet (PI)-1 and PI-2. (a) Collection of AOM isolates stratified by serotype and analysed for the presence of PI-1 and PI-2. *Serotypes with two isolates only (3, 4, 8, 15B, 16F, 18A, 33A) or one isolate only (7B, 9N, 9V, 11A, 23A, 23B, 24F, 31, 33F, 35B, not typable). PI-1 was present only in one of the two serotype 33A isolates and in the 11A isolate. (b) PI-1 and PI-2 positive isolates stratified by clonal complex (CC), determined by E-BURST grouping, after multilocus sequence typing. The serotypes to which the CCs are associated are shown with different colours. CCs have been named according to the sequence typing number of the E-BURST predicted founder. S, singletons. *Serotype 19F isolates positive for both PI-1 and PI-2.

TABLE 1. Antibiotic resistance pattern in selected serotypes, in isolates with and without the pilus islet (PI)-1

	14		19F		23F		33A		6A		6B		Others		Total	
	PII (−)	PII (+)	PII (−)	PII (+)	PII (−)	PII (+)	PII (−)	PII (+)	PII (−)	PII (+)	PII (−)	PII (+)	PII (−)	PII (+)	PII(+)/resistant isolates	
	(*n* = 6)	(*n* = 11)	(*n* = 4)	(*n* = 10)	(*n* = 9)	(*n* = 5)	(*n* = 1)	(*n* = 1)	(*n* = 3)	(*n* = 1)	(*n* = 5)	(*n* = 5)	(*n* = 51)	(*n* = 1)		
Erythromycin resistance	5	2	1	8	0	0	1	0	2	1	4	5	2	0	16/31 (51.6%)	
Penicillin MIC ≥0.1 mg/L	5	11	1	9	6	4	0	0	2	0	3	2	21	1	27/65 (41.5%)	
Penicillin MIC ≥1.0 mg/L	3	2	1	4	4	0	0	0	0	0	0	0	2	0	6/16 (37.5%)	
Multidrug resistance*	5	1	1	8	2	0	0	0	0	1	3	4	2	0	14/27 (51.8%)	
Susceptible to all antibiotics	0	0	3	1	2	0	0	1	0	0	1	0	27	0	PII(+)/susceptible isolates 2/35(5.7%)	

*Resistant to ≥3 drug classes

No correlation was found with age or gender of the children, whereas the percentage of PI positive isolates among the Jewish population was higher (43.6%) compared with to Bedouins (17.2%), although the proportion of antibiotic resistant clones was comparable in the two groups. Moreover, children who had experienced one or more otitis media episodes in the previous year were more likely to be infected with *S. pneumoniae* carrying the pilus-encoding islets than children who had not (46% vs. 18%; p 0.002). The concomitant presence of *H. influenzae* in the infection site did not correlate with PIs positive *S. pneumoniae* (28%).

Because PI-1 was found mainly in serotypes with prevalent antibiotic resistance, we analysed its presence or absence by the antibiotic-resistance pattern in each of the serotypes in which it was described (Table 1). The percentage of PI-1 positive isolates among antibiotic-resistant strains reached 41.5% in penicillin-nonsusceptible isolates (MIC >0.1 mg/L), 51.8% among multidrug-resistant isolates, and 51.6% in erythromycin- resistant isolates. By contrast, the proportion of PI-1 strains in strains susceptible to all tested antibiotics was 5.7% (p 0.001). These findings confirm the previously found association between piliated *S. pneumoniae* and antibiotic resistance [8].

In conclusion, the data obtained in the present study indicate that the incidence of piliated pneumococci in otitis media isolates is not greater than in other invasive disease isolates and that the pilus does not appear to confer an additional selective benefit in the middle ear during otitis media. A limitation of the present study is the small sample size of clinical isolates tested. However, the results obtained confirm the correlation of PI in *S. pneumoniae* with genotype and antibiotic resistance. Further studies are needed to understand the epidemiological relevance of the pilus and its role in disease outcome. Although vaccination with PCV7 reduced the frequency of persistent and recurrent AOM [16], multidrug-resistant nonvaccine serotypes such as serotype 19A are increasing, associated with CC156 [17]. This clone was a prevalent clone in the present study. Therefore, the elucidation of the pathogenesis of AOM may help advance the development of a serotype-independent pneumococcal vaccine for otitis media, and a new generation protein vaccine that includes pilus subunits could reduce otitis media disease.

Transparency Declaration

M. Moschioni, G. De Angelis, S. Melchiorre, V. Masignani and M.A. Barocchi are employees of Novartis Vaccines and Diagnostics. E. Leibovitz has no conflict of interest. R. Dagan

has had the following financial interests and/or arrangements with the corporate organizations listed herebelow in the past 5 years: Grant/Research support – Berna/Crucell, Wyeth/Pfizer, MSD; Scientific Consultancy – Berna/Crucell, GlaxoSmithKline, Novartis, Wyeth/Pfizer, Protea, MSD; Speaker – Berna/Crucell, GlaxoSmithKline, Wyeth/Pfizer; Shareholder – Protea.

References

1. Hausdorff WP, Feikin DR, Klugman KP. Epidemiological differences among pneumococcal serotypes. *Lancet Infect Dis* 2005; 5: 83–93.
2. Rovers MM, Schilder AG, Zielhuis GA, Rosenfeld RM. Otitis media. *Lancet* 2004; 363: 465–473.
3. Barocchi MA, Ries J, Zogaj X *et al.* A pneumococcal pilus influences virulence and host inflammatory responses. *Proc Natl Acad Sci USA* 2006; 103: 2857–2862.
4. Nelson AL, Ries J, Bagnoli F *et al.* RrgA is a pilus-associated adhesin in *Streptococcus pneumoniae*. *Mol Microbiol* 2007; 66: 329–340.
5. Gianfaldoni C, Censini S, Hilleringmann M *et al. Streptococcus pneumoniae* pilus subunits protect mice against lethal challenge. *Infect Immun* 2007; 75: 1059–1062.
6. Aguiar SI, Serrano I, Pinto FR, Melo-Cristino J, Ramirez M. The presence of the pilus locus is a clonal property among pneumococcal invasive isolates. *BMC Microbiol* 2008; 8: 41.
7. Basset A, Trzcinski K, Hermos C *et al.* Association of the pneumococcal pilus with certain capsular serotypes but not with increased virulence. *J Clin Microbiol* 2007; 45: 1684–1689.
8. Moschioni M, Donati C, Muzzi A *et al. Streptococcus pneumoniae* contains 3 *rlr*A pilus variants that are clonally related. *J Infect Dis* 2008; 197: 888–896.
9. Sjostrom K, Blomberg C, Fernebro J *et al.* Clonal success of piliated penicillin nonsusceptible pneumococci. *Proc Natl Acad Sci USA* 2007; 104: 12907–12912.
10. Bagnoli F, Moschioni M, Donati C *et al.* A second pilus type in *Streptococcus pneumoniae* is prevalent in emerging serotypes and mediates adhesion to host cells. *J Bacteriol* 2008; 190: 5480–5492.
11. Hsieh YC, Chang KY, Huang YC *et al.* Clonal spread of highly beta-lactam-resistant *Streptococcus pneumoniae* isolates in Taiwan. *Antimicrob Agents Chemother* 2008; 52: 2266–2269.
12. Mavroidi A, Paraskakis I, Pangalis A *et al.* Spread of the *Streptococcus pneumoniae* Taiwan19F-14 clone among children in Greece. *Clin Microbiol Infect* 2007; 13: 1213–1216.
13. Moore MR, Gertz RE Jr, Woodbury RL *et al.* Population snapshot of emergent *Streptococcus pneumoniae* serotype 19A in the United States, 2005. *J Infect Dis* 2008; 197: 1016–1027.
14. Barkai G, Greenberg D, Givon-Lavi N, Dreifuss E, Vardy D, Dagan R. Community prescribing and resistant *Streptococcus pneumoniae*. *Emerg Infect Dis* 2005; 11: 829–837.
15. Enright MC, Spratt BG. A multilocus sequence typing scheme for *Streptococcus pneumoniae*: identification of clones associated with serious invasive disease. *Microbiology* 1998; 144: 3049–3060.
16. Casey JR, Pichichero ME. Changes in frequency and pathogens causing acute otitis media in 1995–2003. *Pediatr Infect Dis J* 2004; 23: 824–828.
17. Pichichero ME, Casey JR. Emergence of a multiresistant serotype 19A pneumococcal strain not included in the 7-valent conjugate vaccine as an otopathogen in children. *JAMA* 2007; 298: 1772–1778.

Modified sequential multiplex PCR for determining capsular serotypes of invasive pneumococci recovered from Seville

P. Iraurgui[1], M. J. Torres[2], A. Gandia[1], I. Vazquez[1], E. G. Cabrera[2], I. Obando[3], J. Garnacho[4] and J. Aznar[1,2]

1) *Microbiology Service, Hospital Universitario Virgen del Rocío,* 2) *Instituto de Biomedicina de Sevilla, Hospital Universitario Virgen del Rocío/CSIC/Universidad de Sevilla,* 3) *Paediatric Service and* 4) *Intensive Care Unit, Hospital Universitario Virgen del Rocío, Sevilla, Spain*

Abstract

The heptavalent pneumococcal vaccine's introduction resulted in a decline in invasive disease caused by *Streptococcus pneumoniae*, but was accompanied by an increase in non-vaccine serotypes. We evaluated a modified scheme of the sequential multiplex PCRs adapted to the prevalence of serotypes in Seville (Spain) for determining capsular serotypes of *S. pneumoniae* invasive clinical isolates. In adults, the modified scheme allowed us to type 73% with the first three reactions, and 92% with two additional PCRs. In paediatric patients, it allowed us to type 73.5% with the first three reactions, and 90% with the two additional PCRs. The multiplex PCR approach was successfully adapted to target the serotypes most prevalent in Seville.

Keywords: Capsular polysaccharide, invasive infection, multiplex PCR, serotype, *Streptococcus pneumoniae*

Original Submission: 22 July 2009; **Revised Submission:** 18 November 2009; **Accepted:** 19 November 2009
Editor: J.-L. Mainardi
Article published online: 7 December 2009

Clin Microbiol Infect 2010; **16:** 1504–1507
10.1111/j.1469-0691.2009.03129.x

Corresponding author: M. J. Torres, Departamento de Microbiología, Facultad de Medicina, Apdo. 914, 41080 Seville, Spain
E-mail: mjtorres@us.es

Streptococcus pneumoniae causes severe illnesses in the elderly and children. The immunochemistry of the capsular polysaccharide differentiates pneumococci into 91 distinct